Instituto Nacional de Pesquisas da Amazônia – INPA

Universidade do Estado do Amazonas – UEA

Programa de Pós-Graduação em Clima e Ambiente – Cliamb

Estudo do escoamento turbulento atmosférico em diferentes sítios experimentais localizados na Amazônia

Raoni Aquino Silva de Santana

Manaus – Amazonas

Julho, 2017

Raoni Aquino Silva de Santana

Estudo do escoamento turbulento atmosférico em diferentes sítios experimentais localizados na Amazônia

Orientador: Dr. Julio Tóta da Silva

Fonte Financiadora: CAPES – INPA/UEA

Tese apresentada ao Programa de Pós-Graduação em Clima e Ambiente – INPA/UEA, como parte dos requisitos para obtenção do título de doutor em Clima e Ambiente.

Manaus – Amazonas

Julho, 2017

S231 Santana , Raoni Aquino Silva de

Estudo do escoamento turbulento atmosférico em diferentes sítios experimentais localizados na Amazônia / Raoni Aquino Silva de Santana. --- Manaus: [s.n.], 2017.
xvi, 95 f.: il.

Tese (Doutorado) --- INPA, Manaus, 2017.
Orientador: Júlio Tóta da Silva
Área de concentração: Clima e Ambiente

1. Perfil do vento . 2. Turbulência . 3. Amazônia . I. Título.

CDD 551.518

Sinopse:

Este trabalho apresenta um estudo dos diferentes aspectos do escoamento atmosférico em áreas de floresta e sobre um lago na região amazônica, abordando os seguintes temas: observação e modelagem do perfil vertical do vento; estrutura da turbulência; trocas de escalares; espectros da turbulência; e a equação do balanço de energia cinética turbulenta.

Palavras chaves: Perfil do vento; Turbulência; Amazônia; Floresta; Lago.

Dedico este trabalho ao meu pai e minha mãe por terrem me mostrado o caminho da educação como instrumento de transformação social.

AGRADECIMENTOS

Agradeço ao meu orientador, Dr. Julio Tóta, pela paciência, amizade e abertura de portas que possibilitaram meu crescimento na pesquisa, no trabalho e na forma de ver o mundo,

Ao Instituto Nacional de Pesquisas da Amazônia (INPA) e à Universidade do Estado do Amazonas, pela oportunidade de formação,

À Coordenação de Aperfeiçoamento de Pessoal de Nível Superior (CAPES) pela bolsa concedida,

Aos professores do Programa CLIAMB-INPA/UEA, pelo empenho em repassar e orientar seus alunos da melhor forma possível, especialmente ao professor Dr. Leonardo Sá, com quem tive a experiência de ter feito a disciplina de micrometeorologia por duas vezes. Seus ensinamentos foram de fundamental importância para minha formação nesta área,

À Universidade Federal do Oeste do Pará (UFOPA) pelo apoio na formação de seus docentes, especialmente pela minha liberação parcial, sem a qual tornaria a confecção desta tese uma tarefa ainda mais complicada,

Ao Dr. David Fitzjarrald por seus ensinamentos, muitas vezes duros, com a certeza de que foram muito válidos para minha vida profissional,

Ao amigo Cléo Quarema Dias-Júnior que contribuiu enormemente na confecção dos artigos deste trabalho, além do incentivo e da colaboração desde a época do mestrado,

À amiga Eliane Gomes Alves pela parceria científica e por me receber em sua casa, sempre de forma acolhedora, nos períodos que precisei vir à Manaus durante o doutorado.

Ao amigo, colega de classe e de trabalho, Roseilson Souza do Vale, com quem compartilhei muitas tristezas, angustia e principalmente momentos felizes, durante todo o percurso do doutorado. Muito obrigado pelo incentivo e pela colaboração em todos os momentos.

Agradeço aos colegas de doutorado, alunos de mestrado e graduação, pesquisadores nacionais e estrangeiros, ajudantes de campo, os quais seria impossível nominar sem cometer injustiças.

Muito obrigado pela convivência, pela ajuda, pelo incentivo e por todos os momentos durante os numerosos trabalhos de campo que participei durante a pós-graduação,

Sou especialmente grato a minha esposa, Márcia Tais, por estar sempre do meu lado todos esses anos e por me acompanhar desde a época do mestrado em todas as situações da vida.

Agradeço a toda minha família, especialmente a meus pais Núbia e Pedro, meus irmãos Ronilson, Tiago e Luis e meus sobrinhos Cristiano e Pedro Jorge.

"Quando a educação não é libertadora, o sonho do oprimido é ser o opressor." - Paulo Freire

RESUMO

A região amazônica é mundialmente conhecida pela disponibilidade de água e pelo número de ecossistemas, tais como: florestas densas de terra firme, florestas inundadas, planícies de inundação, igapós, campos abertos e fechados. O importante papel que a floresta amazônica exerce nas trocas de energia e massa com a atmosfera e a implicação destas trocas no clima em escala local, regional e global é fato difícil de ser contestado. Uma vez que tais trocas são controladas pela turbulência atmosférica, o entendimento do escoamento turbulento nas diferentes camadas da atmosfera, dentro e acima do dossel da floresta e sobre superfícies aquáticas na Amazônia se faz necessário. Como base nisso, neste trabalho, foram estudados a variabilidade vertical da velocidade do vento, dos momentos estatísticos da turbulência, do fluxo de calor sensível (H) e da taxa de dissipação da energia cinética turbulenta (ε) em diferentes sítios experimentais sobre áreas de floresta na Amazônia. Além disso, foi realizada uma comparação entre os escoamentos turbulentos sobre um destes sítios (tradada como superfície rugosa) e sobre um lago, este também localizado na Amazônia. Com relação ao perfil vertical do vento, foram analisados dados coletados em seis torres de medidas de diferentes sítios experimentais, com objetivo de observar as características gerais do comportamento do referido perfil, além de testar a habilidade de modelos simplificados em reproduzir tais características. De maneira geral, o perfil abaixo do dossel é fortemente afetado pela estrutura da floresta. Do solo até $0{,}65h$ (em que $h = 35\,m$ é a altura média do dossel da floresta), o perfil vertical do vento é aproximadamente constante com a altura e apresenta valores muito baixos, menores do que $1{,}0\,ms^{-1}$. Acima de $0{,}65h$ até $2{,}25h$ a velocidade do vento aumenta com a altura. Quanto aos modelos utilizados, tanto o modelo de Yi quanto o de Souza conseguiram reproduzir de maneira satisfatória o perfil do vento para os diferentes sítios experimentais. Em relação a este último modelo, ainda foi possível diminuir a quantidade de variáveis de entrada necessárias para simular o perfil vertical de velocidade do vento sem prejuízo na tal habilidade mencionada acima. Diferentemente do perfil do vento, para as outras análises realizadas neste trabalho foram analisados dados de apenas dois sítios experimentais. Tais dados foram coletados por anemômetros sônicos bi e tridimensionais dispostos desde próximo ao solo da floresta até cerca de 80 m de altura. Comparando os resultados dos dois sítios estudados neste trabalho com outros dois (investigados por outros autores em trabalhos já publicados) também localizados na Amazônia, verificou-se que estes sítios apresentaram diferenças significativas na eficiência em absorver momentum da

atmosfera, provavelmente devido a pequenas diferenças na estrutura da vegetação de cada sítio. O comportamento dos momentos estatísticos da turbulência evidenciou que vórtices gerados acima do dossel florestal dificilmente penetram a região abaixo de $0.5h$, sendo que tal profundidade pode ser mais facilmente atingida durante condições de ventos fortes. Da mesma forma os valores de H foram maiores durante esta condição, tanto durante o dia quanto a noite. Outra observação importante, acerca do perfil de H, é o fato deste não ser constante com a altura, comprometendo a validade da teoria de similaridade de Monin-Obukhov. Além disso, notou-se que o comportamento do ciclo diário de H é bastante complexo em certas alturas, mudando de positivo para negativo dentro do período diurno. Já o ciclo diário de ε, apresenta o mesmo comportamento em todas as alturas, influenciado pelo ciclo diário da radiação solar. Os maiores valores de ε também foram encontrados durante a atuação de ventos fortes, com um máximo próximo ao topo do dossel da floresta. Comparando as características da turbulência sobre a floresta com as observadas sobre o lago, foi verificado que, em geral, a intensidade da turbulência do ar sobre a floresta foi maior do que sobre o lago durante o dia, devido à alta eficiência da floresta em absorver momentum do escoamento. Durante a noite, a situação se inverte, uma vez que a turbulência do ar tem maior intensidade sobre o lago, exceto em alguns períodos em que rajadas de turbulência intermitente ocorrem sobre a floresta. As escalas integrais da turbulência horizontal (Λ_u) e vertical (Λ_w), calculadas durante o período diurno, foram maiores sobre a floresta do que sobre o lago, da mesma forma que a escala de comprimento vertical (L_w) também é maior sobre a floresta. Por outro lado, a escala de comprimento horizontal (L_u) foi maior sobre o lago. Os compósitos dos espectros de potencia da velocidade vertical obtidos para os períodos diurno e noturno para cada sítio apresentaram comportamento canônico, com a região do subdomínio inercial bem definida, exceto no período noturno acima da floresta. Finalmente, a produção de turbulência por cisalhamento do vento foi o termo dominante da equação do balanço de Energia Cinética Turbulenta (ECT), durante o período diurno em ambos os sítios. Todos os termos desta equação calculados neste trabalho, referente ao período noturno, apresentaram valores muito próximos de zero sobre o lago, indicando que outros termos que não puderam ser calculados, como a advecção de ECT, podem ter contribuído para manter a turbulência durante a noite neste sítio.

Palavras chaves: Perfil do vento; Turbulência; Amazônia; Floresta; Lago.

ABSTRACT

Amazon region is known worldwide for the availability of water and for the number of ecosystems such as dense forests land, flooded forests, flood plains, igapós, open and closed fields. The important role that the Amazon rainforest plays in the energy and mass exchange with the atmosphere and the implication of these changes in the climate at a local, regional and global scale is a fact difficult to be answered. Since such changes are controlled by atmospheric turbulence, the understanding of turbulent flow in the different atmosphere layers, in and above the forest canopy and above water surfaces in the Amazon, becomes necessary. In this work, the vertical variability of the wind velocity, the turbulence statistical moments, the sensible heat flux (H) and the turbulent kinetic energy dissipation rate (ε) in different experimental sites in and above Amazon forest were studied. In addition, a comparison was made between turbulent flows above one of these sites (a rough surface) and above a lake, which is also located in the Amazon. Regarding the vertical wind profile, data collected from six towers of different experimental sites were analyzed, aiming to observe the general characteristics of the behavior of said profile, as well as to test the ability of simplified models to reproduce such characteristics. In general, the profile below the canopy is strongly affected by the forest structure. From the soil up to 0.65h (where $h = 35$ is the average height of the forest canopy), the vertical wind profile is approximately constant with height and has very low values, less than $1.0\,ms^{-1}$. Above $0.65h$ up to $2.25h$ the wind speed increases with height. As for the models used, both the Yi and Souza models were able to reproduce satisfactorily the wind profile for the different experimental sites. In relation to this last model, it was still possible to reduce the amount of input variables required to simulate the vertical wind speed profile without prejudice to the aforementioned ability. Differently from the wind profile, the other analyzes performed in this work were based on data from only two experimental sites. These data were collected by bi and three - dimensional sonic anemometers arranged from near the forest floor to about 80 m high. Comparing the results of the two sites studied in this study with other two (investigated by other authors in published works) also located in Amazonia, these sites showed significant differences in the efficiency of absorbing momentum of the atmosphere, probably due to small differences in the forest structure of each site. The behavior of the turbulence statistical moments showed that eddies generated above the forest canopy hardly penetrate the region below $0.5h$, and that depth can be more easily reached during strong wind conditions. Likewise, H values were higher during

this condition in both during the daytime and nighttime. Another important observation disappears from the H profile is that is not constant with the height, compromising the validity of the Monin-Obukhov's theory similarity. In addition, it has been noted that the behavior of the H diurnal cycle is quite complex at certain times, changing from positive to negative within the daytime period. The ε diurnal cycle shows the same behavior at all heights, influenced by the solar radiation diurnal cycle. The highest values of ε were also found during the strong winds performance, with a maximum close to the forest canopy top. Comparing the turbulence characteristics above the forest with those observed above the lake, it was verified that in general the air turbulence intensity above the forest was higher than above the lake during the daytime, due to the high efficiency of the forest in absorbing momentum of the turbulent flow. During the nighttime the situation was reversed, with greater air turbulence intensity above the lake, except in some periods in which intermittent turbulence bursts occur above the forest. The horizontal (Λ_u) and vertical (Λ_w) eddies scales calculated during the daytime period were higher above forest than above the lake, and the vertical length scale (L_w) was also larger over the forest, but the horizontal length scale (L_u) was higher above lake. The composites of the vertical velocity power spectra obtained for the daytime and nighttime periods for each site showed canonical behavior, with a well-defined inertial subdomain region, except in the nighttime period above the forest. Finally, shear production was the dominant term of the turbulent kinetic energy (TKE) budget equation during the daytime period at both sites. All terms calculated in this work at night showed values close to zero over the lake, indicating that the terms that could not be calculated, such as the TKE advection, may have contributed to maintenance of turbulence overnight at this site.

Keywords: Wind profile; Turbulence; Amazon; Forest; Lake.

SUMÁRIO

LISTA DE TABELAS

Capítulo I. Observing and modeling the vertical wind profile at multiple sites in and above the Amazon rain forest canopy

Capítulo II. Vertical variability and wind speed effect on the atmospheric turbulence structure in the Amazon rainforest

Capítulo III. Comparing the air turbulence above smooth and rough surfaces in the Amazon

LISTA DE FIGURAS

Capítulo I. Observing and modeling the vertical wind profile at multiple sites in and above the Amazon rain forest canopy

Capítulo II. Vertical variability and wind speed effect on the atmospheric turbulence structure in the Amazon rainforest

Capítulo III. Comparing the air turbulence above smooth and rough surfaces in the Amazon

INTRODUÇÃO GERAL

Existem várias questões que motivaram os pesquisadores a intensificar seus estudos sobre a interação floresta amazônica-atmosfera (Nobre et al. 1996; Silva Dias et al. 2002; Andreae et al. 2002; Andreae et al. 2015; Fuentes et al. 2016). Uma delas consiste no importante papel que a floresta amazônica exerce na liberação de energia para a atmosfera tropical (von Randow et al. 2004). Outra questão refere-se à sua participação no ciclo hidrológico, em diferentes escalas espaciais (Wang et al. 2016). A terceira consiste no papel que a floresta amazônica desempenha nos balanços globais de componentes gasosas secundárias da atmosfera, tais como ozônio, gás carbônico, hidrocarbonetos e outros componentes (Alves et al. 2016; Gerken et al. 2016; Freire et al. 2017). Finalmente, há problemas associados ao desmatamento na Amazônia e as mudanças climáticas globais (Gash & Nobre 1997), principalmente por conter em sua biomassa um importante estoque de carbono (Gloor et al. 2012).

O transporte de escalares (tais como CO_2, H_2O, entre outros) da floresta para camadas superiores da atmosfera é realizado por movimentos verticais turbulentos. Estes movimentos, por sua vez, podem ser gerados por efeitos térmicos ou mecânicos. Contudo, vale salientar que o escoamento turbulento próximo de superfícies extremamente rugosas (como é o caso da floresta amazônica) se reveste de considerável complexidade. Um exemplo de tal complexidade é a presença de uma *subcamada rugosa* localizada imediatamente acima do dossel florestal (Zahn et al. 2016; Chor et al. 2017), a qual torna difícil a estimativa, com precisão, das variáveis turbulentas médias (Sakai et al. 2001). Em um contexto de modelagem tal complexidade inclui grandes gradientes verticais da estatística da turbulência, natureza não-gaussiana da turbulência e elevadas taxas de dissipação da energia cinética turbulenta dentro da copa, devido à interação do escoamento com os elementos de folhagem do dossel (Raupach & Thom 1981; Finnigan 2000).

Em todas as interações turbulentas entre a floresta e a atmosfera, a mudança da velocidade do vento com a altura é importante (Fitzjarrald et al. 1990; Dias-Júnior et al. 2013; Dias-Júnior et al. 2017), principalmente devido ao persistente desacoplamento entre escoamento atmosférico acima dossel e aquele do interior da floresta, causada pela estratificação térmica do ar entre as camadas da floresta (Fitzjarrald et al. 1988; Kruijt et al. 2000). Dessa maneira, a turbulência mecânica gerada acima da floresta, ou mesmo aquela

oriunda de altos níveis da atmosfera (Santana et al. 2015; Gerken et al. 2016; Dias-Júnior, et al. 2017), que chegam à superfície por movimentos verticais descendentes, tornam-se fundamentais nos processo de acoplamento entre as camadas atmosféricas na interface floresta-atmosfera. Outro fenômeno importante, relacionado ao perfil vertical do vento dentro do dossel da floresta, é a drenagem de escares, tais como CO_2, em regiões com terrenos que apresentam certo grau de inclinação (Tóta et al. 2008; Tóta et al. 2012; Xu et al. 2017). Tóta et al. (2008) encontram significantes transportes horizontais de CO_2 abaixo de 10 metros da copa da floresta, em um sítio experimental na Amazônia.

Embora seja reconhecida a importância do perfil vertical da velocidade do vento, poucos trabalhos têm sido realizados, tanto do ponto de vista observacional quanto de modelos que representem tal perfil. Sá e Pachêco (2001), utilizando ajustes polinomiais de terceira ordem, conseguiram calcular a altura do ponto de inflexão, a velocidade média do vento no ponto de inflexão e ainda uma escala de comprimento característica, utilizada na normalização do perfil vertical de velocidade do vento, para uma área de floresta na Amazônia. Souza et al. (2016), utilizando os mesmos dados de Sá e Pachêco (2001), propuseram um modelo empírico-analítico que conseguiu reproduzir de maneira satisfatória o perfil do vento observado.

O que há em comum entre a maioria dos trabalhos sobre o perfil vertical de velocidade do vento na Amazônia (Sá e Pachêco, 2001; Sá e Pachêco, 2006; Dias-Júnior et al., 2013; Souza et al., 2016) é a utilização de dados medidos em um único ponto, com boa resolução espacial apenas em parte do perfil, de maneira que este pode ser pouco representativo de áreas de floresta densa na Amazônia. Assim, trabalhos que avaliem simultaneamente o comportamento do perfil vertical do vento em diferentes sítios experimentais na Amazônia, bem como a modelagem de tais perfis se fazem necessários.

Da mesma forma, embora trabalhos como os de Fitzjarrald et al. (1988), Fitzjarrald et al. (1990), Fitzjarrald e Moore (1990), Kruijt et al. (2000), Santos et al. (2016) e Dias-Júnior et al. (2017), tenham ajudado a entender a turbulência atmosférica dentro e acima do dossel da floresta na Amazônia, ainda se fazem necessárias análises mais detalhadas para elucidar questões relacionadas à penetração de vórtices no interior do dossel de florestas dessa região. Algumas perguntas precisam ainda ser respondidas, tais como: até que profundidade os vórtices turbulentos conseguem penetrar o dossel da floresta? Qual o papel da velocidade do vento no processo de acoplamento entre a parte superior e inferior do dossel na Amazônia?

Além das áreas de floresta, a Amazônia também é conhecida pelas planícies de inundação, grandes rios, lagos e igapós. Nos últimos anos as pesquisas tem mostrado que assim como os oceanos, as águas interiores exercem um papel fundamental no ciclo regional e global do carbono (Cole et al. 1994; Cole et al. 2007; Richey et al. 2002). No entanto, poucos estudos têm sido realizados a respeito da turbulência atmosférica sobre lagos em regiões tropicais e medidas de longo prazo sobre esta superfície são praticamente inexistentes (Vale 2016). Mesmos em lagos extratropicais, as informações sobre a estrutura da turbulência acima desta superfície ainda são escassas (Sahlée et al. 2014). A pergunta a ser respondida é a seguinte: quais as características da turbulência atmosférica sobre lagos na Amazônia? Quais as diferenças entre as características desta turbulência sobre lagos e a observada sobre o dossel de florestas?

Este trabalho tenta responder as questões levantadas acima, em três artigos, apresentados nos capítulos I, II e III, que seguem no corpo do texto desta tese, todos escritos na língua inglesa. O primeiro, já publicado, entitulado *"Observing and modeling the vertical wind profile at multiple sites in and above the Amazon rain forest canopy"*, avalia as principais características do perfil vertical do vento em seis sítios experimentais localizados na Amazônia, do ponto de vista observacional e de modelagem matemática. O segundo, em processo de submissão, intitulado "*Vertical variability and wind speed effect on the atmospheric turbulence structure in the Amazon rainforest*", avalia dados da turbulência atmosférica coletados como parte dois grandes experimentos realizados na região amazônica: GoAmazon (Fuentes et al. 2016) e ATTO (Andreae et al. 2015), abordando questões relacionadas a penetração de vórtices turbulentos no interior do dossel da floresta e troca de calor sensível entre a floresta e a atmosfera. Finalmente, no terceiro artigo,*"Comparing the air turbulence above smooth and rough surfaces in the Amazon",* é realizada uma comparação entre a intensidade da turbulência, escalas temporais e de comprimentos dos vórtices turbulentos, espectros de potencia e termos da equação do balanço de energia cinética turbulenta observadas sobre uma região de lago e outra de floresta.

OBJETIVOS

OBJETIVO GERAL

Investigar o escoamento turbulento atmosférico acima e abaixo do dossel florestal de diferentes sítios experimentais localizados na Amazônia, bem como avaliar este mesmo escoamento sobre um lago tropical, também situado na Amazônia.

OBJETIVOS ESPECÍFICOS

- Avaliar as características do perfil vertical de velocidade do vento em regiões de floresta.
- Testar a habilidade de modelos que simulam o perfil vertical do vento em reproduzir as observações, além de propor simplificações em um destes modelos, a fim de diminuir o número de variáveis de entrada necessária para gerar o referido perfil.
- Estudar a estrutura da turbulência avaliando seus principais momentos estatísticos, fluxo de calor sensível e taxa de dissipação da energia cinética turbulenta, bem como verificar a influência da velocidade do vento acima do dossel nesta estrutura.
- Comparar as diferentes características da turbulência do ar sobre superfície lisa (lago) e rugosa (floresta).

Capítulo I

Santana, Raoni Aquino Silva de; Dias-Júnior, Cléo Quaresma; Vale, Roseilson Souza do; Tóta, Júlio; Fitzjarrald, David Roy. Observing and Modeling the Vertical Wind Profile at Multiple Sites in and above the Amazon Rain Forest Canopy. *Advances in Meteorology*, 2017, p.8.

Observing and modeling the vertical wind profile at multiple sites in and above the Amazon rain forest canopy

Abstract

We analyzed the vertical wind profile measured at six experimental tower sites in dense forest in the Amazon Basin, and examined how well two simple models can reproduce these observations. In general, the vertical wind profile below the canopy is strongly affected by the forest structure. From the forest floor to 0.65 *h* (where *h* = 35 m is the average height of the forest canopy for sites considered), the wind profile is approximately constant with height with speeds less than 1 m s^{-1}. Above 0.65 to 2.25 h the wind speed increases with height. Testing these data with the Yi and Souza models showed that each was able to reproduce satisfactorily the vertical wind profile for different experimental sites in the Amazon. Using the Souza Model, it was possible use fewer input variables necessary to simulate the profile.

1. Introduction

There are several issues that have motivated researchers to intensify their studies on the interaction between the Amazon rainforest and the atmosphere [1]–[4]. Among these issues is the role that the Amazonian forest exerts on the liberation of energy in the tropical atmosphere [5], on the hydrological cycle [6] and in the global balance of secondary gaseous components in the atmosphere, such as ozone, carbon dioxide, hydrocarbons and others [7]. Furthermore, there are problems associated with deforestation in the Amazon that could have a direct influence on global climate change [8]. In this context, understanding the processes of energy, mass and momentum exchanges between the Amazon forest and the atmosphere is of fundamental importance. Although considerable progress has been made in this area over the past 30 years [9]–[12], more details on variables controlling the said exchanges are needed.

According to Yi [13] the vertical profile of the wind velocity, together with the Reynolds stress, is of fundamental importance to the characterization of turbulent flow over vegetated surfaces, an assertion particularly relevant in dense forest areas. Studies conducted in Amazon forests have shown persistent decoupling of the atmospheric flow between the lower and upper forest canopy [10], due to reduced penetration of direct solar radiation inside the forest and corresponding static stability near the forest floor [9], a condition that often persists over the entire diurnal cycle [11], [12], [14], [15]. Mechanical turbulence generated at canopy top by the rough canopy becomes a determining factor dominates turbulent mixing processes between the upper and lower forest canopy [16].

An hypothesized, dynamic instability associated with an inflection point in the above-canopy wind profile in what is known as the *roughness sublayer* [17]–[20] is another factor that may contribute to the production of turbulence that penetrates into the lower canopy [21], [22]. Dias-Junior *et al.* [23], working in the Amazon, showed the existence of a strong correlation between the inflection point height and time scales of coherent structures, known to contribute to turbulent mixing in forest areas [21].

Only a few previous studies have been done using to describe the wind profile shape in the rain forest canopy, combining observational data and modeling. Sá and Pachêco [24], using a third order polynomial fit, estimated the inflection point height, the average wind speed at the inflection point as well as a characteristic length scale used to normalize the vertical wind profile in an Amazonian forest. Souza *et al.* [25], using the same data as did Sá

and Pachêco [24], proposed an empirical-analytic model that was able to satisfactorily reproduce the vertical wind profile observed.

What is common among most of the work on the vertical wind profile in the Amazon [23]–[26], is the use of data from a single point of measurements, with good spatial resolution for only part of the profile, raising the question that these studies may be unrepresentative of dense forest areas in the Amazon overall. Thus, the aim of this study was to evaluate the different aspects of the vertical wind profile measured at different experimental sites in the Amazon. In addition, simplified models were used to simulate the profiles. Furthermore, for one of these models an improvement was proposed in its formulation in order to reduce the input variables necessary for the model to generate the wind profile.

2. Materials and Methods

2.1. Study Area and Data

This research used observational data collected in five experimental sites in the Brazilian Amazon, where micrometeorological observation towers were installed, namely: the Rebio-Jaru Forest Reserve [27], located in the state of Rondônia in the Southwest Amazon; the Cuieiras Biological Reserve (also called site K34, [28]), located next to the city of Manaus, Amazonas; the Tapajós National Forest (FLONA, km 67 site) near the city of Santarém, Pará [29]; the Caxiuanã National Forest about 350 km west of the city of Belém , Pará [30]; and the Uatumã Sustainable Development Reserve , in the ATTO site (Amazonian Tall Tower Observatory, [3]), city of Santo Antônio do Uatumã , Amazonas. For the latter experimental site, data from two measurements towers were used, which will be called Triangular Tower (TT) and Square Tower (ST). The experimental design of each site is summarized in Table 1 and the geographical position shown in Figure 1. The data used in this work consists primarily of wind speed averages at different heights within and above the forest canopy at each experimental site, made by sonic (two and three dimensional) and cup anemometers (specification of each instrument is listed in Table 1).

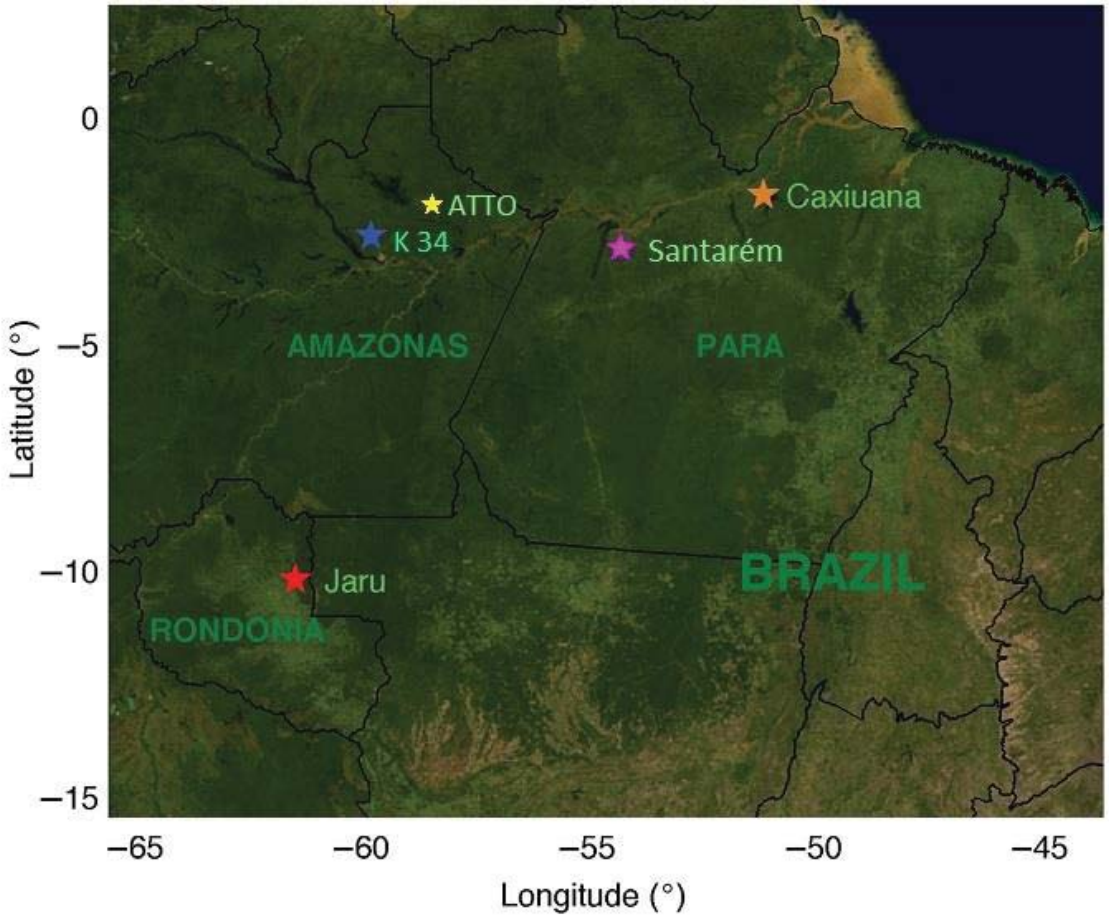

Figure 1. Experimental sites located in the Amazon (Source: Adapted from Zeri *et al.* [31])

Each of these experimental sites is in dense tropical forest with trees ranging from 30 to 40 meters high. The leaf area index values (LAI) for different sites are relatively close. Moura [32] found 5.6 $m^2 m^{-2}$ LAI value for Rebio-Jaru, and for the K34 site, Marque Filho *et al.* [33], using incident solar radiation measurements, estimated LAI at 6.1 $m^2 m^{-2}$, and Tóta *et al.*, [34] measured 7.3 $m^2 m^{-2}$ using a LIDAR. At the Santarém site Asner *et al.,* [35] found LAI to be approximately 6.3 $m^2 m^{-2}$ in October (dry season) and 5.8 $m^2 m^{-2}$ for January (rainy season). In Caxiuanã seasonal variation of LAI is quite sharp, reaching a peak in October, larger than 6 $m^2 m^{-2}$ [30]. Preliminary measures made in September 2013 at the ATTO site indicate LAI of 5.7 ± 0.37 (Giordane Martins, personal communication, November, 2016).

Table 1. Instruments and data periods used.

Experimental sites	Instruments	Reference	Measuremen theights	Sampling rate	Measurement Period
K34 **[4]**	3D-sonic anemometer	CSAT3, Campbell scientific	48.2, 40.4, 34.9, 31.6, 24.5, 22.1, 18.4,13.5, 7.0, 1.5	20 Hz	June 2014 to January 2015
Rebio-Jaru **[23]**	Cup anemometer	Low Power A100L2, Vector Instruments Inc.	55.0, 50.55, 47.7, 42.9, 40.25, 37.8, 32.8, 26.65, 14.30	0.1 Hz	February 1999
Santarém **[29]**	Cup anemometer	5103, R.M. Young Company	64.1, 52, 38.2, 30.7	1 Hz	July to November 2013
	3D-sonic anemometer	CSAT, Campbell scientific	57.8	10 Hz	
	2D-sonic anemometer	CATI/2, Applied Technologies, Inc.	1.8	1Hz	
	3D-sonic anemometer	ATI, Applied Technologies, Inc.	5	10 Hz	
Caxiuanã **[30]**	sonic anemometer	CSAT, Campbell scientific	57.8	10 Hz	April 18-24, 1999
ATTO – Triangular tower **[36]**	3D-sonic anemometer	WindMaster, Gill Instruments Ltd.	78, 41 and 30	10 Hz	February to April 2012
	2D-sonic anemometer	WindSonic, Gill Instruments Ltd.	50,45, 36, and 23	4Hz	
	Automatic weather station	*MetPak*, Gill Instruments Ltd.	72, 60 and 57	1 Hz	
ATTO Square tower **[3]**	3D-sonic anemometer	R3, Gill Instruments Ltd.	80, 40, and 23	10 Hz	January to February 2012
	Cup anemometer	5103, R.M. Young Company	55, 42 and 30	1 Hz	

2.2. Methodology

To obtain the vertical wind speed profiles, averages of the entire time period for which data were available were taken for each height in each experimental site (Table 1). Data from three-dimensional sonic anemometers were used with equation (1) to calculate the wind speed *U*.

$$U = \sqrt{(u^2 + v^2)} \qquad (1)$$

where *u* and *v* are zonal and meridional wind velocity components, respectively.

In this work we use two models to simulate the vertical wind profile above and below the forest canopy. The first, which will be called Yi Model [13], [37], describes the profile:

$$\bar{u}(z) = \bar{u}_h[c_D^h/c_D(z)] \exp\{-0{,}5[LAI - L(z)]\}, \qquad (2)$$

where u_h is the average wind speed at h height (h = 35 m is the average canopy height), $c_D(z)$ is the drag coefficient at z height, $c_D^h = c_D(h)$; *LAI* is the leaf area index; and $L(z)$ is the cumulative leaf area index, defined as

$$L(z) = \int_0^z \alpha(z')dz' \qquad (3)$$

where α is the leaf area density.

The leaf area density was assumed from the values obtained by Tóta *et al.* [34] at the tower K34 site (Figure 2). The drag coefficient was calculated as [10], [38]:

$$c_D(z) = \frac{u_*^2(z)}{U^2(z)}, \qquad (4)$$

where $u_* = [(\overline{u'w'})^2 + (\overline{v'w'})^2]^{1/4}$ is the friction velocity whereinu', v' and w' are the wind turbulent components. This equation was applied to each height for both K34 and ATTO-TT. We then used the cubic interpolation technique to obtain values at other heights in the vertical profile (Figure 2).

The second model used in this study is an empirical-analytical model based on data from sites in the Amazon and mathematical function properties, developed by Souza *et al.* [25] (called the Souza Model from this point forward), given by the equation:

$$\bar{u}(z) = \bar{u}_h \left\{ \left[\frac{-1 + \exp(\mu z)}{\exp(\omega z)} \right] \alpha \; tanh \left[\beta + \gamma \exp\left(-LAI \left(1 - \frac{z}{z_{ip}} \right) \right) \right] \right\}, \quad (5)$$

where μ, ω, α, β and γ are fit parameters of the equation to the observed data, z is the height and z_{ip} is the inflection point height in the vertical wind profile. This model used a larger number of fit parameters, a fact that will be further discussed in the next section.

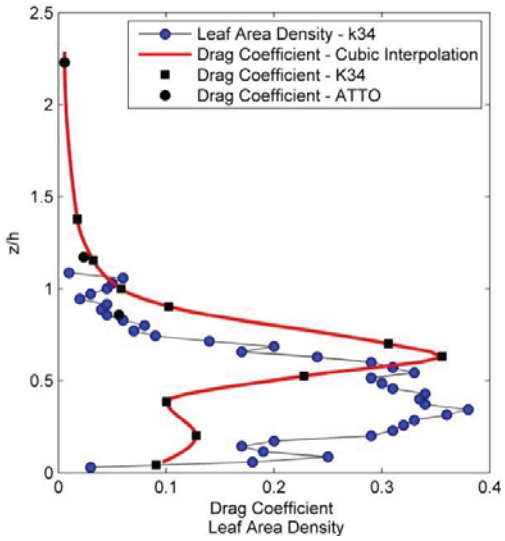

Figure 2. Leaf area density vertical profile (source: Tóta *et al.* [34]) and drag coefficient profile.

3. Results and Discussion

Figure 3 shows the vertical profile of the wind velocity of the K34 and ATTO triangular tower for the daytime (Figure 3a) and nighttime (Figure 3b) periods. Such profiles are complementary: whereas the K34 measurements show wind speed behavior inside the canopy the ATTO data provides more information above the canopy. The shape of the profiles does not change significantly between the daytime and nighttime periods, but in general the speeds recorded during the day, at each height, showed slightly higher values than the nighttime. Due to the vegetation structure below 0.8*h* wind speed showed very low values, lower than 0.25 m s^{-1}, except for at 0.65*h* in the daytime ATTO profile. This point in turn, showed the maximum difference between the profiles observed for an equivalent height, probably caused by differences in the vegetation structure between the sites.

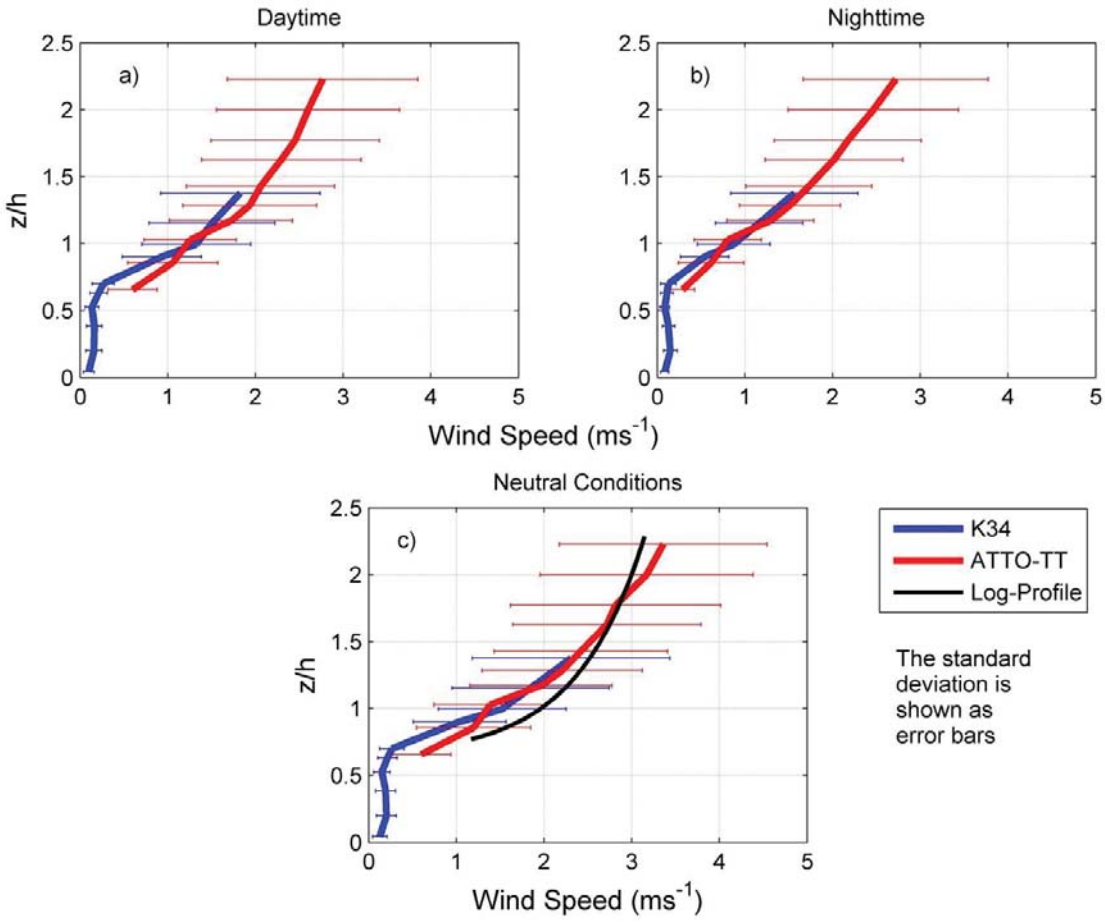

Figure 3. Vertical wind profile for K34 (blue line) and ATTO triangular tower (red line). The horizontal lines represent the standard deviation for each measurement point. The logarithmic profile was obtained through the equation $\bar{u} = \frac{u_*}{k} \ln\left(\frac{z-d}{z_0}\right)$, where k is von Karman's constant, $z_0 = \frac{1}{30}h$ is roughness length and $d = 0.75h$ is displacement height [17].

The atmospheric stability was close to neutral, and the vertical wind profile above the forest canopy is assumed to be the theoretical logarithmic profile [17]. This assumption is approximate for both K34 and ATTO-TT sites, and Figure 3c shows the comparison between said logarithmic profile and the observed data. In this analysis, it is possible to note that from 0.7h to 1.5h the theoretical logarithmic profile overestimates the measured wind speed values; on the other hand, above 1.7h the values observed for the ATTO-TT were slightly higher than said logarithm profile. The reason for these differences is the *roughness sublayer* just above the forest canopy, and this complicates the effort to estimate accurately the relationship between the mean turbulent variables and the canopy structure [39].

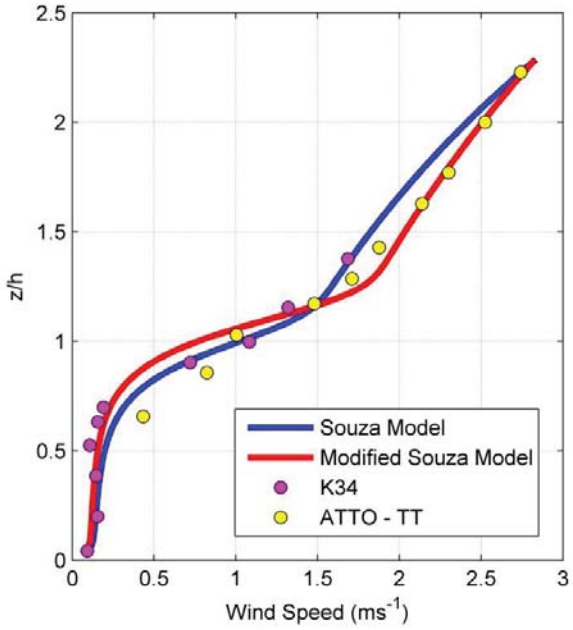

Figure 4. Observed and modeled vertical wind profiles.

Table 2. Souza models fit constants

Constants	Souza Model	Modified Souza Model
μ	1.016	1.012
β	0.1583	0.1
α	0.7275	-------
ω	1	-------
γ	1.973	-------

From the K34 and ATTO-TT data we obtained the fitting constants required for the Souza model, using the least squares technique (Table 2). The constants were obtained in two ways: first by using the original equation proposed by Souza *et al.* [25] (equation 5) in which five constants are required; in the second case, we used a formulation proposed here, where only two constants are used.

$$\bar{u}(z) = \bar{u}_h \left\{ \left[\frac{-1 + \exp(\mu z)}{\exp(z)} \right] tanh \left[\beta + \exp\left(-LAI \left(1 - \frac{z}{z_{ip}} \right) \right) \right] \right\}, \qquad (6)$$

For both equations 5 and 6 the Souza model fit very well to the K34 and ATTO–TT data, with a coefficient of determination (r^2) of 0.98 and 0 .97, respectively (Figure 4). Thus,

equation 6 is more advantageous because it has a smaller number of necessary constants for the mathematical fit (the model of equation 6 will be called Modified Souza Model from this point forward).

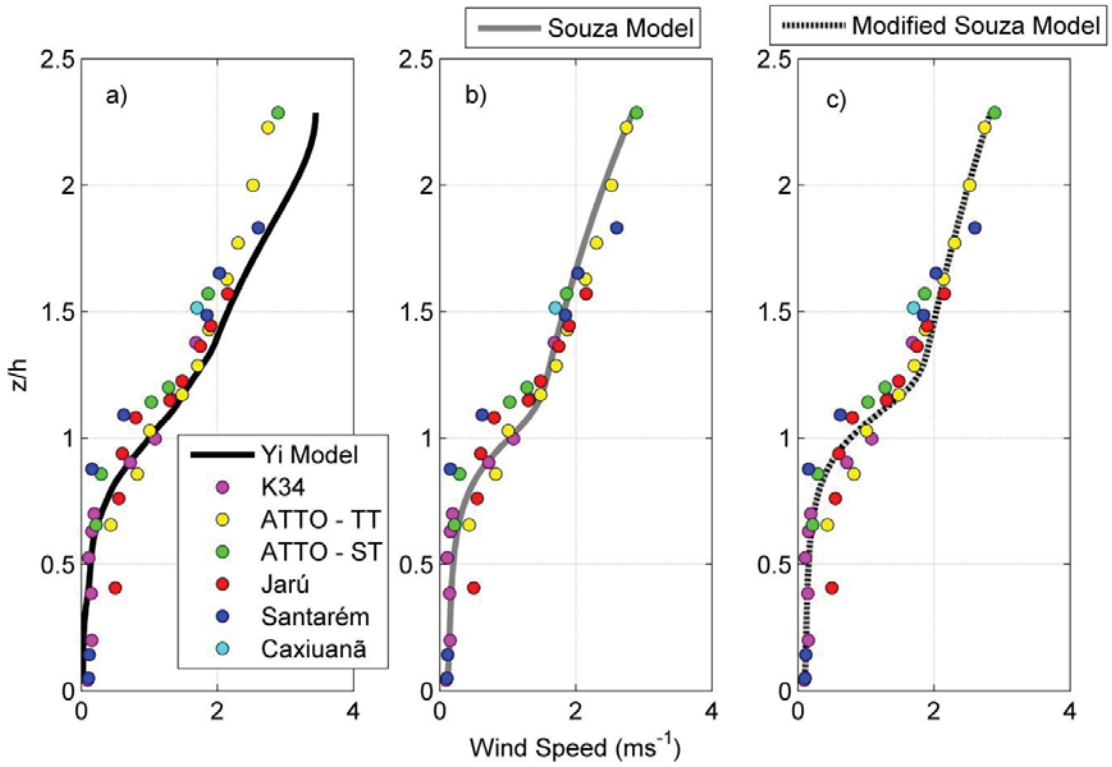

Figure 5. Vertical wind profile observed and modeled in different experimental sites in the Amazon.

An important question is whether the Souza models (original and modified), which fit the K34 and ATTO-TT data very well, can be used to represent the vertical wind profile for other experimental sites in the Amazon. Also, a good test to see if the model represents such profiles is to compare their performance with that of another model that has already been tested in other conditions, such as the Yi Model, for example.

We can conclude from this analysis that all models represented fairly well the vertical profile of the wind velocity for different Amazonian experimental sites (Figure 5), although there are differences among both the models and simulated and observed wind speed values, to a greater or lesser degree, for some heights. In Figure 6 (a, b, and c) the observed wind speed values were plotted against the model output to measure the degree to which data points approach the line with an 45° angular coefficient, and which model better represents the observations at each point. Among the models, the Yi Model was the one that presented, on

average, the greatest distance of observed values. The two versions of the Souza models have similar behavior, but the modified Souza Model has a slightly higher coefficient of correlation (0.973) compared to the original Souza Model (0.967).

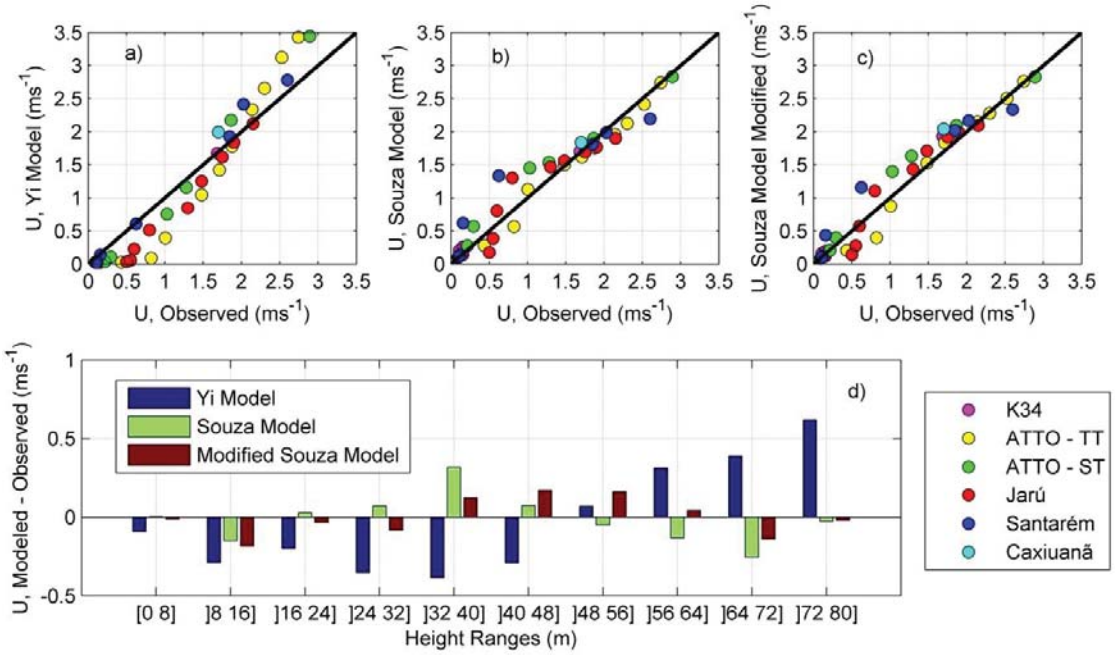

Figure 6. Wind speed (U) observed versus modeled for the three models used in this study (a, b and c). Part d shows the modeled minus observed wind speed for different intervals of heights, above and below the forest canopy.

To verify the ability of each model at different heights, an average of the observed and simulated wind speed values were calculated at intervals of 8 meters in height and then the difference between the modeled and observed values was calculated (Figure 6d). The results show that the Yi Model overestimated the wind velocity values above 48 m in height, with a greater difference between 72 and 80 m, while at the same time underestimated values below 48 m, with a mean-squared error (MSE) of 0.12 ms^{-1}. The Souza Model had its maximum divergence between 32 and 40 m, with a difference of 0.3 ms^{-1} between the modeled value and the observed value. The Modified Souza Model was the one that presented the smallest absolute value at its point of maximum difference between the heights of 8 and 16 m and also presented the lowest MSE, 0.04 ms^{-1}. Again, this shows that a smaller number of fit parameters in the Souza Model do not change the model's ability to simulate the vertical wind profile for different sites in the Amazon.

Each of the three models has satisfactory performance; using one or the other model depends on each situation. In the Souza Model the constants must be different for other forest types, after which calculations for a given profile may be extrapolated to others with similar vegetation structure. Since the Yi Model requires, in addition to other input variables, the profile drag coefficient, this, in turn, needs to be calculated for the type of vegetation.

4. Conclusions

In this work we examined the vertical wind profile measured at different experimental sites in Amazonia. Measurements with high resolution below the canopy, performed at the K34 site, and above the canopy at the ATTO triangular tower, represent the first time that such data have been compiled in a single work, and have provided a broader view of the wind vertical profile behavior in the Amazon forest. Under the forest canopy the wind speed values were very low due to the vegetation structure, while above the canopy wind increases with height in an approximately logarithmic behavior. Furthermore, with data from the two sites mentioned above, it was possible to obtain a new formulation for the Souza Model, with a reduced number of input variables, which facilitates the use of the model for future applications. Both Souza models (original and modified) and the Yi Model managed to satisfactorily represent the vertical wind profile for different sites in the Amazon.

Acknowledgements

We acknowledge the funding provided by the Coordination of Higher Education and Personnel Training (CAPES) and all who participated in the GoAmazon project at K34 and ATTO IOP-1-2012 for the excellent quality of the collected data.

References

[1] M. A. F. Silva Dias, S. Rutledge, P. Kabat, P. L. Silva Dias, C. Nobre, G. Fisch, A. J. Dolman, E. Zipser, M. Garstang, A. O. Manzi, J. D. Fuentes, H. R. Rocha, J. Marengo, A. Plana-Fattori, L. D. A. Sá, R. C. S. Alvalá, M. O. Andrcae, P. Artaxo, R. Gielow, and L. Gatti, "Cloud and rain processes in a biosphere-atmosphere interaction context in the Amazon Region," *J. Geophys. Res. D Atmos.*, vol. 107, no. 20, 2002.

[2] M. O. Andreae, D. Rosenfeld, P. Artaxo, A. A. Costa, G. P. Frank, K. M. Longo, and M. A. F. Silva-Dias, "Smoking Rain Clouds over," vol. 303, no. 0036–8075, pp. 1337–13242, 2004.

[3] M. O. Andreae, O. C. Acevedo, A. Araújo, P. Artaxo, C. G. G. Barbosa, H. M. J. Barbosa, J. Brito, S. Carbone, X. Chi, B. B. L. Cintra, N. F. Da Silva, N. L. Dias, C. Q. Dias-Júnior, F. Ditas, R. Ditz, A. F. L. Godoi, R. H. M. Godoi, M. Heimann, T. Hoffmann, J. Kesselmeier, T. Könemann, M. L. Krüger, J. V. Lavric, A. O. Manzi, A. P. Lopes, D. L. Martins, E. F. Mikhailov, D. Moran-Zuloaga, B. W. Nelson, A. C. Nölscher, D. Santos Nogueira, M. T. F. Piedade, C. Pöhlker, U. Pöschl, C. A. Quesada, L. V. Rizzo, C. U. Ro, N. Ruckteschler, L. D. A. Sá, M. De Oliveira Sá, C. B. Sales, R. M. N. Dos Santos, J. Saturno, J. Schöngart, M. Sörgel, C. M. De Souza, R. A. F. De Souza, H. Su, N. Targhetta, J. Tóta, I. Trebs, S. Trumbore, A. Van Eijck, D. Walter, Z. Wang, B. Weber, J. Williams, J. Winderlich, F. Wittmann, S. Wolff, and A. M. Yáñez-Serrano, "The Amazon Tall Tower Observatory (ATTO): Overview of pilot measurements on ecosystem ecology, meteorology, trace gases, and aerosols," *Atmos. Chem. Phys.*, vol. 15, no. 18, pp. 10723–10776, 2015.

[4] J. Fuentes, M. Chamecki, R. Nascimento dos Santos, C. Von Randow, P. Stoy, G. Katul, D. Fitzjarrald, A. Manzi, T. Gerken, A. Trowbridge, L. Friere, J. Ruiz-Plancarte, J. Maia, J. Tota, N. Dias, G. Fisch, C. Schumacher, O. Acevedo, and J. Mercer, "Linking meteorology, turbulence, and air chemistry in the Amazon rainforest during the GoAmazon project," *Bull. Am. Meteorol. Soc.*, p. in review, 2016.

[5] C. von Randow, A. O. Manzi, B. Kruijt, P. J. de Oliveira, F. B. Zanchi, R. L. Silva, M. G. Hodnett, J. H. C. Gash, J. A. Elbers, M. J. Waterloo, F. L. Cardoso, and P. Kabat, "Comparative measurements and seasonal variations in energy and carbon exchange over forest and pasture in South West Amazonia," *Theor. Appl. Climatol.*, vol. 78, no. 1–3, pp. 5–26, 2004.

[6] J. Wang, P. Artaxo, and J. Brito, "Amazon boundary layer aerosol concentration sustained by vertical transport during rainfall," *Nature*, vol. 539, no. 7629, pp. 416–419, 2016.

[7] T. Gerken, D. Wei, R. J. Chase, J. D. Fuentes, C. Schumacher, L. A. T. Machado, R. V. Andreoli, M. Chamecki, R. A. Ferreira de Souza, L. S. Freire, A. B. Jardine, A. O. Manzi, R. M. Nascimento dos Santos, C. von Randow, P. dos Santos Costa, P. C. Stoy, J. Tóta, and A. M. Trowbridge, "Downward transport of ozone rich air and implications for atmospheric chemistry in the Amazon rainforest," *Atmos. Environ.*, vol. 124, no. 1352–2310, pp. 64–76, 2016.

[8] J. H. C. Gash and C. A. Nobre, "Climatic Effects of Amazonian Deforestation: Some Results from ABRACOS," *Bull. Am. Meteorol. Soc.*, vol. 78, no. 5, pp. 823–830, 1997.

[9] W. J. Shuttleworth, “Observations of radiation exchange above and below Amazonian forest,” *Q. J. R. Meteorol. Soc.*, vol. 110, pp. 1163–1169, 1984.

[10] D. R. Fitzjarrald, B. L. Stormwind, G. Fisch, and O. M. R. Cabral, “Turbulent transport observed just above the Amazon forest,” *J. Geophys. Res.*, vol. 93, no. D2, p. 1551, 1988.

[11] B. Kruijt, Y. Malhi, J. Lloyd, A. D. Nobre, A. C. Miranda, M. G. P. Pereira, A. Culf, and J. Grace, “Turbulence statistics above and within two Amazon rain forest canopies,” *Boundary-Layer Meteorol.*, vol. 94, no. 2, pp. 297–331, 2000.

[12] D. M. Santos, O. C. Acevedo, M. Chamecki, J. D. Fuentes, T. Gerken, and P. C. Stoy, “Temporal Scales of the Nocturnal Flow Within and Above a Forest Canopy in Amazonia,” *Boundary-Layer Meteorol.*, pp. 1–26, 2016.

[13] C. Yi, “Momentum transfer within canopies,” *J. Appl. Meteorol. Climatol.*, vol. 47, no. 1, pp. 262–275, 2008.

[14] D. R. Fitzjarrald, K. E. Moore, O. M. R. Cabral, J. Scolar, A. O. Manzi, and L. D. de Abreu Sá, “Daytime turbulent exchange between the Amazon forest and the atmosphere,” *J. Geophys. Res. Atmos.*, vol. 95, no. D10, pp. 16825–16838, 1990.

[15] D. R. Fitzjarrald and K. E. Moore, “Mechanisms of nocturnal exchange between the rain forest and the atmosphere,” *J. Geophys. Res. Atmos.*, vol. 95, no. D10, pp. 16839–16850, 1990.

[16] C. Q. Dias-júnior, L. D. A. Sá, E. P. Marques, R. A. Santana, M. Mauder, and A. O. Manzi, “Turbulence regimes in the stable boundary layer above and within the Amazon forest,” *Agric. For. Meteorol.*, vol. 233, pp. 122–132, 2017.

[17] J. C. Kaimal and J. J. Finnigan, *Atmospheric Boundary LayerFlows - Their Structureand Measurement*. 1994.

[18] P. Cellier and Y. Brunet, “Flux Gradient Relationships above Tall Plant Canopies,” *Agric. For. Meteorol.*, vol. 58, no. 1–2, pp. 93–117, 1992.

[19] M. R. Raupach, J. J. Finnigan, and Y. Brunei, “Coherent eddies and turbulence in vegetation canopies: The mixing-layer analogy,” *Boundary-Layer Meteorol.*, vol. 78, no. 3–4, pp. 351–382, 1996.

[20] J. Finnigan, “Turbulence in plant canopies,” *Annu. Rev. Fluid Mech.*, vol. 32, pp. 519–571, 2000.

[21] C.-H. Lu and D. R. Fitzjarrald, “Seasonal and diurnal variations of coherent structures over a deciduous forest,” *Boundary-Layer Meteorol.*, vol. 69, pp. 43–69, 1994.

[22] C. Q. Dias-Júnior, L. D. de A. Sá, E. P. Marques Filho, R. A. S. de Santana, M. Mauder, and A. O. Manzi, “Turbulence regimes in the stable boundary layer above and within the Amazon forest,” *Agric. For. Meteorol.*, 2016.

[23] C. Q. Dias Júnior, L. D. A. Sá, V. B. Pachêco, and C. M. de Souza, “Coherent structures detected in the unstable atmospheric surface layer above the Amazon forest,” *J. Wind Eng. Ind. Aerodyn.*, vol. 115, pp. 1–8, 2013.

[24] L. D. A. Sá and V. B. Pachêco, “Relações de similaridade para os perfis de velocidade média do vento dentro da copa da floresta amazônica em Rondônia,” *Rev. Bras. Meteorol.*, vol. 16, no. 1, pp. 81–89, 2001.

[25] C. M. Souza, C. Q. Dias-Júnior, J. Tóta, and L. D. de A. Sá, “An empirical-analytical model of the vertical wind speed profile above and within an Amazon forest site,” *Meteorol. Appl.*, vol. 23, no. 1, pp. 158–164, 2016.

[26] L. D. de A. Sá and V. B. Pachêco, “Wind velocity above and inside amazonian rain forest in Rondônia,” *Rev. Bras. Meteorol.*, vol. 21, no. 3a, pp. 50–58, 2006.

[27] M. O. Andreae, P. Artaxo, C. Brandão, F. E. Carswell, P. Ciccioli, A. L. Da Costa, A. D. Gulf, J. L. Esteves, J. H. C. Gash, J. Grace, P. Kabat, J. Lelieveld, Y. Malhi, A. O. Manzi, F. X. Meixner, A. D. Nobre, C. Nobre, M. D. L. P. Ruivo, M. A. Silva-Dias, P. Stefani, R. Valentini, J. Von Jouanne, and M. J. Waterloo, “Biogeochemical cycling of carbon, water, energy, trace gases, and aerosols in Amazonia: The LBA-EUSTACH experiments,” *J. Geophys. Res. D Atmos.*, vol. 107, no. 20, 2002.

[28] A. C. Araújo, A. D. Nobre, B. Kruijt, J. A. Elbers, R. Dallarosa, P. Stefani, C. Von Randow, A. O. Manzi, A. D. Culf, J. H. C. Gash, R. Valentini, and P. Kabat, “Comparative measurements of carbon dioxide fluxes from two nearby towers in a central Amazonian rainforest: The Manaus LBA site,” *J. Geophys. Res.*, vol. 107, pp. 1–20, 2002.

[29] J. Tóta, D. R. Fitzjarrald, R. M. Staebler, R. K. Sakai, O. M. M. Moraes, O. C. Acevedo, S. C. Wofsy, and A. O. Manzi, “Amazon rain forest subcanopy flow and the carbon budget: Santarém LBA-ECO site,” *J. Geophys. Res. Biogeosciences*, vol. 114, no. 1, pp. 1–15, 2008.

[30] F. E. Carswell, A. L. Costa, M. Palheta, Y. Malhi, P. Meir, J. D. P. R. Costa, M. D. L. Ruivo, L. D. S. M. Leal, J. M. N. Costa, R. J. Clement, and J. Grace, “Seasonality in CO2 and H2O flux at an eastern Amazonian rain forest,” *J. Geophys. Res. D Atmos.*, vol. 107, no. 20, 2002.

[31] M. Zeri, L. D. A. Sá, and C. A. Nobre, “Contribution of coherent structures to the buoyancy heat flux under different conditions of stationarity over Amazonian forest sites,” *Atmos. Sci. Lett.*, vol. 16, no. 3, pp. 228–233, 2015.

[32] R. G. de Moura, “Estudos Das Radiações Solar E Terrestre Acima E Dentro De Uma Floresta Tropical Úmida,” 2001.

[33] A. O. Marques Filho, R. G. Dallarosa, and V. B. Pachêco, “Radiação solar e distribuição vertical de área foliar em floresta Reserva Biológica do Cuieiras ZF2, Manaus,” *Acta Amaz.*, vol. 35, no. 4, pp. 427–436, 2005.

[34] J. Tóta, D. Roy Fitzjarrald, and M. A. F. da Silva Dias, “Amazon Rainforest Exchange of Carbon and Subcanopy Air Flow: Manaus LBA Site—A Complex Terrain Condition,” *Sci. World J.*, vol. 2012, pp. 1–19, 2012.

[35] G. P. Asner, D. Nepstad, G. Cardinot, and D. Ray, “Drought stress and carbon uptake in an Amazon forest measured with spaceborne imaging spectroscopy,” *Proc Natl Acad Sci U S A*, vol. 101, no. 16, pp. 6039–6044, 2004.

[36] L. Newton, “Sobre as características de formação de estrutura coerente e turbulência

em uma floresta densa de terra firme com medidas em até 80m de altura: Projeto ATTO-CLAIRE / IOP - 1 - 2012.," 2014.

[37] C. Yi, R. K. Monson, Z. Zhai, D. E. Anderson, B. Lamb, G. Allwine, A. A. Turnipseed, and S. P. Burns, "Modeling and measuring the nocturnal drainage flow in a high-elevation, subalpine forest with complex terrain," *J. Geophys. Res. Atmos.*, vol. 110, no. 22, pp. 1–13, 2005.

[38] L. Mahrt, X. Lee, A. Black, H. Neumann, and R. M. Staebler, "Nocturnal mixing in a forest subcanopy," *Agric. For. Meteorol.*, vol. 101, no. 1, pp. 67–78, 2000.

[39] R. K. Sakai, D. R. Fitzjarrald, and K. E. Moore, "Importance of Low-Frequency Contributions to Eddy Fluxes Observed over Rough Surfaces," *J. Appl. Meteorol.*, vol. 40, no. 12, pp. 2178–2192, 2001.

Capítulo II

Santana, Raoni Aquino Silva de; Tóta, Júlio; et al. Vertical variability and wind speed effect on the atmospheric turbulence structure in the Amazon rainforest. Manuscrito em preparação para Agricultural and Forest Meteorology.

Vertical variability and wind speed effect on the atmospheric turbulence structure in the Amazon rainforest

Abstract

In this work, the atmospheric turbulence structure in and above the forest canopy area was analyzed in two experimental sites located in the Amazon region, in order to identify patterns of turbulent flow and to elucidate questions related to the eddies´ penetration in the canopy and changes of scalars of this region. For this, we used data provided by bi- and three-dimensional sonic anemometers arranged from near the forest floor to about 80 m in height. The main variables that describe the behavior of atmospheric turbulence, turbulent sensible heat flux (H) and the turbulent kinetic energy dissipation rate (ε) were analyzed. The behavior of each mentioned variable was also verified under weak (WW) and strong (SW) wind conditions. Comparing the results of the two sites studied in this work with two others also located in Amazonia that were investigated by other authors in published works, these sites showed significant differences in the efficiency of absorbing momentum of the atmosphere, probably due to small differences in the structure of each site. The behavior of the turbulence statistical moments showed that eddy generated above the canopy hardly penetrated the region below $0.5h$, and that depth can be more easily reached during SW, mainly during the nighttime period. It was also observed that the highest values of H occur during the SW condition, during both day and nighttime periods. In addition, the H profile is not constant with height, compromising the validity of Monin-Obukhov's similarity theory. Finally, it was noted that the behavior of the H diurnal cycle is quite complex at certain times, changing from positive to negative within the daytime period. The ε diurnal cycle shows the same behavior in each height, influenced by the solar radiation diurnal cycle. The highest ε values were also found during SW, with a maximum close to the top of the forest canopy.

Keywords: Turbulence; Wind; Forest; Amazon;

1. Introduction

The study of the energy, mass and momentum exchanges between the vegetated surface and the atmosphere is an essential part of the understanding of the processes associated with biosphere-atmosphere interactions (Raupach & Thom 1981; Finnigan 2000). In particular, tropical forest regions, especially the Amazon rainforest, play a key role not only in these exchanges (Fitzjarrald et al. 1988; Kruijt et al. 2000; Fuentes et al. 2016), but also in the carbon cycling related to biomass an important carbon stocks (Gloor et al. 2012).

The transport of scalars (such as CO_2, H_2O, among others) from the forest to the free atmosphere is performed by turbulent vertical motions. Thermal or mechanical effects generate these movements. In dense forest regions, such as the Amazon rainforest, little incident solar radiation can reach the soil (about 1 to 3%, according Shuttleworth et al. (1984)), The result is that within the forest canopy a statically stable atmospheric layer is formed, persisting for almost the entire diurnal cycle (Fitzjarrald et al. 1990; Santos et al. 2016; Dias-Júnior et al. 2017).

This feature makes a possible coupling (i.e., a time period in which turbulent mixing occurs between different levels of the atmosphere (Acevedo & Fitzjarrald 2003; Freire et al. 2017)) between the top and bottom of the forest canopy difficult to occur due to turbulence generated by thermal effects. Thus, the mechanical turbulence generated above the forest, or even that arising from high levels in the atmosphere (Santana et al. 2015; Gerken et al. 2016; Dias-Júnior et al. 2017), which reach the surface by downward vertical movements, become important in the energy and mass exchange in dense forest regions. Lu & Fitzjarrald (1994) showed that during certain time intervals coherent eddies (or coherent structures) have the ability to penetrate the interior of a deciduous forest canopy in Ontario, Canada. Such eddies may be directly related to the aerodynamic instability caused by the inflection point in the vertical wind speed profile (Raupach et al. 1996). Dias-Júnior et al. (2013) showed that there is a direct relationship between the temporal scales of occurrences of the structures consistent with the inflection point height in the wind profile.

Although previous studies Fitzjarrald et al. (1988), Fitzjarrald et al. (1990), Fitzjarrald & Moore (1990), Kruijt et al. (2000), Santos et al. (2016), Dias-Júnior et al. (2017) have helped to understand the atmospheric turbulence in and above the Amazon forest canopy, further analysis is needed to elucidate questions related to the characteristic eddies reaching

different levels of the forest canopy. Some questions still need to be answered, such as: how deep can the turbulence penetrate the forest canopy? What is the role of wind speed in the coupling process between the upper and bottom of the Amazon rainforest canopy?

To try to elucidate these questions, this research evaluates the turbulence structure above and below the forest canopy of two experimental sites in the Amazon. In each of these sites, 10 measurement levels, carried out over long term periods, were used. The vertical variability turbulence statistic was calculated and compared with that of Kruijt et al. (2000) (hereafter, KJ2000) for moderately unstable atmospheric conditions. These profiles were also analyzed under weak and strong wind conditions over the forest. Other analyses were also conducted based on weak and strong wind classes to: evaluate the diurnal cycle of turbulence statistics, sensible heat flux and turbulent kinetic energy dissipation rate for different levels within and above the rainforest.

2. Material and methods

2.1. Experimental sites and data

The data used in this research were collected at two experimental sites, both located in the state of Amazonas, Brazil. These sites are areas of dense forest with trees ranging from 30 to 40 meters in height. The first, called K34, is located in the biological reserve of Cuieiras (54° 58’ O, 2° 51’ S), which is about 60 km northwest of the city of Manaus (Araújo et al. 2002). The forest had a leaf area index estimated at 6.1 (Marques Filho et al. 2005) and 7.3 $m^2 m^{-2}$ (Tóta et al. 2012). The second site is known as ATTO (Amazon Tall Tower Observatory) and is located in the city of São Sebastião do Uatumã, within the Sustainable Development Reserve (2° 8’ 32.42” S, 59° 0’ 3.50” W, (Andreae et al. 2015)). The leaf area index estimated for this site in September 2013 was $5.7 \pm 0.37\ m^2 m^{-2}$ (Santana et al. 2017; Chor et al. 2017).

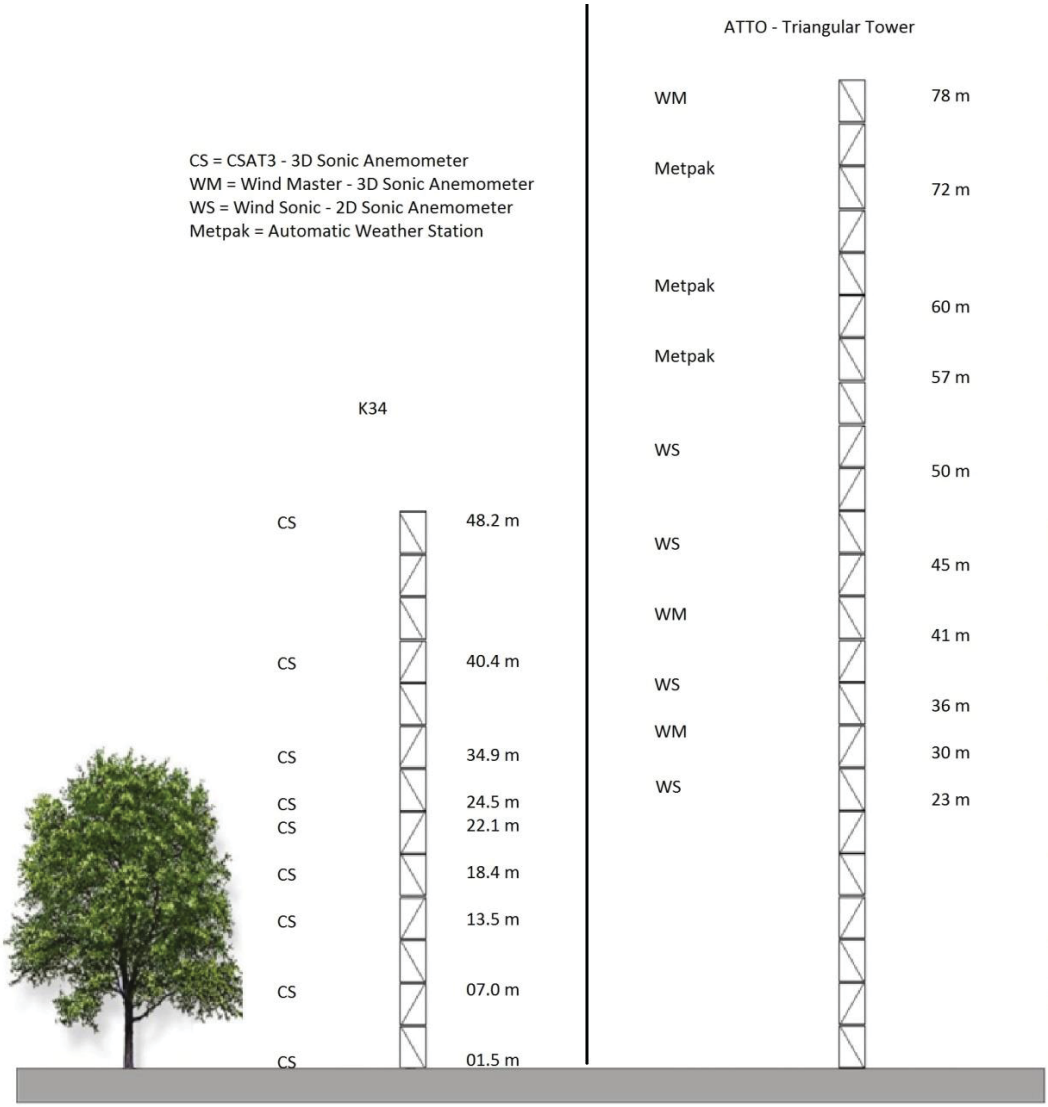

Figure 1. Illustrative figure representing the measurement instruments installed in the K34 and ATTO experimental sites.

At the K34 site, 10 three-dimensional sonic anemometers (model CSAT3, Campbell 128 Scientific Inc., Logan, UT) were arranged from 1.5 to 48.2 m above ground during the period from April 2014 to January 2015 as part of the GoAmazon project (Fuentes et al. 2016, see Table and Figure 1 for detailing all measurement heights). The data were collected at the sampling frequency of 20 Hertz, and included the three wind components (u, v, and w) and the virtual sonic temperature (T_V).

Table 1 - Measurements levels, variables, sampling rate and instruments models used in the K34 and ATTO experimental sites.

K34			
Levels (m)	Variables	Sampling rate (Hz)	Instruments
1.5, 7.0, 13.5, 18.4, 22.1, 24.5, 31.6, 34.9, 40.4, 48.2	Virtual temperature and wind speed components (vertical, zonal and meridional)	20	Three-dimensional sonic anemometer (CSAT)
ATTO – Triangular Tower			
78, 41 and 30	Virtual temperature and wind speed components (vertical, zonal and meridional)	10	Three-dimensional sonic anemometer (Gill)
57, 60 and 72	Air temperature, humidity, pressure and wind speed and direction	1	Metpak-automatic weather station coupled to a two-dimensional sonic anemometer (Gill)
23, 36, 45 and 50	Wind speed and direction	4	Two-dimensional sonic anemometer (Gill)

The ATTO data were collected from February to April 2012, on a triangular tower of 84 m height, as part of the ATTO-CLAIRE/IOP-1-2012 experiment (Lima 2014). In this experiment, three-dimensional and two-dimensional sonic anemometers were deployed over 10 different heights on the tower. At some heights two-dimensional sonic anemometers were coupled to temperature and humidity sensors, and this set is referred to as “metpak”. These metpaks (*MetPak*, Gill Instruments Ltd, Lymington, Hampshire, UK.) were installed above the forest canopy at 57, 62 and 70 m height, with 1 Hz sampling rate. Three-dimensional sonic anemometers (WindMaster, Gill Instruments Ltd, Lymington, Hampshire, UK) were installed at 30, 41 and 78 m height and sent data at a 10 Hz sampling rate. In turn, the two-dimensional sonic anemometers were installed at 23, 36, 45 and 50 m in height, at a sampling rate of 4 Hz (Table 2).

ATTO data have advantages and disadvantages compared to K34 data. At the ATTO site, not all instruments are three-dimensional as in K34, which means that vertical velocity data are not available at all heights. In addition, the low sampling rate of two-dimensional sonics may not capture all eddies, especially those of smaller length scales. Even so, ATTO data are relevant as they provide information on heights above the canopy that were not

considered at the K34 site due to the limitation of the measurement tower, which is only 50 m high.

2.2. Methodology

To compare the results with those found in the work of KJ2000, we calculated the variables of the so-called "Family Portraits" of turbulence (Raupach et al. 1996), for each measurement height. The time interval used to calculate these quantities was 5 minutes for the nighttime period, in order to minimize the effects of non-turbulent scales, and 30 minutes for the daytime period (Vickers & Mahrt 1997). The overall horizontal wind speed was obtained by the equation $U = \sqrt{u^2 + v^2}$, where u and v are zonal and meridional wind components. The u standard deviation was calculated as $\sigma_u = \left[\overline{(u')^2}\right]^{1/2}$, with u oriented along with the mean wind direction. Similarly, the standard deviation of the wind vertical component, w, was defined as $\sigma_w = \left[\overline{(w')^2}\right]^{1/2}$. We also calculated the kinematic momentum flux, $-\overline{u'w'}$, the correlation coefficient between u and w, $-r = -\overline{u'w'}/\left(\sigma_u \sigma_w\right)$, as well as higher order statistical moments: u e w Skewness ($Sk_u = \overline{(u')^3}/\sigma_u^3$ and $Sk_w = \overline{(w')^3}/\sigma_w^3$); and u and w Kurtosis ($k_u = \overline{(u')^4}/\sigma_u^4$ and $k_w = \overline{(w')^4}/\sigma_w^4$).

In addition to the Family Portraits variables, the sensible heat flux was also calculated according to the equation $H = \rho c_p \overline{T_v' w'}$, wherein ρ is the air density; c_p is the air specific heat at constant pressure; and T_v is the virtual temperature; as well as the turbulent kinetic energy dissipation rate, ε. In order to calculate ε we used inertial subrange properties of the power spectra established by Kolmogorov (Kaimal & Finnigan 1994) and the assumption of the Taylor's hypothesis validity (Stull 1988). Thus we obtain the following equation:

$$\varepsilon = \frac{2\pi f^{5/2} S_u^{3/2}}{U \alpha^{3/2}}$$

Where f is the frequency; S_u is the u power spectra; e $\alpha = 0.55$ is the Kolmogorov's constant (Kaimal et al. 1972; Kaimal & Finnigan 1994). In order to select only values of S_u that were inside the inertial subrange, we used values of the frequency range $1.0 > f < 2.5$ Hz, which, according to Bolzan & Vieira (2006), have always been in the part of the desired spectrum, in a study carried out over a forest area in the Amazon. The same frequency ranges were used by Dias-Júnior et al. (2017) for the same site.

With the objective of verifying the influence of wind speed variation above the canopy on the behavior of the previously mentioned variables, four classes of data were defined based on the quartile analysis of the wind speed measured at the top of the canopy at each experimental site. To make possible differences more visible and simplify the analyses, only two of these classes were used, which contain 25% of the data with the lowest wind speeds and 25% with the highest wind speeds. In addition, the data were also separated into diurnal and nocturnal datasets. Thus, different wind speed thresholds above the canopy were defined, for each period of the day (daytime and nighttime) and for each experimental site. These thresholds are summarized in Table 2.

Table 2. Wind speed thresholds based on the quartile analysis for the daytime and nighttime periods for the K34 and ATTO sites.

	Experimental sites	**Q1 (m/s)**	**Q2 (m/s)**	**Q3 (m/s)**
Daytime	K34	1.00	1.44	1.86
	ATTO	0.94	1.28	1.70
Nighttime	K34	0.57	0.84	1.19
	ATTO	0.51	0.70	0.97

3. Results and discussion

3.1. Turbulence statistical moments - comparison with KJ2000

In this section a comparison between the results obtained in this work (for the K34 and ATTO sites) with the those of KJ2000 (for the C14 and Jaru sites) is made. Initially, the vertical profiles of some turbulence statistical moments will be compared (Figure 2). KJ2000 calculated such moments for moderately unstable atmospheric conditions in two forest areas in the Amazon, and compare their results with the "family portraits" summarized by Raupach et al. (1996). Figure 2 shows the profiles of KJ2000 with those obtained in this research.

It is important to note that comparing these profiles is convenient not only to confirm some observations made by KJ2000 but also to add new information to the turbulence statistical moments data using a more complete data set. As an example, the standard profiles obtained in the ATTO offer information at levels above $1.5\,h$ ($h = 35\,m$). In the work of

KJ2000, information measured only below $1.5\ h$ was used due to data limitation. In addition, in this work we could count on more levels of measurements for the K34 site than KJ2000 had.

The normalized wind speed profiles (U/U_h, Figure 2a) were quite similar between the studied sites, and a strong attenuation in the wind intensity below 0.75 h was observed, besides a positive gradient above this height. A similar result was found by Santana et al. (2017), who compared the wind speed profile of different sites in the Amazon (including the same profiles as ATTO and K34 shown here). This result suggests that U_h is a good normalization parameter, in terms of horizontal variability, for moderately unstable atmospheric conditions. Furthermore, it was possible to observe that above 1.5 h the U/U_h profile calculated for the ATTO, U_h behaves as an extension of the profiles obtained for the other sites studied (Figure 2a).

In addition to the U/U_h profile, the σ_u/u_{*zs}, σ_w/u_{*zs} e $-\langle u'w'\rangle/(u_{*zs})^2$ profiles also rapidly decay to as they move towards the inside of the canopy (Figures 2 b, c and d, respectively). However, it is possible to observe some differences between the profiles investigated for each site, mainly for the last two profiles. The main differences are the following: i) The value of σ_w/u_{*zs}, in the region just above the canopy, was much higher in the Jaru site when compared to the value of σ_w/u_{*zs} found for the other sites analyzed (Figure 2c, a profile with this behavior was found for the K34 site, for the daytime period under weak wind conditions, details will be discussed in the next section); ii) The $-\langle u'w'\rangle/(u_{*zs})^2$ profile found for the K34 and C14 sites have maximum values at height h. Although there are few levels of measurements for the momentum flux, such behavior does not appear to occur for the ATTO site, since a profile of approximately constant values in the region above h was observed. For Jaru, it is not possible to say anything about a maximum in $z = h$, because of the lack of data at this site (Figure 2d).

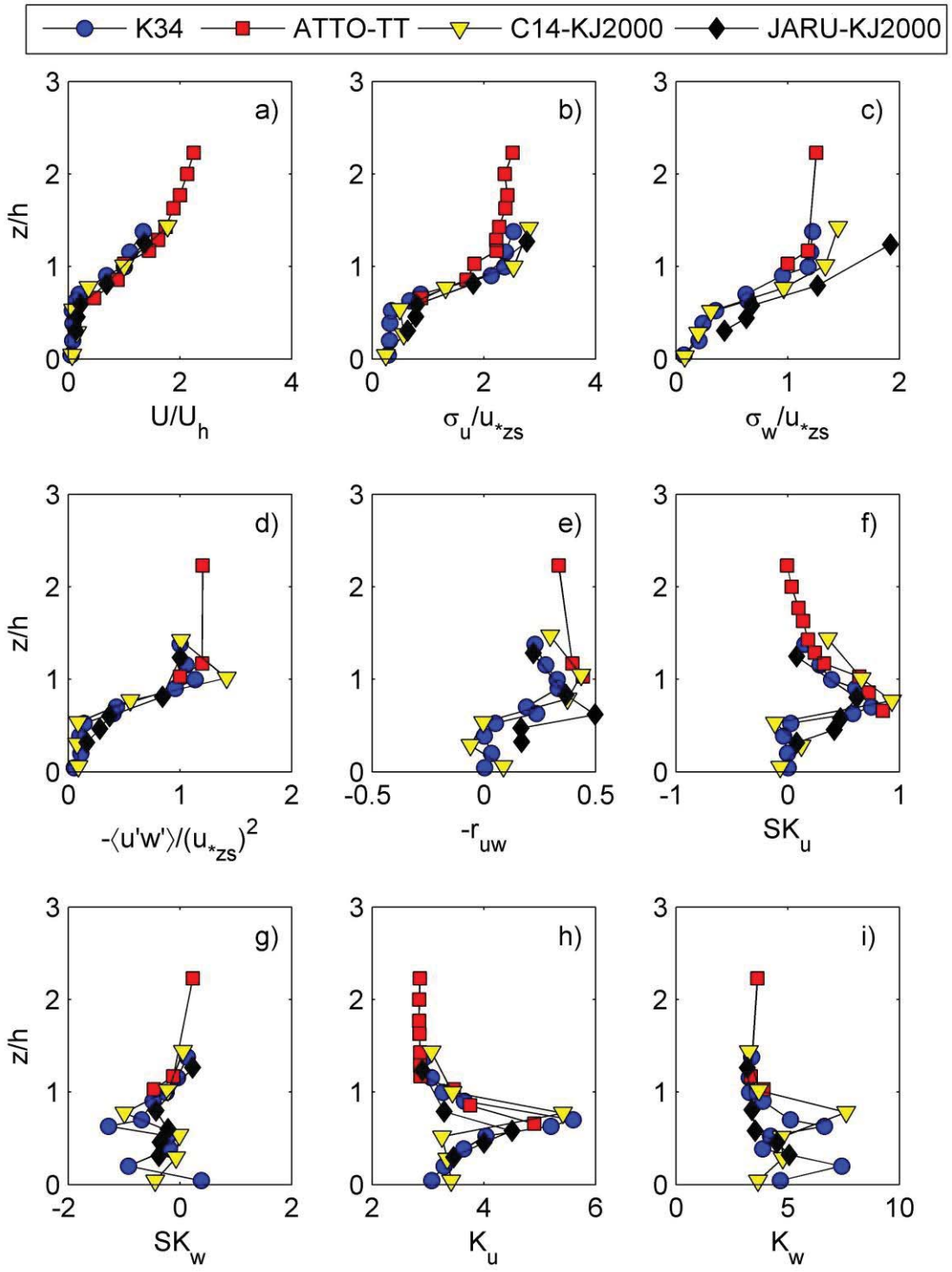

Figure 2. Vertical profiles in (a) U/U_h; (b) σ_u/u_{*zs}; (c) σ_w/u_{*zs}; (d) $-\langle u'w'\rangle/(u_{*zs})^2$; (e) $-r = -\overline{u'w'}/(\sigma_u\sigma_w)$; (f) $Sk_u = \overline{(u')^3}/\sigma_u^3$, (g) $Sk_w = \overline{(w')^3}/\sigma_w^3$); (h) $k_u = \overline{(u')^4}/\sigma_u^4$; e (i) $k_w = \overline{(w')^4}/\sigma_w^4$), for K34, ATTO, C14 and Jaru sites. Table 3 provides a summary of the heights at which the u_{*zs} measurements were performed.

An important property of the *roughness sublayer* above the forest is that the turbulence characteristics depend directly on the arrangement of trees (Kaimal & Finnigan 1994; Poggi et al. 2004). In other words, forest heterogeneity influences the canopy efficiency to absorb momentum from the atmospheric flow. The $-r_{uw}$ profile (Figure 2e) shows that even forests with a certain degree of similarity (all the forests studied here are dense rainforests) may be more or less efficient in absorbing momentum from the atmospheric flow. With this in mind, it was possible to observe that at $z = h$, the ATTO and C14 sites had the highest $-rw$ values as compared to the K34 and Jaru sites. Unlike the other sites, Jaru presented the $-r_{uw}$ maximum value at 0.65 h. According to KJ2000, this behavior is explained by the Jaru leaf area density whose maximum values are observed close to this height.

In addition to $-r_{uw}$, the ratio $U_h/\ u_{*zs}$ can also be understood as a measure of canopy efficiency in absorbing momentum of the atmospheric flow. The values of this ratio obtained in this work and those calculated by KJ2000 are summarized in Table 3. One site is more efficient than the other as the U_h/u_{*zs}value is lower, so, according to the values in Table 3, the C14 and K34 sites were the most and least efficient, respectively.

Another issue concerns the penetration of vortices inside the forest canopy. Vertical profiles of turbulent statistical moments of higher order, such as skewness and kurtosis may help to understand this process. It is important to keep in mind that the u and w skewness, i.e., Sk_u and Sk_w, respectively, are related to the degree of asymmetry of the u and w probability distribution around their mean values (Baldocchi & Meyers 1988). The values of such variables provide useful information about vertical transport at the forest-atmosphere interface. Nonzero values of Sk_u and Sk_w are related to typical manifestations of the existence of heterogeneous turbulence (Lumiley & Panosky 1964), as it exists in the Amazon roughness sublayer.

KJ2000 found that the vertical profiles of Sk_u and Sk_w for the C14 and Jaru sites exhibit marked differences when compared to the Raupach et al. (1996) 'family portraits' profiles. According to Raupach et al. (1996), Sk_u shows values of 0.5 to 1 and Sk_w values of -0.5 to -1 at the region below the canopy, typically. For the sites studied in this work, Sk_u values were close to zero in the region between the soil and $0.5\,h$ (Figure 2f). From this height to about 0.75 h there is a rapid increase in Sk_u values with increasing height until reaching a maximum value, then there is a gradual decay with height and a tendency for Sk_u values to approach zero again. Although fewer Sk_w observations have been performed above

the canopy, the same trend of values approaching gradually to zero can be inferred. In addition, an overall minimum value is observed around $0.75\,h$. Below this height, the values tend to approach zero, except for the K34 site, where a secondary minimum value appears near the forest floor in the Sk_w vertical profile.

The results of the Sk_u and Sk_w vertical profiles suggest that turbulence in the region between $0.5h > z < h$ is highly dominated by sweeps, with "excess" of negative w and positive u (Antonia 1981; Raupach et al. 1996; Katul et al. 1997). On the other hand, due to the high density and heterogeneity of the Amazon forest, little turbulence is able to penetrate the region $z < 0.5h$. This result differs from others performed in wind tunnels with dense crowns (Poggi et al. 2004) or in more homogeneous canopies (Sylvain Dupont & Patton 2012; Chamecki 2013; Launiainen et al. 2007), where values of Sk_u around 0.5 and Sk_w of approximately -0.5 were verified even below 0.5h. It also differs from the results of Dias-Júnior et al. (2015), who used LES (Larger Eddy Simulation) models to represent the turbulent flow above and within the forest canopy at the Jaru site. The main differences between the results found here and the results found by these authors refer to the values of SK_u and SK_w for the interior of the canopy. These differences may be related to the fact that their model cannot account for all the heterogeneity of the Amazon forest.

The u and w kurtosis provide an idea of turbulence intermittence (Lumiley & Panosky 1964). If the values of these variables are greater than 3, the u and w probability distribution is higher (tapered) and more concentrated than the normal distribution, indicating that during short periods the turbulence was more intense than its average behavior at a given level (Baldocchi & Meyers 1988). KJ2000 highlighted the differences in the K_u and K_w vertical profiles between the C14 and Jaru sites, with more emphasis on the K_w profile. The additional information provided by the ATTO and K34 sites shows a certain pattern in the K_u profile, with maximum values in the range of 4 to 6 occurring between 0.5 and $0.75h$ at each site. A clear pattern is not observed in the K_w profile. The C14 site has a maximum in the region between 0.5 and 0.75 h and at the K34 site an atypical maximum occurs at $z = 0.2h$. This maximum may be related to the wake generation due to advection in the forest subcanopy (Tóta et al. 2008; Tóta et al. 2012; Santos et al. 2013)

Table 3. u_{*zs} measurement height, U_h/u_{*zs} with standard error for different sites. The u_{*zs} measurements heights for the K34 and ATTO sites were chosen because they are closest to those used by KJ2000.

	u_{*zs} measurement height (m)	U_h/u_{*zs}	Standard error
K34	48.2	5.4	3.6
ATTO	41	3.8	0.57
C14 (KJ2000)	46.5	2.5	0.19
Jaru (KJ2000)	50	4.5	0.45

3.2. Wind speed effect on the turbulence statistical moments

In the previous section it was shown that there are differences of efficiency in the atmosphere momentum absorption by the forest cover of the different experimental sites studied. Figure 3 shows that such efficiency also varies according to wind speed. The U_h/u_{*zs}values were low for $U_h < 0.25$ m/s for both ATTO and K34 sites. The U_h/u_{*zs}, peaks, i.e., the points where the canopy is less efficient in absorbing momentum, occur at $U_h \approx 0.5$ and $U_h \approx 0.8$ m/s for the ATTO and K34 sites, respectively. From these peaks the canopy efficiency tends to increase with the increase in U_h. .

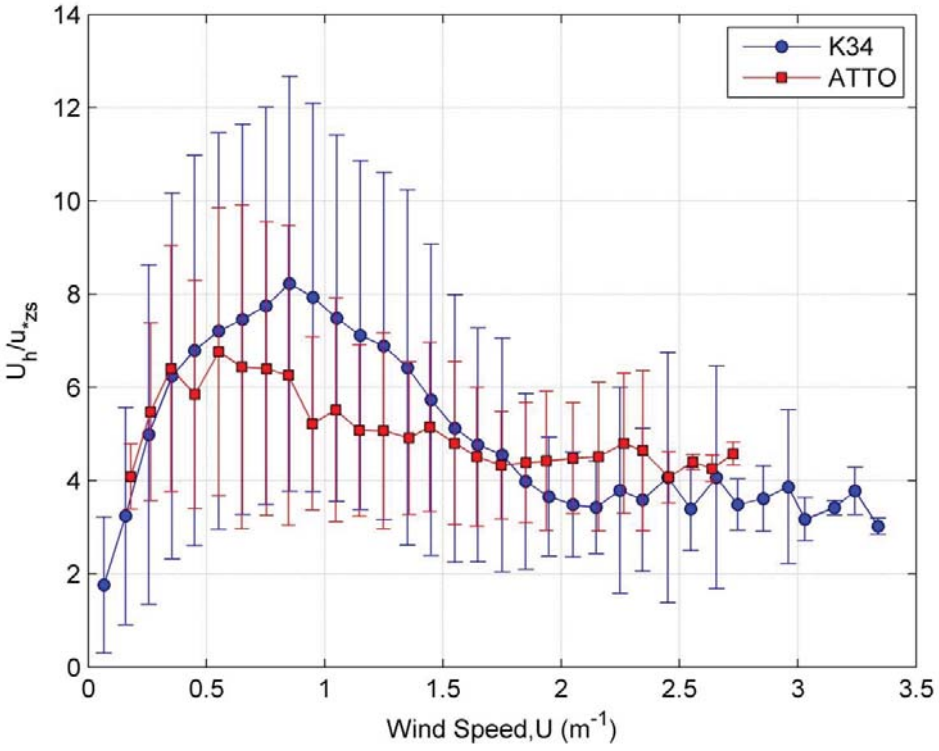

Figure 3. Relationship between wind speed at h height and U_h/u_{*zs} ratio for both K34 ATTO site. The standard deviation is shown as error bars.

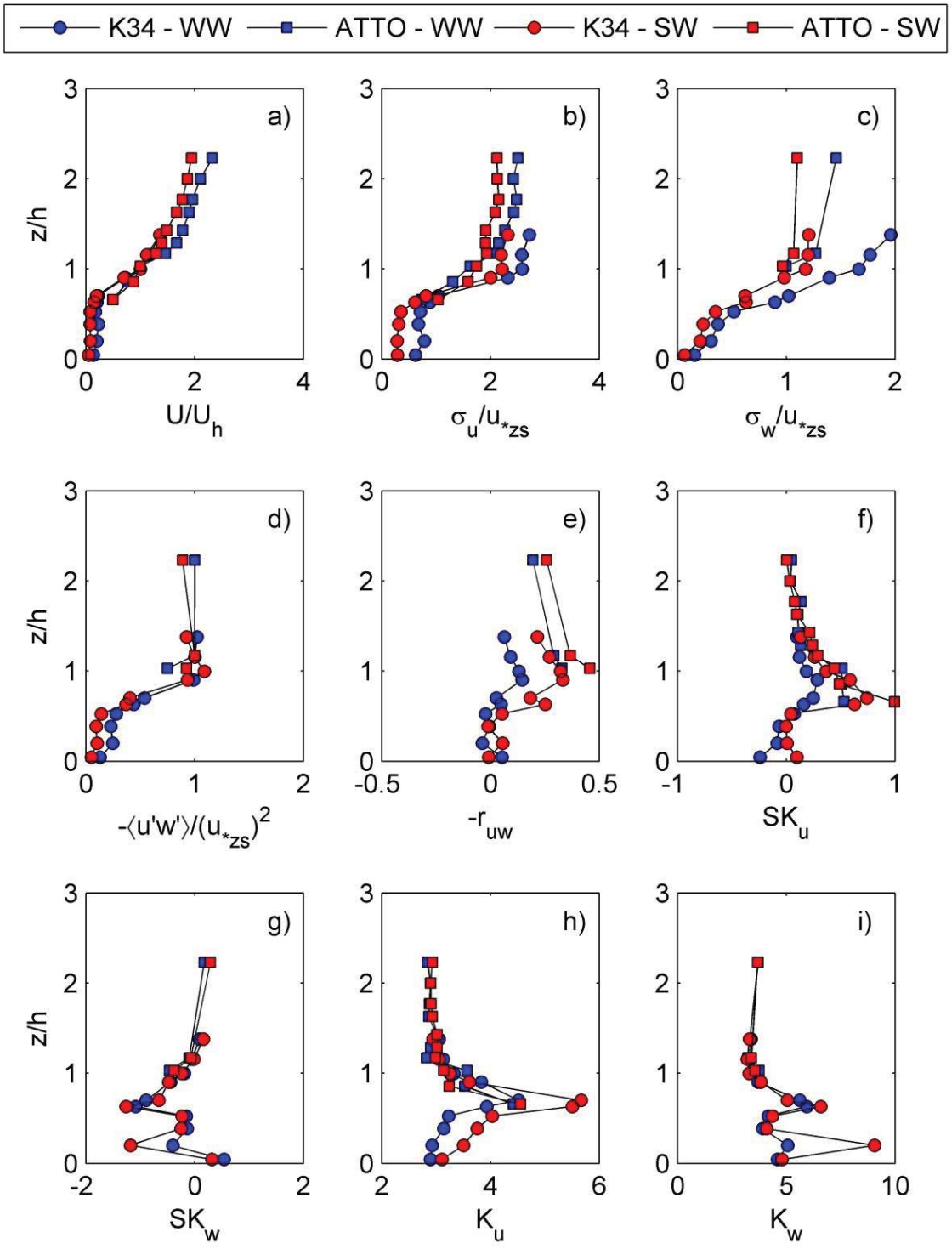

Figure 4. Vertical profiles in (a) U/U_h; (b) σ_u/u_{*zs}; (c) σ_w/u_{*zs}; (d) $-\langle u'w'\rangle/(u_{*zs})^2$; (e) $-r = -\overline{u'w'}/(\sigma_u\sigma_w)$; (f) $Sk_u = \overline{(u')^3}/\sigma_u^3$, (g) $Sk_w = \overline{(w')^3}/\sigma_w^3$); (h) $k_u = \overline{(u')^4}/\sigma_u^4$; e (i) $k_w = \overline{(w')^4}/\sigma_w^4$), for K34 and ATTO sites. The heights at which the u_{*zs} measures were performed are summarized in Table 3. Daytime period under weak wind (WW, blue color) and strong wind (SW, red color).

In addition to the efficiency of momentum absorption being different for different wind speeds, the vertical profiles of the turbulence statistical moments, shown in Figure 2, also vary for different wind speed values above the canopy. Figures 4 and 5 show these profiles for daytime and nighttime periods, respectively, under weak wind (WW) and strong wind (SW) conditions.

The main characteristics observed for the daytime period are: i) among the normalized profiles, the U/U_h, σ_u/u_{*zs} and $-\langle u'w'\rangle/(u_{*zs})^2$ profiles (Figures 4 a, b and d, respectively) were the ones that presented the highest similarity between the profiles calculated for both WW and SW conditions. This indicates that the normalizations are apparently adequate for these profiles; ii) In Figure 3c it is possible to observe that above the canopy the σ_w/u_{*zs} profile for the Jaru site there is a much larger gradient than at the other study sites since the σ_w/u_{*zs} value was approximately 2 for the highest measurement height. The same behavior was observed for the K34 site in WW conditions during the daytime (Figure 4c). A possible explanation for such behavior is that the variance of w is being created by forced turbulence by buoyancy, at the same time as the K34 canopy is inefficient in absorbing momentum for certain wind speed ranges (values between 0.5 and $1\ m/s$, for example); iii) the $-r_{wu}$ values at their maximum point ($-r_{wu}(h)$) were lower at the K34 than ATTO site under similar wind conditions. Furthermore, for each the difference between the calculated values $-r_{wu}(h)$ during SW and WW site are also higher at the K34 site, indicating that this site is more susceptible to efficiency of change in absorbing momentum due to wind speed variation; iv) in the SK_u and K_u profiles the maximum values were more pronounced for SW than WW for both sites. For Sk_w and K_w profiles the behavior is practically the same for both WW and SW conditions, except at $z = 0.2h$, where more pronounced peaks appear during SW. This result reinforces the idea that turbulence is being generated due to advection in the forest subcanopy (Tóta et al. 2008; Tóta et al. 2012; Santos et al. 2013).

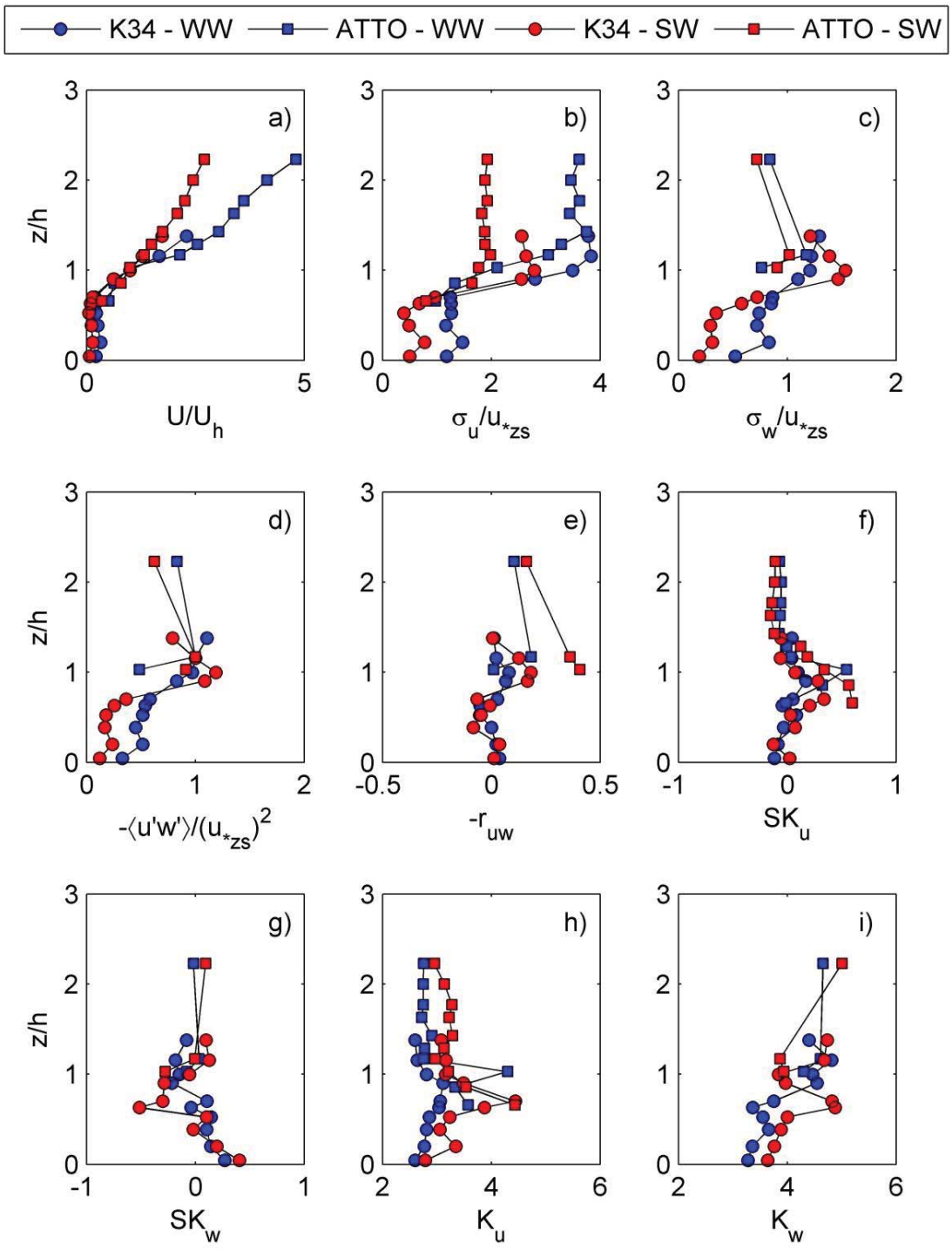

Figure 5. Vertical profiles in (a) U/U_h; (b) σ_u/u_{*zs}; (c) σ_w/u_{*zs}; (d) $-\langle u'w'\rangle/(u_{*zs})^2$; (e) $-r = -\overline{u'w'}/(\sigma_u\sigma_w)$; (f) $Sk_u = \overline{(u')^3}/\sigma_u^3$, (g) $Sk_w = \overline{(w')^3}/\sigma_w^3$); (h) $k_u = \overline{(u')^4}/\sigma_u^4$; e (i) $k_w = \overline{(w')^4}/\sigma_w^4$), for K34, ATTO, C14 and Jaru sites. The heights at which the u_{*zs} measures were performed are summarized in Table 3. Nighttime period under weak wind (WW, blue color) and strong wind (SW, red color).

For the nocturnal period some behaviors call attention such as: i) unlike the daytime period, the normalizations in U, σ_u, σ_w and $-\langle u'w' \rangle$ profiles fail completely in both above and below the forest canopy (Figures 5 a, b, c and d, respectively); ii) in WW conditions, the σ_w/u_{*zs} and $-\langle u'w' \rangle/(u_{*zs})^2$ profiles showed a maximum at $z = h$ at the site of K34, that does not occur in WW conditions. Santos et al. (2016) also found a maximum at $z = h$ in the σ_w/u_{*zs} profile for the K34 site, averaging for the nighttime period, for same data used in this work; iii) even in SW conditions the efficiency of the canopy to absorb momentum is low for this site. The ATTO site showed a different behavior, the $-r_{wu}$ values were close to values observed during the daytime in the SW condition (Figure e); iv) The peaks observed at $0.75h$ in the Sk_u and K_u profiles were much less pronounced than those calculated during the daytime period (Figures f and h, respectively). For the Sk_w and K_w profiles, such peaks exist only during SW (Figures g and i, respectively).

3.3. Sensible heat flux

There are many studies that have evaluated the sensible heat flux above forested regions. In the Amazonian forest, measures of this variable have been made since the end of the 1980's (Fitzjarrald et al. 1990; Malhi et al. 2002; Von Randow et al. 2008; Shuttleworth et al. 1984a). However, information about vertical profiles in the landscapes is still scarce, even for extratropical regions (Santos et al. 2016; Dupont & Patton 2012; Thomas & Foken 2007). Santos et al. (2016) studied the sensitive heat kinematic flux profile at the K34 site during the nighttime, using the same data set of this work.. However, these authors did not analyze the H profile for the different conditions of weak and strong winds, as realized here. Santos et al. (2016) found that on average the H values were positive above 0.75 h and negative below this height.

Figure 6d shows the H profiles for WW and SW conditions. In WW conditions the H values above $0.75h$ were approximately constant with the height, around $-1.7\ W/m^2$. On the other hand, under SW conditions the vertical H profile presents a maximum value of the $-15\ W/m^2$ at $z = h$ and a negative gradient above this height. The finding that the wind speed influences directly the H during the nighttime period is consistent with the result found by Fitzjarrald & Moore (1990) at the Ducke Reserve site in the Amazon, where these researchers observed H values 10 times greater in strong wind conditions, when compared with the average for the whole period. Dias-Júnior et al. (2017), also during the nighttime

period, observed that during higher turbulence regimes, associated with strong winds, about 72% of all H observed occurs in the Jaru site.

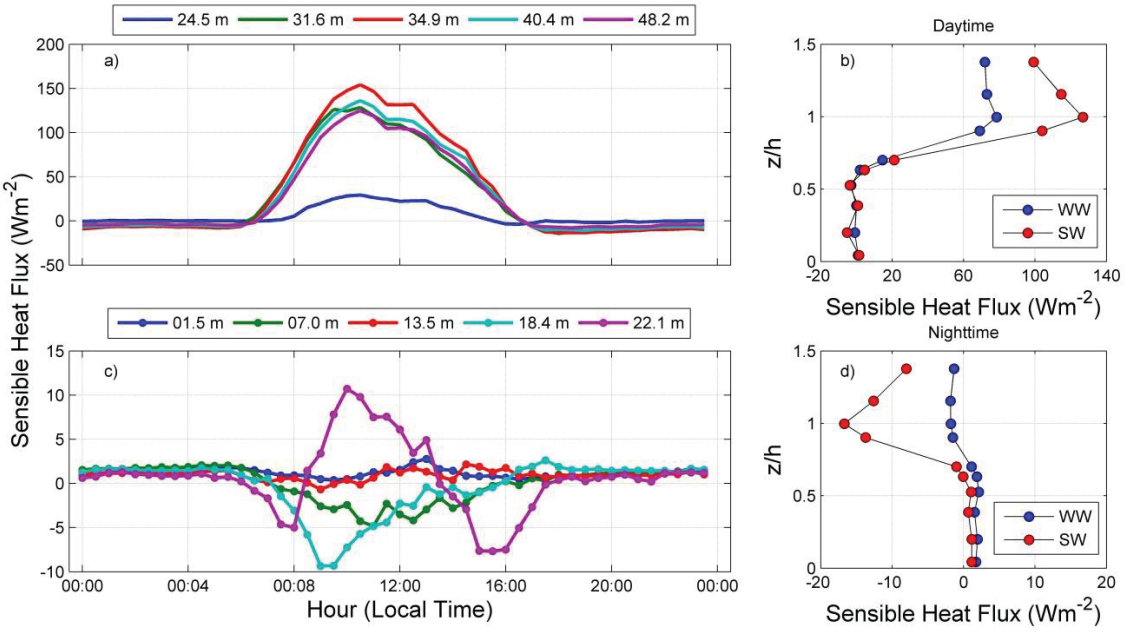

Figure 6. Diurnal cycle of the sensible heat flux for different heights for both inside and above and the canopy forest for the K34 site in a and c. Sensible heat flux profile for weak (WW) and strong (SW) wind conditions for daytime (b) and nighttime (d) periods.

During the daytime the H profiles under WW and SW conditions are quite similar below $0.75h$ and different above this height (Figure 6b). In both profiles a maximum occurs at $z = h$, but much more pronounced in the H profile under SW conditions. In addition, above the canopy it was also possible to observe that H presented higher values and a more marked negative gradient during SW when compared to the WW condition (Figure 6b).

An important observation about H profiles is related to general flux gradient formulations, such as Monin-Obukhov Similarity Theory (MOST). One of the assumptions of this theory is that the H is constant with the height, a condition that is not verified in the profiles shown in Figure 6, especially under WW conditions. This result corroborates that observed by Sun et al. (2012) who studied turbulence in the nocturnal boundary layer (NBL). These authors classified the turbulence in the NBL in three different regimes, which present different relations between turbulence intensity and wind speed. In regime 2 they observed that the turbulence intensity increases systematically with the turbulent kinetic energy

increase and with the wind speed increase. Sun et al. (2012) suggest that in regime 2 the turbulence generation occurs mainly by the vertical wind shear coming from the entire atmospheric boundary layer, and therefore, in this regime it would be expected that MOST will fail.

In addition to the H profiles evaluation, the sensible heat flux behavior in different levels above and below the forest crown (Figure 6 a e c), would yield useful information because with this it will be possible to better understand the processes of heat exchanges and even of other scales in different layers above and within the forest canopy. Figure 6a shows that H values between 31.6 to 48.2 m heights were approximately equal and follow the daily cycle of radiation. At the $24.5\,m$ height the H diurnal cycle still shows a behavior following that of the upper heights, but the increase in H starts only near 8 am (local time), an hour later than the upper heights, besides declining to close zero values earlier (around 4 pm). Such behavior may be related to the fact that the vertical temperature profile minimum\maximum at the canopy top at night\day, i.e., is a consequence of the radiation budget. Clearly, there is a net loss of energy in the trees' crown region through radiative processes, in which the outgoing longwave radiation component is not completely balanced by the incoming longwave radiation component.

Molion (1987) in analysis of the energy budget´s diurnal variability at Ducke reserve (central Amazonia region), showed that the budget had a diurnal deficit due to longwave radiation that is on the order of $40\ W/m^2$ at all times of a typical day. With this information it is possible to state that the upper canopy will emit heat during the day to the lower canopy levels, and will receive heat during the night from these same levels. Therefore, it is expected that in the early morning when the sunshine begins, the canopy top will warm up and only after some time the canopy inside will receive heat from the top, in the late afternoon the process is reversed.

The downward H cycle during the daytime period at the height of $22.1m$ shows a very irregular behavior compared to the H cycle above the canopy. It is possible to observe that at this height the H values alternate between positive and negative values (Figure 6 c). This behavior evidences the complexity of the exchange mechanisms that occur between the forest and the atmosphere, even during the day, when the atmospheric turbulence is quite developed, a certain level inside the canopy can change scales with its lower part and an instant of time later with the atmosphere above. It is worth mentioning here the results of Shuttleworth et al. (1984a), one of the pioneers in the analysis of turbulent time series above and within the

Amazon forest. According to them the lower 2/3 of the forest canopy is almost always decoupled from the higher levels. This decoupling between the two air layers above and within the canopy intensifies when there is a decrease in turbulent activity above the canopy and consequently the radiative processes in the lower layer near the forest floor and between the inner layers of the vegetation are responsible for the equilibrium of the thermal balance.

3.4. Turbulent kinetic energy dissipation rate

The momentum absorption by the forest canopy occurs due to the impact of the flow against the vegetation structure, thus generating turbulent mats and consequently converting turbulent kinetic energy (TKE) into heat. Therefore, with the TKE loss rate, i.e., the TKE dissipation rate (ε) can be calculated for different levels inside and above the forest canopy and for different atmospheric stability conditions (daytime and nighttime, Figure 7).

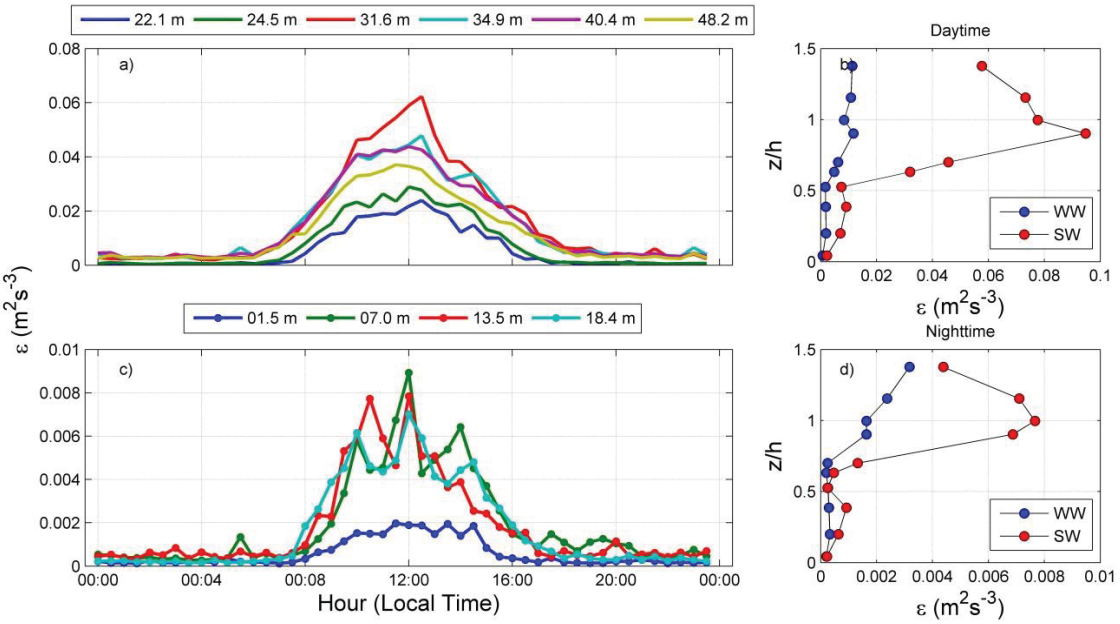

Figure 7. ε diurnal cycle in a and c. Vertical ε profile for weak and strong wind conditions during daytime (b) and nighttime (d) periods.

The ε diurnal cycle is strongly affected by the solar radiation diurnal cycle (Figures 7 a and c) with the peak, at each height, occurring in the period of greatest sunshine. Such peaks occur even at heights where little direct solar radiation is able to penetrate, although the ε

magnitude drops drastically at heights below $0.5h$ (Figures 7a and c). During SW conditions ε values tend to be higher than when WW occur, mainly above $0.5h$ and $0.75h$ for both daytime and nighttime periods, respectively (Figures 7 b and d). This result corroborates previous findings (Dias-Júnior et al. 2017) that indicated ε values change in a magnitude of at least an order of magnitude higher during nighttime periods when the wind speed exceeded $3.0\ m/s$ (turbulent regime 2), compared to periods where the wind was below this threshold (turbulent regime 1).

The vertical ε profiles for SW conditions have a rather pronounced maximum a little below at $z = h$ during the daytime and at $z = h$ during the nighttime period (Figures 7b and d, respectively). On flat surfaces the TKE dissipation rate is often larger near the surface and then decreases with the height at the surface layer (Stull 1988). As previously mentioned, due to the vegetation structure, little turbulence can penetrate the forest canopy, so the higher ε values were observed near the canopy top. In addition, according to (Stull 1988) the higher dissipation rates are often found where the TKE production is also higher.

4. Conclusions

The turbulence structure of two experimental sites in the Amazon was studied in this work. The most important turbulence statistics of these sites were compared with those obtained by KJ2000 for two other sites. The new data added more information from these statistics from below and above the forest crown. The studied sites presented significant differences in the efficiency of absorbing momentum from atmospheric flow, probably due to small differences in the vegetation structure of each site. The mentioned efficiency is higher during strong winds and the turbulence reaches deeper layers of the canopy in this condition. It was verified that the turbulence generated above the canopy hardly penetrates the region below $0.5h$ and between $0.5h > z < h$ the turbulence is quite intermittent and dominated by sweeps.

The sensible heat flux is not constant with the height, especially under strong wind conditions, which affects the assumptions of the Monin-Obukhov similarity theory and reinforces the indication of previous works that such a theory does not apply to the roughness sublayer above the Amazon rainforest. The highest H values were also observed during strong wind conditions for both daytime and nighttime periods. The H diurnal cycle at different heights below the canopy is quite variable, and at some times the flow passes from positive to

negative even during the day, evidencing the complexity of the scalar exchange between the forest and atmosphere.

Using turbulence power spectrum properties the diurnal cycle at different heights and the TKE dissipation rate the profile was calculated. The behavior of this variable follows the diurnal radiation cycle, with maximum values at each height close to the periods of greatest sunshine. Under strong wind conditions, the ε profile presents a maximum near the top of the canopy. This result reflects the observation that higher dissipation rates are often found where TKE production values are also higher.

Acknowledgements

The first author thanks CAPES for the PhD grant awarded through the Programa de Pós-graduação em Clima e Ambiente and the Universidade Federal do Oeste do Pará (UFOPA) for the partial release (20 hours a week), which allowed for the accomplishment of this work. The authors would like to thank all the development and teaching and research institutions that provided financial and human resources to obtain the data of this study, namely: Fundação de Amparo à Pesquisa do Estado do Amazonas (FAPEAM), Fundação de Amparo à Pesquisa do Estado de São Paulo (FAPESP), Universidade do Estado do Amazonas (UEA), Instituto Nacional de Pesquisas da Amazônia (INPA) e Programa de Grande Escala da Biosfera-Atmosfera na Amazônia (LBA).

Bibliography

Acevedo, O.C. & Fitzjarrald, D.R., 2003. In the core of the night – effects of intermittent mixing on a horizontally heterogeneous surface. *Boundary-Layer Meteorology*, 106, pp.1–33.

Andreae, M.O. et al., 2015. The Amazon Tall Tower Observatory (ATTO): Overview of pilot measurements on ecosystem ecology, meteorology, trace gases, and aerosols. *Atmospheric Chemistry and Physics*, 15(18), pp.10723–10776.

Antonia, R.A., 1981. Conditional Sampling Measurement. *Annual Review of Fluid Mechanics*, 13(d), pp.131–156.

Araújo, A.C. et al., 2002. Comparative measurements of carbon dioxide fluxes from two nearby towers in a central Amazonian rainforest: The Manaus LBA site. *Journal of*

Geophysical Research, 107, pp.1–20.

Baldocchi, D. & Meyers, P., 1988. Turbulence structure in a deciduous forest. *Boundary-Layer Meteorology*, 43, pp.345–364.

Bolzan, M.J.A. & Vieira, P.C., 2006. Wavelet Analysis of the Wind Velocity and Temperature Variability in the Amazon Forest. *Brazilian Journal of Physics*, 36(4), pp.1217–1222.

Chamecki, M., 2013. Persistence of velocity fluctuations in non-Gaussian turbulence within and above plant canopies. *Physics of Fluids*, 25(11).

Chor, T.L. et al., 2017. Flux-variance and flux-gradient relationships in the roughness sublayer over the Amazon forest. *Agricultural and Forest Meteorology*, 239, pp.213–222. Available at: http://dx.doi.org/10.1016/j.agrformet.2017.03.009.

Dias-Júnior, C.Q. et al., 2013. Coherent structures detected in the unstable atmospheric surface layer above the Amazon forest. *Journal of Wind Engineering and Industrial Aerodynamics*, 115, pp.1–8.

Dias-Júnior, C.Q., Luís Dias, N., et al., 2017. Convective storms and non-classical low-level jets during high ozone level episodes in the Amazon region: An ARM/GOAMAZON case study. *Atmospheric Environment*, 155, pp.199–209.

Dias-Júnior, C.Q., Sá, L.D.A., et al., 2017. Turbulence regimes in the stable boundary layer above and within the Amazon forest. *Agricultural and Forest Meteorology*, 233, pp.122–132. Available at: http://dx.doi.org/10.1016/j.agrformet.2016.11.001.

Dias-Júnior, C.Q., Marques Filho, E.P. & Sá, L.D.A., 2015. A large eddy simulation model applied to analyze the turbulent flow above Amazon forest. *Journal of Wind Engineering and Industrial Aerodynamics*, 147, pp.143–153. Available at: http://dx.doi.org/10.1016/j.jweia.2015.10.003.

Dupont, S. & Patton, E.G., 2012. Influence of stability and seasonal canopy changes on micrometeorology within and above an orchard canopy: The CHATS experiment. *Agricultural and Forest Meteorology*, 157, pp.11–29. Available at: http://dx.doi.org/10.1016/j.agrformet.2012.01.011.

Dupont, S. & Patton, E.G., 2012. Momentum and scalar transport within a vegetation canopy following atmospheric stability and seasonal canopy changes: The CHATS experiment. *Atmospheric Chemistry and Physics*, 12(13), pp.5913–5935.

Finnigan, J., 2000. Turbulence in plant canopies. *Annu. Rev. Fluid Mech.*, 32, pp.519–571.

Fitzjarrald, D.R. et al., 1990. Daytime turbulent exchange between the Amazon forest and the atmosphere. *Journal of Geophysical Research: Atmospheres*, 95(D10), pp.16825–16838.

Available at: http://onlinelibrary.wiley.com.ezaccess.libraries.psu.edu/doi/10.1029/JD095iD10p16825/abstract%5Cnhttp://onlinelibrary.wiley.com.ezaccess.libraries.psu.edu/store/10.1029/JD095iD10p16825/asset/jgrd1658.pdf?v=1&t=hqo99iy3&s=de2805634c3f9dc537af9c1a7aefb80baad.

Fitzjarrald, D.R. et al., 1988. Turbulent transport observed just above the Amazon forest. *Journal of Geophysical Research*, 93(D2), p.1551. Available at: http://dx.doi.org/10.1029/JD093iD02p01551.

Fitzjarrald, D.R. & Moore, K.E., 1990. Mechanisms of nocturnal exchange between the rain forest and the atmosphere. *Journal of Geophysical Research: Atmospheres*, 95(D10), pp.16839–16850. Available at: http://onlinelibrary.wiley.com.ezaccess.libraries.psu.edu/doi/10.1029/JD095iD10p16839/abstract%5Cnhttp://onlinelibrary.wiley.com.ezaccess.libraries.psu.edu/store/10.1029/JD095iD10p16839/asset/jgrd1659.pdf?v=1&t=hqo8tmps&s=83093cd151da7fecce29b4966cbffa60550.

Freire, L.S. et al., 2017. Turbulent mixing and removal of ozone within an Amazon rainforest canopy. *Journal of Geophysical Research: Atmospheres*, 122(5), pp.2791–2811.

Fuentes, J. et al., 2016. Linking meteorology, turbulence, and air chemistry in the Amazon rainforest during the GoAmazon project. *Bulletin of the American Meteorological Society*, p.in review.

Gerken, T. et al., 2016. Downward transport of ozone rich air and implications for atmospheric chemistry in the Amazon rainforest. *Atmospheric Environment*, 124(January 2016), pp.64–76.

Gloor, M. et al., 2012. The carbon balance of South America : a review of the status , decadal trends and main determinants. *Biogeosciences*, 9, pp.5407–5430.

Kaimal, J.C. et al., 1972. Spectral characteristics of surface-layer turbulence. *Quarterly Journal of the Royal Meteorological Society*, 98(417), pp.563–589.

Kaimal, J.C. & Finnigan, J.J., 1994. *Atmospheric Boundary LayerFlows - Their Structureand Measurement*, New York.: Oxford University Press.

Katul, G. et al., 1997. the Ejection-Sweep Character of Scalar Fluxes in the Unstable Surface Layer. *Boundary-Layer Meteorology*, 83(1), pp.1–26. Available at: http://link.springer.com/article/10.1023/A:1000293516830.

Kruijt, B. et al., 2000. Turbulence statistics above and within two Amazon rain forest canopies. *Boundary-Layer Meteorology*, 94(2), pp.297–331.

Launiainen, S. et al., 2007. Vertical variability and effect of stability on turbulence characteristics down to the floor of a pine forest. *Tellus*, 59(5), pp.919–936.

Lima, N., 2014. *Sobre as características de formação de estrutura coerente e turbulência em uma floresta densa de terra firme com medidas em até 80m de altura: Projeto ATTO-CLAIRE / IOP - 1 - 2012*. Instituto Nacional de Pesquisas da Amazônia.

Lu, C.-H. & Fitzjarrald, D.R., 1994. Seasonal and diurnal variations of coherent structures over a deciduous forest. *Boundary-Layer Meteorology*, 69, pp.43–69.

Lumiley, J.L. & Panosky, H.A., 1964. *The Structure Of Atmospheric Turbulence*, New York: Interscience Publishers.

Malhi, Y. et al., 2002. Energy and water dynamics of a central Amazonian rain forest. *Journal of Geophysical Research Atmospheres*, 107(20), pp.1–17.

Marques Filho, A.O., Dallarosa, R.G. & Pachêco, V.B., 2005. Radiação solar e distribuição vertical de área foliar em floresta Reserva Biológica do Cuieiras ZF2, Manaus. *Acta Amazônica*, 35(4), pp.427–436. Available at: http://acta.inpa.gov.br/fasciculos/35-4/BODY/v35n4a06.html.

Molion, L.C.B., 1987. On the dynamic climatology of the Amazon Basin and associated rain-producing mechanisms. In R. E. Dickinson, ed. *In Geophysiology of Amazonia*. pp. 391–407.

Poggi, D. et al., 2004. The effect of vegetation density on canopy sub-layer turbulence. *Boundary-Layer Meteorology*, 111(3), pp.565–587.

Von Randow, C. et al., 2008. Exploring eddy-covariance and large-aperture scintillometer measurements in an Amazonian rain forest. *Agricultural and Forest Meteorology*, 148(4), pp.680–690.

Raupach, M.R., Finnigan, J.J. & Brunei, Y., 1996. Coherent eddies and turbulence in vegetation canopies: The mixing-layer analogy. *Boundary-Layer Meteorology*, 78(3–4), pp.351–382.

Raupach, M.R. & Thom, A.S., 1981. Turbulence in and above plant canopies. *Annual Review of Fluid Mechanics*, 13(1), pp.97–129.

Santana, R.A.S. de et al., 2015. Estabilidade e estrutura da turbulência sob a influência de jatos de baixos níveis noturnos no sudoeste da Amazônia. *Revista Brasileira de Meteorologia*, 30(4), pp.405–414.

Santana, R.A.S. de et al., 2017. Observing and Modeling the Vertical Wind Profile at Multiple Sites in and above the Amazon Rain Forest Canopy. *Advances inMeteorology*, 2017, p.8.

Santos, A.B. et al., 2013. Dinâmica do Escoamento de Ar Acima e Dentro de uma Floresta Tropical Densa sobre Terreno Complexo na Amazônia. *Revista Brasileira de Geografia Física*, 6(2), pp.308–319.

Santos, D.M. et al., 2016. Temporal Scales of the Nocturnal Flow Within and Above a Forest Canopy in Amazonia. *Boundary-Layer Meteorology*, pp.1–26.

Shuttleworth, W.J. et al., 1984a. Eddy correlation measurements of energy partition for Amazonian forest. *Quarterly Journal of the Royal Meteorological Society*, 110, pp.1143–1162.

Shuttleworth, W.J. et al., 1984b. Observations of radiation exchange above and below Amazonian forest. *Quarterly Journal of the Royal Meteorological Society*, 110, pp.1163–1169.

Stull, R.B., 1988. *An introduction to boundary layer meteorology*, Dordrecht: Kluwer Academic Publishers.

Sun, J. et al., 2012. Turbulence Regimes and Turbulence Intermittency in the Stable Boundary Layer during CASES-99. *Journal of the Atmospheric Sciences*, 69(1), pp.338–351. Available at: http://journals.ametsoc.org/doi/abs/10.1175/JAS-D-11-082.1.

Thomas, C. & Foken, T., 2007. Flux contribution of coherent structures and its implications for the exchange of energy and matter in a tall spruce canopy. *Boundary-Layer Meteorology*, 123(2), pp.317–337.

Tóta, J. et al., 2008. Amazon rain forest subcanopy flow and the carbon budget: Santarém LBA-ECO site. *Journal of Geophysical Research: Biogeosciences*, 114(1), pp.1–15.

Tóta, J., Roy Fitzjarrald, D. & da Silva Dias, M.A.F., 2012. Amazon Rainforest Exchange of Carbon and Subcanopy Air Flow: Manaus LBA Site—A Complex Terrain Condition. *The Scientific World Journal*, 2012, pp.1–19. Available at: http://www.hindawi.com/journals/tswj/2012/165067/.

Vickers, D. & Mahrt, L., 1997. Quality Control and Flux Sampling Problems for Tower and Aircraft Data. *Journal of Atmospheric and Oceanic Technology*, 14, pp.512–526.

Capítulo III

Santana, Raoni Aquino Silva de; Tóta, Júlio; et al. Comparing the air turbulence above smooth and rough surfaces in the Amazon. Manuscrito em preparação para Meteorological Applications.

.

Comparing the air turbulence above smooth and rough surfaces in the Amazon

Abstract

The goal of this work is to compare the main air turbulence characteristics of two common areas in the Amazonian landscape: a dense forest (rough surface) and a water surface (smooth surface). Using wind components data collected at high frequency by sonic anemometers located just above these surfaces turbulence intensity, temporal and length scales of the largest eddies, turbulence power spectra, as well as the main terms of the TKE budget (TKE = turbulent kinetic energy) were evaluated for each surface type. The results showed that in general the air turbulence intensity above the forest was higher than above the lake during the daytime, due to the high efficiency of the forest in absorbing momentum of the turbulent flow. During the nighttime the situation was reversed, with greater air turbulence intensity above the lake, except in some periods in which intermittent turbulence bursts occur above the forest. The horizontal (Λ_u) and vertical (Λ_w) eddies scales calculated during the daytime period were higher above forest than above the lake, and the vertical length scale (L_w) was also larger over the forest, but the horizontal length scale (L_u) was higher above lake. The composites of the vertical velocity power spectra obtained for the daytime and nighttime periods for each site showed canonical behavior, with a well-defined inertial subdomain region, except in the nighttime period above the forest. Finally, shear production was the dominant term of the TKE budget equation during the daytime period at both sites. All terms calculated in this work at night showed values close to zero on the lake, indicating that the terms that could not be calculated, such as the TKE advection, may have contributed to maintenance of turbulence overnight at this site.

Keywords: Turbulence; Forest; Lake.

1. Introduction

The Amazon region is known worldwide for its water resources and the great diversity of its ecosystems, such as dense forest lands, flooded forests, floodplains, igapós, and open and closed fields. The region, during the high water period (May - June), has a flooded area of 350,000 km^2, or about 20% of the volume of the mainstream (Richey et al. 2002). Between August 2015 and July 2016, the Amazon lost 7,989 km^2 of forest, the highest rate since 2008, according to a survey by the Amazon Environmental Research Institute (IPAM, Azevedo et al. (2017)).

Turbulence processes in the atmospheric surface layer play a major role in the transport of momentum, sensible and latent heat in the atmosphere (Arya 2001), particularly in the surface layer where the turbulent fluxes are essential for mediating atmosphere-surface interactions. The behavior of turbulence above the Amazon rainforest has been intensively studied (Fitzjarrald et al. 1990; Fitzjarrald & Moore 1990; Kruijt et al. 2000; Santos et al. 2016; Dias-Júnior et al. 2017; Chor et al. 2017; Freire et al. 2017) more than on the surface of water (Sheppard et al. 1972; Garratt 1972; Fairall et al. 1996; Edson & Fairall 1998; Marques Filho et al. 2008), and therefore the surface layer turbulent structures on horizontally homogeneous surfaces are yet well known (Kaimal & Wyngaard 1990).

However, few observational studies of the turbulent spectra above the canopy in forest environments have been published, especially in the tropical rainforest (Moraes et al. 2008), and there are fewer still that have been conducted studying the air turbulence over lakes. The spectra at the top of the canopy differs from the spectra found for flat surfaces due to wake and wave effects over the canopy (Kaimal & Finnigan 1994). Studies show that the spectral curves are more peaked, a possible indication that some variance is being lost due to the interaction of the wind flow with the canopy for frequencies in the inertial subrange (Anderson et al. 1986; Lee 1996; Moraes et al. 2008). Fitzjarrald et al. (1990) observed the −2/3 inertial subrange above and within the Amazon forest canopy.

Most of these studies have been conducted over land, and only occasional spectra and cospectra from eddy-covariance measurements of greenhouse gases measurements over sea have been presented (Ohtaki et al. 1989; McGillis et al. 2001; Sahlée et al. 2008). Studies of Sahlée et al. (2014) taken at a Swedish lake show that the turbulence structure was highly influenced by the surrounding land during daytime and the variance spectra of both horizontal velocity and scalars during both unstable and stable stratification displayed a low frequency

peak. Turbulence spectra obtained from water side measurements from ADV (Acoustic Doppler Velocimeter) in a shallow estuary followed the general shape of the Kaimal et al. (1972) curves and turbulent power laws; however, the curves were all shifted toward higher frequencies and spectral lags effects (Walter et al. 2011).

The goal of this work is to compare the main characteristics of the air turbulence of two common areas in the Amazonian landscape: a dense forest (rough surface) and a water surface (smooth surface). Using data from the wind components collected at high frequency, turbulence intensity, temporal and length scales of the largest vortices, turbulence power spectra, as well as the main terms of the turbulent kinetic energy budget were evaluated for each surface type. These areas contribute significantly to the total energy, mass and momentum budget in this region. The differences highlighted in this study are very useful for modeling processes concerning parameterizations above surfaces with different roughness.

2. Material and Methods

2.1. Study area

The data were collected in two sites located in the Brazilian Amazon. The first site was K34 located in the Cuieiras Biological Reserve - Manaus (AM) and the second at the Curuá-Una Hydroelectric Power Plant located in Santarém (PA) (Figure 1). The Cuieiras Biological Reserve is located in the Rio Negro Environmental Preservation Area - Setor Sul - Rio Cuieiras is approximately 80 km north of Manaus and comprises about 10 thousand ha (02º36'33 "S and 60º12'33" W) (Araújo et al. 2002). It is an undisturbed area with primary lowland vegetation and is in the Igarapé Asu watershed. This area is reserved for ecological, botanical and meteorological surveys. The Curuá-Una dam ('Dark River' in Tupi-Guarani) is located in the Lower Amazon River Basin (41.531,51 km^2) in the Curuá-Una River, at the waterfall Palhão (2°50' S and 54°18' W), 70 km southeast of Santarém, in Pará State. The Curuá-Una hydropower plant was the second to be built in the Amazon and the reservoir was filled in 1977, occupying an area of 72 km^2 at the operational level, has 30.3 MW capacity, and is 68 m above sea level (Fearnside 2005). Eletronorte is working on a plan to expand the generation capacity of the Curuá-Una Hydropower Plant up to 40.3 MW.

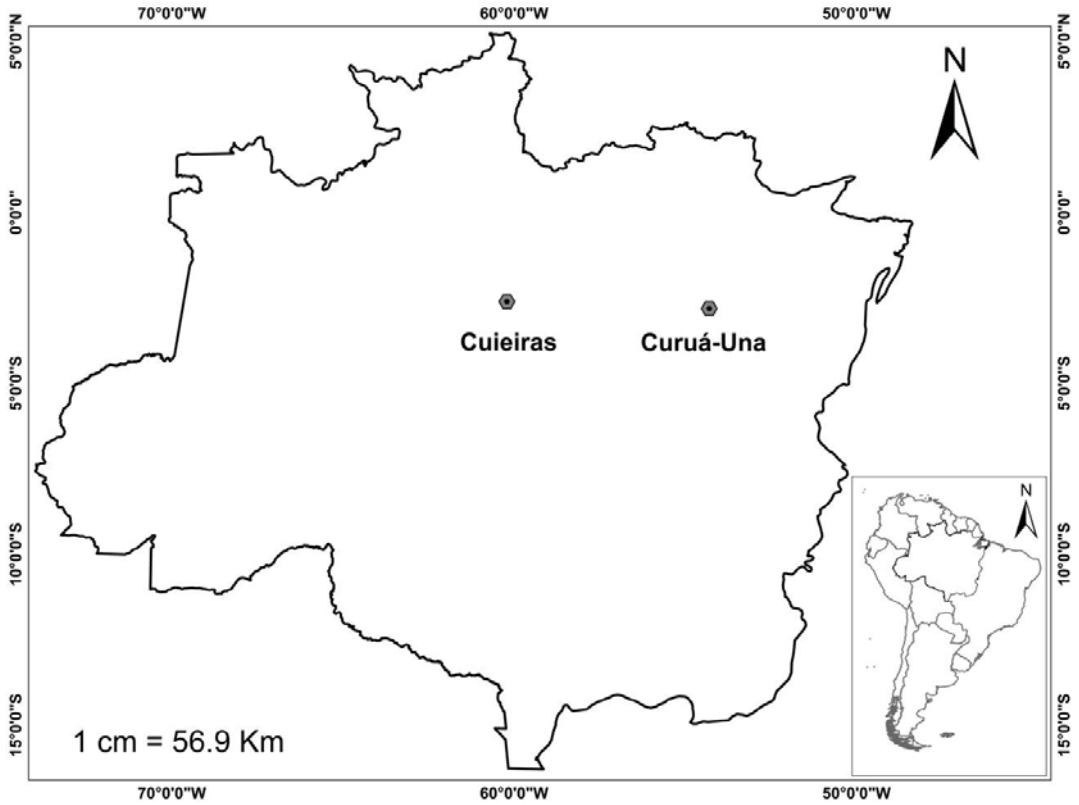

Figura 1. Map with the location of two study sites: Cuieiras (dense forest) near Manaus (AM) and Curuá-Una (lake) near Santarém (PA), both located in the Amazon region.

2.2. Data

At the K34 site, 10 three-dimensional sonic anemometers (CSAT3 model, Campbell 128 Scientific Inc., Logan, UT) were arranged from 1.5 to 48.2 m above ground during the period from April 2014 to January 2015, as part of the GoAmazon project (Fuentes et al., 2016). The data used in this work corresponds to the three highest sonic anemometers, one at the canopy height ($35\ m$) and two others installed at 40.4 and 48.2 m above the forest floor. The wind components and the virtual sonic temperature data were collected at a rate of 20 Hz.

Data from the Curuá-Una (CU) site were collected from a fluctuating micrometeorological platform with shape of a regular pentagon, four anchor points, and a nearby floating power supply platform (Vale (2016)). The floating micrometeorological platform is equipped with high and low frequency sensors for both water and air measurements. In this study we used data from the high frequency system (10 Hz) to measure the flux (open path EC 150 – Campbell Scientific, Inc.). The system consists of a gas analyzer that measures the absolute densities of CO_2 and H_2O, a sonic anemometer (CSAT3A -

Campbell Scientific, Inc), which measures the orthogonal components of the wind, and a thermometer, which determines the air temperature sonically. The system is 3 m above the surface of the water. Complementarily, data from two two-dimensional sonics (WindSonic, Gill Instruments Ltd, UK), which provide wind speed and direction at 4 Hz rate, were used. These sonics were installed in 1.5 and 4.5 m on the floating buoy structure.

2.3. Metodology

In order to minimize the effects of rain on measures of turbulence, measurements were conducted in the month of September, the month which presents the lowest rainfall values for the region. Four days of data were used in each experimental site (September 13 to 16, 2014 for the K34 site and September 15 to 18, 2015 for the CU site). The days were chosen based on the continuity of measurements at each site.

To describe the atmospheric turbulent flow at the K34 and CU sites, data were calculated in intervals of 30 minutes, and the following equations were used: the wind speed $U = \sqrt{u^2 + v^2}$, where u and v are the zonal and meridional wind components, respectively; the vertical velocity (w) standard deviation, $\sigma_w = \sqrt{(w')^2}$; friction velocity, $u_* = \sqrt{(\overline{u'w'})^2 + (\overline{v'w'})^2}$; the drag coefficient, $C_D = \frac{u_*^2}{U^2}$ (Mahrt et al. 2000; Fitzjarrald et al. 1988); and local free convection velocity scale, $w_{Lf} = [(g/\theta_V).\overline{w'\theta_V'}.z]^{1/3}$.

The horizontal (Λ_u) and vertical (Λ_w) integral scales of the largest eddies were also calculated, based on the u and w correlograms, respectively. Figure 2 shows an example of how such scales were obtained. After obtaining the autocorrelation according to the equation:

$$r_x(\xi) = \frac{\overline{x(t)x(t+\xi)}}{\sigma_x^2}$$

where $x = u, w$; ξ is the time lag with respect to time, the values of the integral scales will be numerically equal to the area under the curve in the interval between $t = 0$ and t for the first r root, i.e., where the curve touches the abscissa axis for the first time (Kaimal & Finnigan 1994, Kundu and Cohen, 2002).

Therefore,

$$\Lambda_x = \int_0^\infty r_x(\xi)\, d\xi$$

Using the Taylor hypothesis we obtained the length scales of the largest eddies, $L_x = U\Lambda_x$.

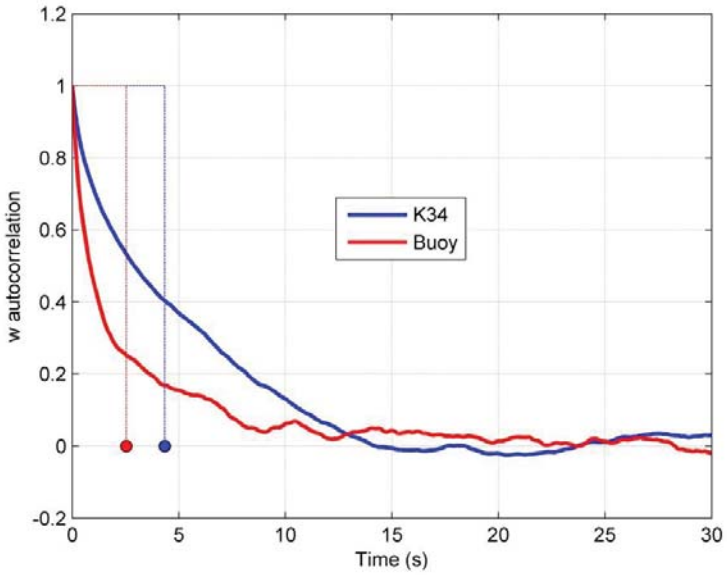

Figure 2. Correlogram of the vertical velocity. Each curve refers to 30 minutes data from both sites. The circles represent the Λ_w values for both CU (red) and K34 (blue) sites. Such values are numerically equal to the areas formed under the curves of each site.

Using the fast fourier transform (FFT) the w power spectra of the wind vertical (S_w) and horizontal (S_u) velocities were obtained. From S_u and assuming the applicability of the Taylor's hypothesis as well as the spectral properties established by Kolmogorov, the turbulent kinetic energy (TKE) dissipation rate was calculated according to the equation:

$$\varepsilon = \frac{2\pi f^{5/2} S_u^{3/2}}{U\alpha^{3/2}}$$

Where f is the frequency; S_u is the u power spectra; e $\alpha = 0.55$ is Kolmogorov's constant (Kaimal et al. 1972; Kaimal & Finnigan 1994). In order to select only values of S_u that were inside the inertial subrange, we used values of the frequency range $1.0 > f < 2.5$ Hz (Dias-Júnior et al. 2016).

In addition to ε, two other TKE budget equation terms were calculated: buoyancy, $(g/\bar{\theta}_V)\,\overline{\theta_V' w'}$, where g is the acceleration of gravity and θ_V virtual potential temperature, and wind shear production, $\overline{u'w'}\,\frac{\partial U}{\partial z}$, where z is the height.

3. Results and Discussion

In general the turbulence intensity in the atmospheric boundary layer (ABL) presents its highest values close to the surface (Stull 1988), since momentum is extracted from the flow at this surface. The results presented in Figure 3 show that the way the flow interacts with the surface differs greatly between the rough surface, above the K34 forest canopy, and the smooth surface, above the CU lake.

The wind regime showed strong differences during the four days of observation at each site. The behavior of the diurnal cycle of the expected wind speed in CLA is that it presents low values during the night, due to the negative net radiation, and increases gradually during the day following the radiation diurnal cycle. The U cycles were quite regular on the lake during the studied period, different from those observed over the forest canopy. In addition, the wind velocity values observed during the daytime were higher above lake than above the forest (Figure 3), even though the measurement height of this variable on the lake was closer to the surface (3 m in CU and 5 m above in the K34 canopy), and considering that the wind is expected to increase with increasing height in the surface layer (Kaimal & Finnigan 1994; Yi 2008; Santana et al. 2017).

Figures 3d and 3e show the σ_w and u_* time series, respectively. The behavior of these variables shows that although the wind speed is higher above the lake during the day, the turbulence intensity is much higher over the forest in this period. The σ_w values close to midday were about twice those over the forest than over the lake. This behavior reflects the ability of each surface to absorb momentum from the atmospheric flow. During the night the situation is reversed, although the turbulence intensity above the lake is weak, it is greater than above the forest, except in moments of intermittent turbulence bursts (Oliveira et al. 2013; Santos et al. 2016; Dias-Júnior et al. 2017; Freire et al. 2017), which are apparently more frequent above the forest. Far from these moments of intermittent events the σ_w values were very close to zero above the forest during the nighttime period.

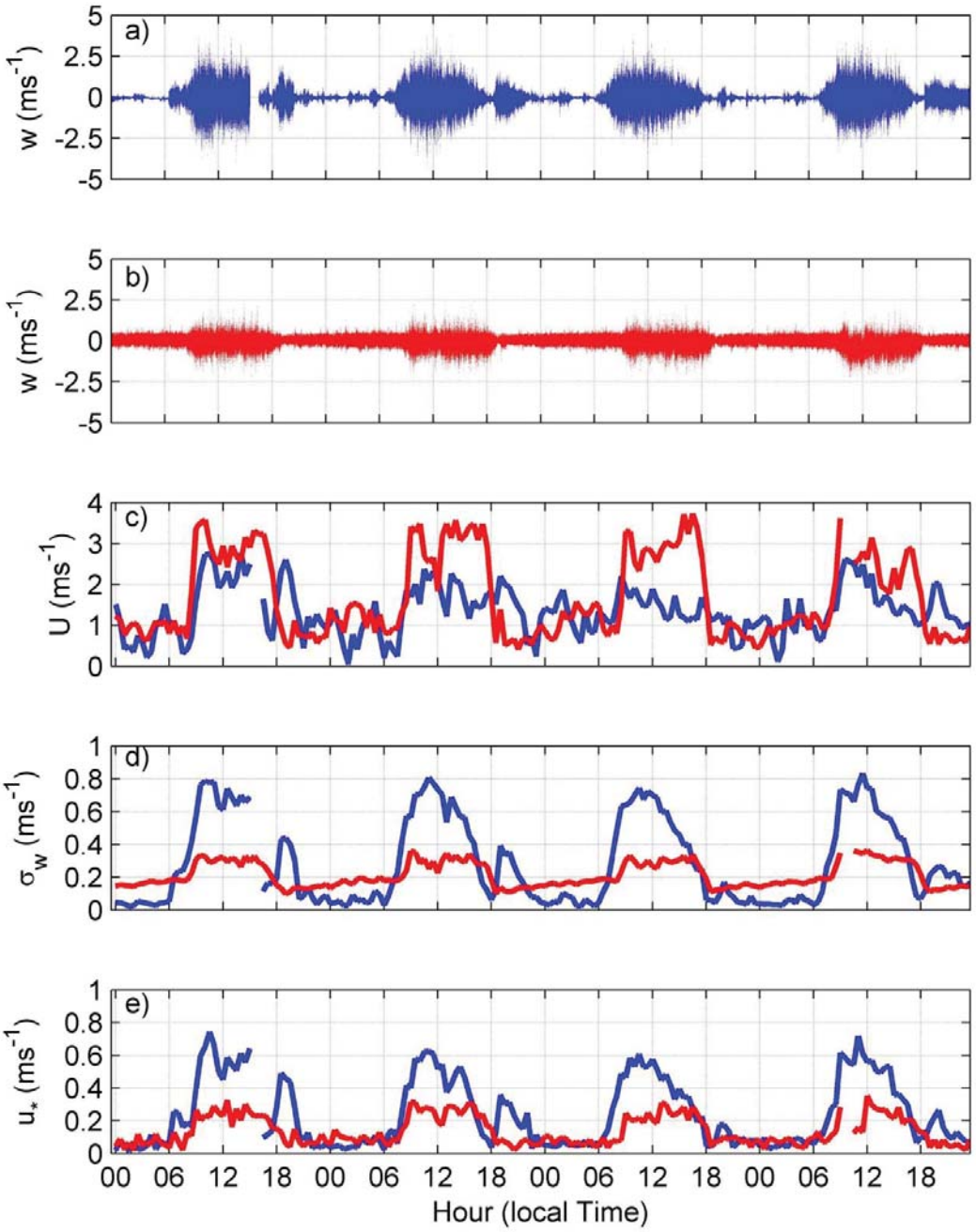

Figure 3. Time series of the *w* wind component (a and b), mean wind (c), *w* standard deviation (d) and friction velocity (e) for K34 (blue) and CU (red) sites.

Many parametrizations of atmospheric models or questions involving the turbulence closure make it necessary to know the time and length scales of the largest eddies in the ABL. Table 1 lists these scales calculated during the daytime period on the of K34 and CU sites, since the turbulence is more developed during this period at both sites. One variable that is

used precisely to quantify drag at a surface in a fluid environment is the drag coefficient. This variable presented values eight times higher above the forest than above the lake. The integral scales of the horizontal (Λ_u) and vertical (Λ_w) wind components, which can be understood in this case (measured at a single point during a certain period of time), as the time in these series needed to maintain a significant correlation with itself (Lumiley & Panosky 1964; Shaw et al. 1995). The integral scales presented higher values at the forest than those observed at the lake; however, such difference is more expressive in Λ_w, considering that the variability Λ_u at the lake was great.

The limiting condition of $u_* \to 0$ for the unstable ABL is usually referred to as free convection, where all turbulent energy is generated by buoyancy forces and where the mean horizontal wind vanishes (Businger 1973). Because the ABL vertical structure data were not available for both sites, and direct measurements of the ABL height have not been performed, we chose to use a local free convection velocity scale (w_{LF}) instead of a convective velocity scale (w_*) (Table 1). Furthermore, turbulence in the surface layer might be influenced by the ground more than the influence of the capping inversion, therefore, z_i is not a relevant parameter, but z is (Stull 1988). These conditions may be considered local free convection (Tennekes 1970; Wyngaard et al. 1971; Businger 1973).

The value of w_{LF} during the day (night) was higher (lower) for K34 (Table 1). However, when the daytime and nighttime periods are compared for the same site, the value of w_{LF} for K34 shows an inversion in its magnitude, while CU has practically the same magnitude. The inversion of w_{LF} in K34 occurs due to the radiative cooling at the forest canopy and consequently $\overline{w'\theta_v'} < 0$. On CU, the daily temperature gradient is less than 1 ° (while in K34 it is 9.5 °), presenting $\overline{w'\theta_v'} > 0$, even for the nighttime (Vale, 2016).

From the values of the time scales the length scales of the largest eddies were obtained assuming the validity of Taylor's hypothesis, with the recognition that such hypothesis is not always valid for forest areas, where, for the standard deviation of the mean wind velocity (σ_u), the relation $\sigma_U < 0.5U$ is rarely observed (Shaw et al. 1995). The L_u and L_w values obtained for the forest were comparable to those found by Kruijt et al. (2000) for forest canopy in the Amazon. Taking the average height of the forest canopy at K34 ($35\ m$) (Fuentes et al., 2016), the values of these length scales fit the pattern observed by Raupach et al. (1996), who observed $L_u \approx h$ e $L_w \approx h/3$, studying different canopies. The L_w value above the lake was lower than over the forest, but the same result does not happen with L_u, which is greater

above the lake. Measurements of these variables on lakes are scarce, considering the difficulty of making measurements using the eddy covariance technique over this surface (Vesala et al. 2012).

Table 1. Time and length scales of the turbulent flow in the atmospheric boundary layer for the K34 and CU site. The variables are: drag coefficient (C_D), integral scale of the horizontal (Λ_u) and vertical (Λ_w) component of the wind, scale length of turbulent vortices for horizontal (L_u) and vertical wind component (L_w) and local free convection velocity scale for day (w_{LFD}) and night (w_{LFN}).

	K34	**CU**
C_D	0.08 ± 0.03	0.01 ± 0.005
Λ_u(s)	18.3 ± 15.6	16.6 ± 20.9
Λ_w(s)	6.0 ± 2.7	3.5 ± 2.4
L_u(m)	35.2 ± 28.2	$48.0 + 60.8$
L_w(m)	11.1 ± 3.2	9.3 ± 5.4
w_{LFD}(m/s)	0.0068 ± 0.0039	0.0006 ± 0.00031
w_{LFN}(m/s)	-0.00015 ± 0.00029	0.00073 ± 0.00021

The time and length scales calculated above refer to the scales of the largest vortices (Lumiley & Panosky 1964; Kaimal & Finnigan 1994). However, the turbulent flow in the ABL encompasses different sized eddies, which distinctly contribute to total kinetic energy of the flow (Stull 1988), and the power spectrum in function of the frequency is a variable which describes such characteristics (Stull 1988). In Figure 4 shows composites of the w power spectra for the K34 and CU sites obtained during the daytime and nighttime periods at each site. The behavior of these spectra present considerable differences between the sites and even between the periods studied in a given site.

It is well documented and consolidated in the literature that the spectra of the wind velocity components when plotted as a function of frequency have a linear decay region with a coefficient of $-5/3$, called Kolmogorov's five-third law of spectrums (Kundu & Cohen 2002). In this region, called inertial subrange, energy is neither produced or dissipated but handed down to smaller and smaller scales (Kaimal & Finnigan 1994). At the K34 site this region is well defined during the daytime and starts at $f \cong 10^{-1.9} \cong 0.013\,Hz$, thus

continuing to higher frequencies (Figure 4a). On the other hand, during the night period said decay only appears from $f > 1\ Hz$ (Figure 4b)

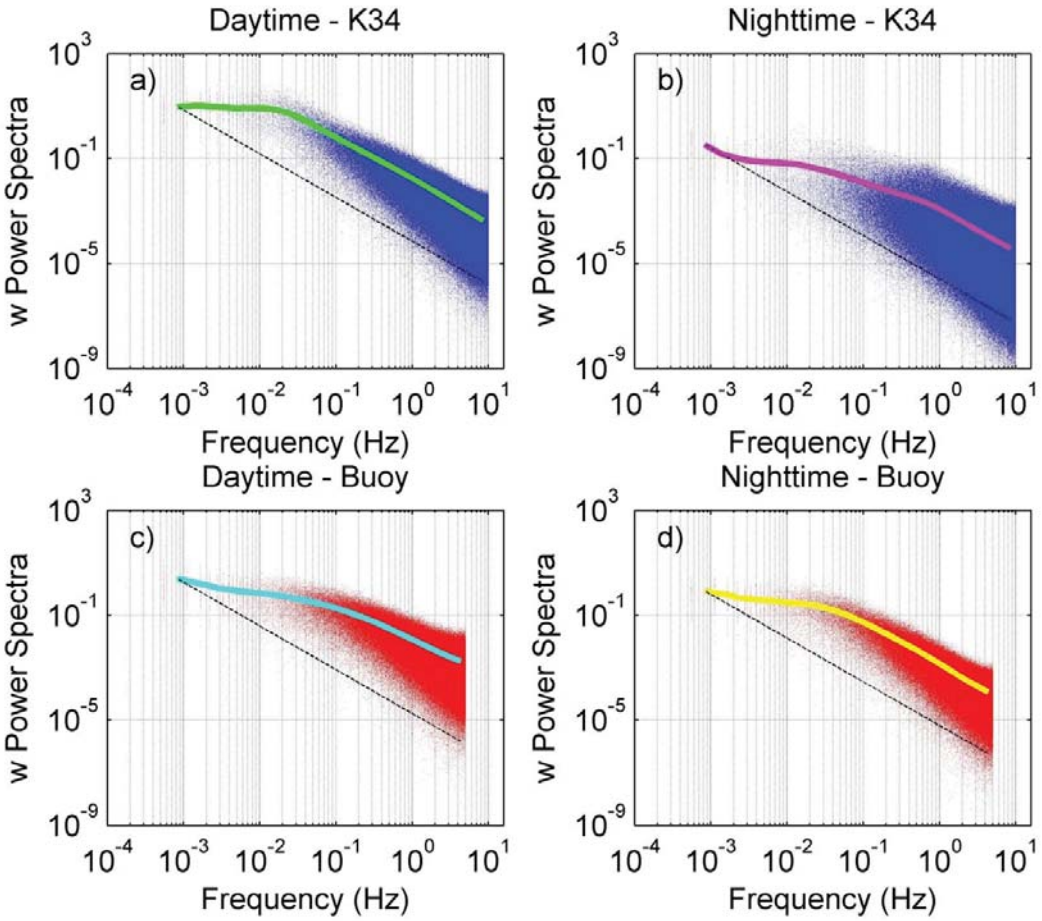

Figure 4. Power spectra of the vertical wind component to the K34 (4a and 4b) and CU (4c and 4d) sites for the daytime and nighttime, respectively.

Moraes et al. (2008) studying the turbulence spectra and cospectra in two areas in the Amazon (one with forest and another deforested) observed that many of these spectra obtained in wind conditions lower than $1\ m/s$ during the nighttime did not show the decay of $-5/3$ in the inertial subrange. Kruijt et al. (2000) found relative deficit of power at mid-frequencies and an excess at the highest frequencies under conditions of atmospheric stability above the canopy of two forest sites in the Amazon. During the 4 days of data chosen for the analyses of the present study, 50% of the time the wind speed was below $1\ m/s$ during the nocturnal period (Figure 3c). As the result shown in Figure 4b is a composite with all periods of the night, the decay of $-5/3$ still appears in a region of high frequencies, due to the

contribution to the spectrum of periods in which wind speed exceeded $1\,m/s$. According to Moraes et al. (2008), in this condition the turbulence spectra presented ~~the~~ canonical behavior, with the decay of $-5/3$.

Unlike the forest, the spectra calculated above the lake showed the decay region in both day and nighttime. Moreover, the inertial subrange of the night spectrum seems clearer than the daytime spectrum (Figures 4c and d). The behavior of these two spectra differs subtly in the region of low frequencies of the spectrum, evidencing the presence of larger vortices during the daytime period compared to the nocturnal period above the lake. The fact that the nighttime w spectrum above the lake resembles canonical behavior indicates that turbulence is well developed in this period, which does not occur in the forest in at least 50% of the nighttime period. An important fact, which may help to explain this turbulence above the lake, is that the atmosphere is almost always over unstable conditions or close to neutrality over the CU lake, favoring the vertical mixing of the atmosphere above (Vale 2016).

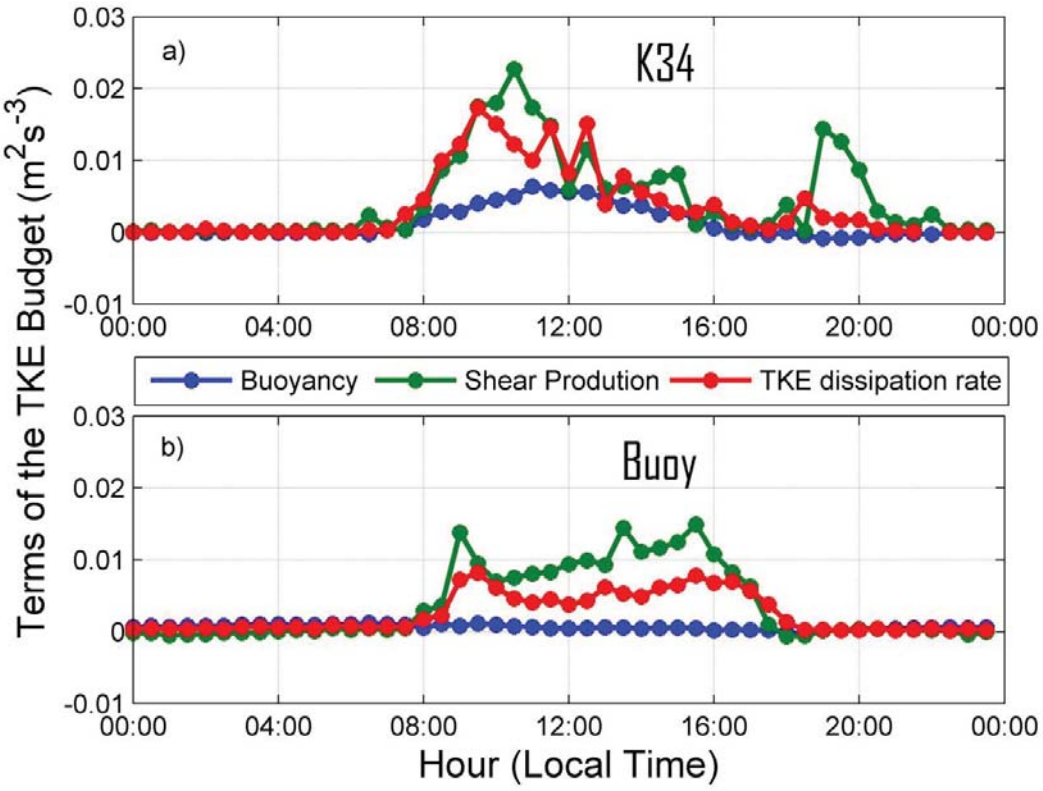

Figure 5. Diurnal cycle of the terms of the TKE budget for K34 (a) and CU (b) sites.

An important question about the air turbulence on the surfaces studied in this work (smooth and rough) is to know how the terms of the turbulent kinetic energy budget equation vary during their diurnal cycle. Figure 5 shows the cycles of buoyancy, shear production and TKE dissipation rate (ε) for k34 (Figure 5a) and CU (Figure 5b) sites. For both forest and lake, shear production was greater than buoyancy during the daytime, a result expected for measurements very close to the surface. However, the possible explanation for the difference between these two terms at each site should be different. As previously seen, wind speed above the lake is higher than above the forest during the daytime, but as the surface is inefficient in absorbing momentum from the atmosphere flow this does not translate into greater turbulence intensity (Figure 3). Even so, shear production dominates during the day due to the lake's great thermal inertia. In the forest this occurs due to the high efficiency in absorbing momentum from the atmosphere.

Comparing the shear production with ε also during the diurnal period at each site, the curves of these variables are closer to each other in the forest than in the lake. This result shows that a surface that is efficient in "generating" turbulence is also efficient in dissipating it (Stull 1988). At the k34 site the shear production and ε curves were coincident in almost every daily cycle, but there is a prominent peak in shear production that occurs at 19:00 (local time). Such a peak is a result of intermittent turbulence bursts which, curiously, occurred preferentially early in the night at the K34 site.

As previously shown, air turbulence above the lake is well developed during the nighttime period (Figures 3 and 4d). However, the results show that all terms of the TKE balance equation are very close to zero. Even though buoyancy was slightly positive during this period (i.e., producing turbulence), the values seem too low to maintain nighttime turbulence above the lake. A possible explanation for the maintenance of this turbulence may be associated with the advection term of the TKE budget equation (Stull 1988; Sahlée et al. 2014)

4. Conclusions

In this work the characteristics of the atmospheric turbulence on a smooth surface (lake) and a rough surface (forest) were compared. At each site turbulence intensity, temporal and length scales of the largest eddies, turbulence power spectra, as well as the main terms of the TKE budget (TKE = turbulent kinetic energy) were measured.

During the daytime the turbulence intensity above the forest was greater than above the lake. The σ_w values calculated for the forest were approximately twice as high as those calculated for the lake, close to mid-day. In the nighttime period the situation was reversed, and the turbulence above the lake was practically continuous, with higher values of σ_w than the forest, except for periods in which intermittent turbulence bursts occur in K34. These bursts occurred primarily in the early evening on the days studied here.

The time and length scale of the largest eddies in the horizontal and vertical directions were calculated. The values obtained for the forest were close to those found in the literature for this surface, for example, the values of L_u and $L_w$were related to canopy height ($L_u = 35.2$, $L_w = 11.1$ and $h = 35\ m$), as indicated by Raupach et al. (1996). The scales obtained for the lake were probably the first on this surface in tropical regions. These scales had lower values than at the forest, except for the horizontal length scale ($L_u = 48.0\ m$, above the lake).

The composites of the w power spectra showed a very similar behavior to the canonical ones above the lake. The region of the inertial subdomain with decay of $-5/3$ appears in both in day and nighttime periods above this surface. Above the forest this spectrum is well defined only during the daytime. In the nighttime period spectrums obtained during the performance of weak winds, below $1\ m/s$, contributed to the deformation of the spectrum in the region of medium frequency.

The buoyancy, shear production and TKE dissipation rate (ε), which are terms of the TKE budget equation, were calculated. Shear production was the term that most contributed to the generation of turbulence on both surfaces during the daytime. In the forest the buoyancy values were comparable to those of shear production from 12 to 16 hour (local time). On the other hand, in the lake, the buoyancy values were very close to zero during the whole diurnal cycle. The behavior of ε follows the same trend as shear production. All terms calculated in this work had values very close to zero on the lake at night, indicating that other terms that could not be calculated, such as TKE advection, may have contributed to the turbulence overnight at this site.

Acknowledgements

The authors are grateful to Daniel Jati for the preparation of Figure 1 of this paper, as well as help in assembling the floating buoy experiment in Curuá-Una site. The first author thanks the Coordenação de Aperfeiçoamento de Pessoal de Nível Superior **(**CAPES**)** for the PhD grant awarded through the Programa de Pós-graduação em Clima e Ambiente and the Universidade Federal do Oeste do Pará (UFOPA) for the partial release (20 hours a week), which allowed for the accomplishment of this work. The authors also thank these institutions for their financial and logistical support in obtaining data on Lake Curuá-Uma. The authors would like to thank all the development and teaching and research institutions that provided financial and human resources to obtain the data at the k34 site, namely: Fundação de Amparo à Pesquisa do Estado do Amazonas (FAPEAM), Fundação de Amparo à Pesquisa do Estado de São Paulo (FAPESP), Universidade do Estado do Amazonas (UEA), Instituto Nacional de Pesquisas da Amazônia (INPA) e Programa de Grande Escala da Biosfera-Atmosfera na Amazônia (LBA).

References

Anderson, D.E. et al., 1986. Turbulence spectra of CO2, water vapor, temperature and velocity over a deciduous forest. *Agricultural and Forest Meteorology*, 38(7664), pp.81–99.

Araújo, A.C. et al., 2002. Comparative measurements of carbon dioxide fluxes from two nearby towers in a central Amazonian rainforest: The Manaus LBA site. *Journal of Geophysical Research*, 107, pp.1–20.

Arya, P., 2001. *Introduction to Micrometeorology*, San Diego: Academic Press.

Azevedo, A. et al., 2017. *P Anorama Sobre O D Esmatamento Na a Mazônia Em 2016*, Brasília, DF. Available at: http://ipam.org.br/wp-content/uploads/2016/12/panorama-desmatamento-amazônia-2016.pdf.

Businger, J.A., 1973. A note on free convection. *Boundary-Layer Meteorology*, 4(1–4), pp.323–326.

Chor, T.L. et al., 2017. Flux-variance and flux-gradient relationships in the roughness sublayer over the Amazon forest. *Agricultural and Forest Meteorology*, 239, pp.213–222. Available at: http://dx.doi.org/10.1016/j.agrformet.2017.03.009.

Dias-Júnior, C.Q. et al., 2017. Turbulence regimes in the stable boundary layer above and within the Amazon forest. *Agricultural and Forest Meteorology*, 233, pp.122–132. Available at: http://dx.doi.org/10.1016/j.agrformet.2016.11.001.

Dias-Júnior, C.Q. et al., 2016. Turbulence regimes in the stable boundary layer above and within the Amazon forest. *Agricultural and Forest Meteorology*.

Edson, J.B. & Fairall, C.W., 1998. Similarity Relationships in the Marine Atmospheric Surface Layer for Terms in the TKE and Scalar Variance Budgets*. *Journal of the Atmospheric Sciences*, 55(13), pp.2311–2328. Available at: http://journals.ametsoc.org/doi/abs/10.1175/1520-0469%281998%29055%3C2311%3ASRITMA%3E2.0.CO%3B2.

Fairall, C.W. et al., 1996. Bulk parameterization of air-sea fluxes for Tropical Ocean-Global Atmosphere Coupled-Ocean Atmosphere Response Experiment. *Journal of Geophysical Research: Oceans*, 101(C2), pp.3747–3764. Available at: http://doi.wiley.com/10.1029/95JC03205.

Fearnside, P.M., 2005. Do hydroelectric dams mitigate global warming? The case of Brazil's Curuá-Una Dam. *Mitigation and Adaptation Strategies for Global Change*, 10(4), pp.675–691.

Fitzjarrald, D.R. et al., 1990. Daytime turbulent exchange between the Amazon forest and the atmosphere. *Journal of Geophysical Research: Atmospheres*, 95(D10), pp.16825–16838. Available at: http://onlinelibrary.wiley.com.ezaccess.libraries.psu.edu/doi/10.1029/JD095iD10p16825/abstract%5Cnhttp://onlinelibrary.wiley.com.ezaccess.libraries.psu.edu/store/10.1029/JD095iD10p16825/asset/jgrd1658.pdf?v=1&t=hqo99iy3&s=de2805634c3f9dc537af9c1a7aefb80baad.

Fitzjarrald, D.R. et al., 1988. Turbulent transport observed just above the Amazon forest. *Journal of Geophysical Research*, 93(D2), p.1551. Available at: http://dx.doi.org/10.1029/JD093iD02p01551.

Fitzjarrald, D.R. & Moore, K.E., 1990. Mechanisms of nocturnal exchange between the rain forest and the atmosphere. *Journal of Geophysical Research: Atmospheres*, 95(D10), pp.16839–16850. Available at: http://onlinelibrary.wiley.com.ezaccess.libraries.psu.edu/doi/10.1029/JD095iD10p16839/abstract%5Cnhttp://onlinelibrary.wiley.com.ezaccess.libraries.psu.edu/store/10.1029/JD

095iD10p16839/asset/jgrd1659.pdf?v=1&t=hqo8tmps&s=83093cd151da7fecce29b4966cbffa60550.

Freire, L.S. et al., 2017. Turbulent mixing and removal of ozone within an Amazon rainforest canopy. *Journal of Geophysical Research: Atmospheres*, 122(5), pp.2791–2811.

Garratt, J.R., 1972. Studies of turbulence in the surface layer over water (Lough Neagh). Part II. Production and dissipation of velocity and temperature fluctuations. *Q. J. R. Meteorol. Soc.*, 98, p.642–657.

Kaimal, J.C. et al., 1972. Spectral characteristics of surface-layer turbulence. *Quarterly Journal of the Royal Meteorological Society*, 98(417), pp.563–589.

Kaimal, J.C. & Finnigan, J.J., 1994. *Atmospheric Boundary LayerFlows - Their Structureand Measurement*, New York.: Oxford University Press.

Kaimal, J.C. & Wyngaard, J.C., 1990. The Kansas and Minessota Experiments. *Boudary-Layer Meteorlogy*, 50(1952), pp.31–47.

Kruijt, B. et al., 2000. Turbulence statistics above and within two Amazon rain forest canopies. *Boundary-Layer Meteorology*, 94(2), pp.297–331.

Kundu, P.K. & Cohen, I.M., 2002. *Fluid Mechanics*, ACADEMIC PRESS. Available at: http://wobl.engineeringvillage.com/wobl/9780121782511/9780121782511.pdf?expires=1327426759207&ticket=f900c3de4a50f7f517e7dcc12fac5e70&custid=1001720&EISESSION=1_969c291350044e6b453bbses4.

Lee, X., 1996. Turbulence spectra and eddy diffusivity over forests. *Journal of Applied Meteorology*, 35(8), pp.1307–1318.

Lumiley, J.L. & Panosky, H.A., 1964. *The Structure Of Atmospheric Turbulence*, New York: Interscience Publishers.

Mahrt, L. et al., 2000. Nocturnal mixing in a forest subcanopy. *Agricultural and Forest Meteorology*, 101(1), pp.67–78.

Marques Filho, E.P. et al., 2008. Atmospheric surface layer characteristics of turbulence above the Pantanal wetland regarding the similarity theory. *Agricultural and Forest Meteorology*, 148(6–7), pp.883–892.

McGillis, W.R., Hare, J.E. & Fairall, C.W., 2001. Direct covariance air-sea CO2 fluxes. *Journal of Geophysical Research*, 106(C8), pp.729–745.

Moraes, O.L.L. et al., 2008. Comparing spectra and cospectra of turbulence over different surface boundary conditions. *Physica A: Statistical Mechanics and its Applications*, 387(19–20), pp.4927–4939.

Ohtaki, E., Iwatani, Y. & Mitsuta, Y., 1989. Measurements of the Carbon Dioxide Flux over the Ocean. *Meteolorogical Society of Japan*, 67(4), pp.541–554.

Oliveira, P.E.S. et al., 2013. Nocturnal Intermittent Coupling Between the Interior of a Pine Forest and the Air Above It. *Boundary-Layer Meteorology*, 146(1), pp.45–64.

Raupach, M.R., Finnigan, J.J. & Brunei, Y., 1996. Coherent eddies and turbulence in vegetation canopies: The mixing-layer analogy. *Boundary-Layer Meteorology*, 78(3–4), pp.351–382.

Richey, J.E. et al., 2002. Outgassing from Amazonian rivers and wetlands as a large tropical source of atmospheric CO2. *Nature*, 416(6881), pp.617–620. Available at: http://www.nature.com/doifinder/10.1038/416617a.

Sahlée, E. et al., 2014. Influence from Surrounding Land on the Turbulence Measurements Above a Lake. *Boundary-Layer Meteorology*, 150(2), pp.235–258.

Sahlée, E. et al., 2008. Spectra of CO2 and Water Vapour in the Marine Atmospheric Surface Layer. *Boundary-Layer Meteorology*, 126(2), pp.279–295. Available at: http://link.springer.com/10.1007/s10546-007-9230-5.

Santana, R.A.S. de et al., 2017. Observing and Modeling the Vertical Wind Profile at Multiple Sites in and above the Amazon Rain Forest Canopy. *Advances inMeteorology*, 2017, p.8.

Santos, D.M. et al., 2016. Temporal Scales of the Nocturnal Flow Within and Above a Forest Canopy in Amazonia. *Boundary-Layer Meteorology*, pp.1–26.

Shaw, R.H. et al., 1995. A wind tunnel study of air flow in waving wheat: Two-point velocity statistics. *Boundary-Layer Meteorology*, 76(4), pp.349–376.

Sheppard, P.A., Tribble, D.T. & Garratt, J.R., 1972. Studies of turbulence in the surface layer over water (Lough Neagh). Part I. Instrumentation, programme, profiles. *Quarterly Journal of the Royal Meteorological Society*, 98(417), pp.627–641.

Stull, R.B., 1988. *An introduction to boundary layer meteorology*, Dordrecht: Kluwer Academic Publishers.

Tennekes, H., 1970. Free convection in the turbulent Ekman layer of the atmosphere. *Journal of the Atmospheric sciences*, 27(7), pp.1027–1034.

Vale, R.S. do, 2016. *Medições de gases de efeito estufa e variáveis ambientais em reservatórios hidrelétricos na amazônia central.* Instituto Nacional de Pesquisas da Amazônia - Universidade do Estado do Amazonas.

Vesala, T., Eugster, W. & Ojala, A., 2012. Eddy covariance measurements over lake fluxes. In M. Aubinet, T. Vesala, & D. Papale, eds. *Eddy Covariance - A Practical Guide to Measurement and Data Analysis*. Springer Atmospheric Sciences.

Walter, R.K., Nidzieko, N.J. & Monismith, S.G., 2011. Similarity scaling of turbulence spectra and cospectra in a shallow tidal flow. *Journal of Geophysical Research: Oceans*, 116(10), pp.1–14.

Wyngaard, J.C., Coté, O.R. & Izumi, Y., 1971. Local free convection, similarity, and the budgets of shear stress and heat flux. *Journal of the Atmospheric Sciences*, 28(7), pp.1171–1182.

Yi, C., 2008. Momentum transfer within canopies. *Journal of Applied Meteorology and Climatology*, 47(1), pp.262–275.

SÍNTESE E CONSIDERAÇÕES FINAIS

Neste trabalho foi estudado o escoamento turbulento do ar, dentro e acima do dossel florestal, de diferentes sítios experimentais localizados na floresta amazônica. Além disso, as características deste escoamento sobre um dos sítios de floresta foi comparada com ao escoamento turbulento observado sobre um lago, também localizado na região amazônica. As seguintes análises foram realizadas: observação e modelagem do perfil vertical de velocidade do vento (medidas realizadas em seis torres de observação espalhadas pela Amazônia); estudo dos perfis verticais da estatística da turbulência, fluxo de calor sensível e taxa de dissipação da ECT (energia cinética turbulenta) em sítios de floresta; comparação das características da turbulência do ar sobre floresta (superfície rugosa) e lago (superfície lisa).

Pela primeira vez as medidas do perfil vertical de velocidade do vento realizadas na floresta amazônica foram compiladas em um único trabalho, tais medidas forneceram uma visão mais ampla do comportamento do referido perfil sobre está região. Abaixo do dossel da floresta os valores de velocidade do vento foram muito baixos, devido à atenuação pela estrutura da vegetação. Acima do dossel o vento aumenta com a altura em um comportamento logarítmico, levemente modificado devido à presença da subcamada rugosa. Os modelos utilizados para simular o perfil vertical de velocidade do vento conseguiram capturar suas características tanto acima quanto abaixo do dossel da floresta. A simplificação na formulação de um destes modelos não alterou sua habilidade em representar o este perfil na Amazônia.

Os sítios de floresta estudados apresentaram diferenças significativas na eficiência em absorver momentum da atmosfera, provavelmente devido a pequenas diferenças na estrutura da vegetação de cada sítio. Esta eficiência é função também da velocidade do vento, tipicamente, a eficiência aumenta com o aumento da velocidade do vento. A partir da análise das estatísticas da turbulência nos diferentes sítios, pode-se dizer que existe um padrão na profundidade que a turbulência gerada acima da floresta consegue penetrar o seu dossel. Dificilmente esta turbulência penetra a região abaixo de $0.5h$, sendo esta altura mais facilmente alcançada em condições de vento forte.

O fluxo de calor sensível não é constante com a altura acima da floresta, principalmente sob condições de ventos fortes, fato que afeta os pressupostos da teoria de similaridade de Monin-Obukhov e reforça a indicação de trabalhos anteriores de que tal teoria não se aplica na subcamada rugosa acima da floresta amazônica. Os maiores valores de H

foram também observados durante a atuação de ventos fortes nos dois períodos estudados, diurno e noturno. O ciclo diário de H em diferentes alturas abaixo dossel é bastante variável, em algumas alturas o fluxo passa de positivo para negativo, mesmo durante o dia, evidenciado a complexidade das trocas de escares entre a floresta a atmosfera.

Utilizando propriedades do espectro de potencia da turbulência, o ciclo diário em diferentes alturas e o perfil da taxa de dissipação de ECT pôde ser calculado. O comportamento desta variável obedece o ciclo diário de radiação, com valores máximos, em cada altura, próximos aos períodos de maior insolação. Em condições de ventos fortes, o perfil de ε apresenta um máximo próximo ao topo do dossel. Resultado que reflete a observação de que maiores taxas dissipação são frequentemente encontradas onde os valores de produção de ECT também são maiores.

Comparado as característica da turbulência atmosférica sobre a floresta e o lago, observou-se que durante o dia a intensidade da turbulência sobre a floresta foi maior do que sobre o lago. Os valores de σ_w calculados para a floresta foram aproximadamente duas vezes maiores do que aqueles calculados para o lago, próximo ao meio dia. No período noturno a situação é invertida, a turbulência sobre o lago foi praticamente contínua, com maiores valores de σ_w do que a floresta, com exceção de períodos em que rajadas de turbulência intermitente ocorrem na floresta. Estas rajadas ocorreram prioritariamente no inicio da noite nos dias estudados aqui.

As escalas de tempo e comprimento dos maiores vórtices nas direções horizontal e vertical foram calculadas. Os valores obtidos para a floresta ficaram próximos aos encontrados na literatura para esta superfície, como exemplo, os valores de L_u e L_w foram da ordem da atura do dossel ($L_u = 35.2$, $L_w = 11.1$ e $h = 35\ m$), como indicado por Raupach et al. (1996). As escalas obtidas para o lago foram, provavelmente, os primeiros sobre esta superfície, em regiões tropicais. Estas escalas tiveram valores menores do que sobre a floresta, com exceção da escala de comprimento horizontal ($L_u = 48.0\ m$, sobre o lago).

Os compósitos dos espectros de potencia de w mostraram um comportamento bastante semelhante ao canônico sobre o lago. A região do subdomínio inercial com decaimento de $-5/3$ aparece tanto no período diurno quanto a noite, sobre esta superfície. Sobre a floresta este espectros são bem definidos apenas durante o dia. No período noturno os espectro obtidos durante a atuação de ventos fracos, abaixo de $1\ m/s$, contribuíram para a deformação do espectro na região de médias frequência.

A flutuabilidade, a produção por cisalhamento e a taxa de dissipação de ECT (ε), todos termos da equação do balanço de energia cinética turbulenta, foram calculados para a floresta e para o lago. A produção por cisalhamento foi termo que mais contribuiu para a geração de turbulência sobre ambas as superfícies durante o dia. Na floresta os valores de flutuabilidade foram comparáveis aos da produção por cisalhamento das 12 às 16, hora local. Por lado, no lago está variável apresentou valores muito próximos de zero durante todo o ciclo diário. O comportamento de ε segue o a mesma tendência da produção por cisalhamento. Todos os termos calculados neste trabalho apresentaram valores muito próximos de zero sobre o lago durante a noite, indicando que outros termos que não puderam ser calculados, como a advecção de ECT, podem ter contribuído para manter a turbulência durante a noite neste sítio.

Como sugestão para trabalhos futuros seguem os seguintes tópicos:

I. Aplicar o modelo de Souza apresentado no Capítulo I desta tese em áreas de floresta de outros tipos, como apresentado por Yi (2008).
II. Estudar as estatísticas da turbulência em uma maior resolução, ou seja, sem utilizar valores médios, capturando sua variabilidade, a fim de investigar possíveis momentos em que a turbulência gerada acima do dossel consegue ultrapassar a região abaixo de $h/2$.
III. Investigar o fluxo de outro escalares, como CO_2, por exemplo, nos momentos em que escoamento acima do dossel é acoplado e não-acoplado com a região abaixo do dossel.
IV. Estudar a ocorrência de rajadas de turbulência intermitente sobre a floresta e o lago durante o período noturno, identificando horários de preferência destes eventos e tentar relacioná-los a fenômenos de escalas maiores, como Jatos de Baixos Níveis, Brisa de rio, tempestades, entre outros.
V. Verificar o efeito da advecção da turbulência sobre as medidas sobre o lago, utilizando medidas em mais de um ponto, modelagem numérica e propriedade dos espectros de potencia.

REFERÊNCIAS

Acevedo, Otávio C., and David ROY Fitzjarrald. 2003. “In the Core of the Night – Effects of Intermittent Mixing on a Horizontally Heterogeneous Surface.” *Boundary-Layer Meteorology* 106: 1–33.

Alves, Eliane G., Kolby Jardine, Julio Tota, Angela Jardine, Ana Maria Yãnez-Serrano, Thomas Karl, Julia Tavares, et al. 2016. “Seasonality of Isoprenoid Emissions from a Primary Rainforest in Central Amazonia.” *Atmospheric Chemistry and Physics* 16 (6): 3903–25. doi:10.5194/acp-16-3903-2016.

Anderson, Dean E, Shashi B Verma, Robert J Clement, Dennis D Baldocchi, and Detlef R Matt. 1986. “Turbulence Spectra of CO2, Water Vapor, Temperature and Velocity over a Deciduous Forest.” *Agricultural and Forest Meteorology* 38 (7664): 81–99.

Andreae, M. O., O. C. Acevedo, A. Araújo, P. Artaxo, C. G G Barbosa, H. M J Barbosa, J. Brito, et al. 2015. “The Amazon Tall Tower Observatory (ATTO): Overview of Pilot Measurements on Ecosystem Ecology, Meteorology, Trace Gases, and Aerosols.” *Atmospheric Chemistry and Physics* 15 (18): 10723–76. doi:10.5194/acp-15-10723-2015.

Andreae, M. O., P. Artaxo, C. Brandão, F. E. Carswell, P. Ciccioli, A. L. Da Costa, A. D. Gulf, et al. 2002. “Biogeochemical Cycling of Carbon, Water, Energy, Trace Gases, and Aerosols in Amazonia: The LBA-EUSTACH Experiments.” *Journal of Geophysical Research D: Atmospheres* 107 (20). doi:10.1029/2001JD000524.

Andreae, M. O., D. Rosenfeld, P. Artaxo, A. A. Costa, G. P. Frank, K. M. Longo, and M. A. F. Silva-Dias. 2004. “Smoking Rain Clouds over” 303 (0036–8075): 1337–13242. doi:10.1126/science.1092779.

Antonia, R A. 1981. “Conditional Sampling Measurement.” *Annual Review of Fluid Mechanics* 13 (d): 131–56.

Araújo, A C, A D Nobre, B Kruijt, J A Elbers, R Dallarosa, P Stefani, C Von Randow, et al. 2002. “Comparative Measurements of Carbon Dioxide Fluxes from Two Nearby Towers in a Central Amazonian Rainforest: The Manaus LBA Site.” *Journal of Geophysical Research* 107: 1–20. doi:10.1029/2001JD000676.

Arya, Paul. 2001. *Introduction to Micrometeorology*. San Diego: Academic Press.

Asner, G P, D Nepstad, G Cardinot, and D Ray. 2004. “Drought Stress and Carbon Uptake in an Amazon Forest Measured with Spaceborne Imaging Spectroscopy.” *Proc Natl Acad Sci U S A* 101 (16): 6039–44. doi:10.1073/pnas.0400168101.

Azevedo, Andrea, Ane Alencar, Paulo Moutinho, Vivian Ribeiro, Tiago Reis, Marcelo Stabile, and André Guimarães. 2017. “P Anorama Sobre O D Esmatamento Na a Mazônia Em 2016.” Brasília, DF. doi:10.13140/RG.2.2.30526.08002.

Baldocchi, D, and P Meyers. 1988. “Turbulence Structure in a Deciduous Forest.” *Boundary-Layer Meteorology* 43: 345–64.

Bolzan, Maurício José Alves, and Paulo Cesar Vieira. 2006. “Wavelet Analysis of the Wind

Velocity and Temperature Variability in the Amazon Forest." *Brazilian Journal of Physics* 36 (4): 1217–22.

Businger, J. A. 1973. "A Note on Free Convection." *Boundary-Layer Meteorology* 4 (1–4): 323–26. doi:10.1007/BF02265241.

Carswell, F. E., A. L. Costa, M. Palheta, Y. Malhi, P. Meir, J. De P R Costa, M. De L Ruivo, et al. 2002. "Seasonality in CO2 and H2O Flux at an Eastern Amazonian Rain Forest." *Journal of Geophysical Research D: Atmospheres* 107 (20). doi:10.1029/2000JD000284.

Cellier, P, and Y Brunet. 1992. "Flux Gradient Relationships above Tall Plant Canopies." *Agricultural and Forest Meteorology* 58 (1–2): 93–117. doi:10.1016/0168-1923(92)90113-I.

Chamecki, Marcelo. 2013. "Persistence of Velocity Fluctuations in Non-Gaussian Turbulence within and above Plant Canopies." *Physics of Fluids* 25 (11). doi:10.1063/1.4832955.

Chor, Tomás L, Nelson L Dias, Alessandro Araújo, Stefan Wolff, Einara Zahn, Antônio Manzi, Ivonne Trebs, Marta O Sá, Paulo R Teixeira, and Matthias Sörgel. 2017. "Flux-Variance and Flux-Gradient Relationships in the Roughness Sublayer over the Amazon Forest." *Agricultural and Forest Meteorology* 239. Elsevier B.V.: 213–22. doi:10.1016/j.agrformet.2017.03.009.

Cole, J. J., N. F. Caraco, G. W. Kling, and T. K. Kratz. 1994. "Carbon Dioxide Supersaturation in the Surface Waters of Lakes." *Science* 265 (5178): 1568–70. doi:10.1126/science.265.5178.1568.

Cole, J. J., Y. T. Prairie, N. F. Caraco, W. H. McDowell, L. J. Tranvik, R. G. Striegl, C. M. Duarte, et al. 2007. "Plumbing the Global Carbon Cycle: Integrating Inland Waters into the Terrestrial Carbon Budget." *Ecosystems* 10 (1): 171–84. doi:10.1007/s10021-006-9013-8.

Dias-Júnior, Cléo Quaresma, Nelson Luís Dias, Jos D Fuentes, and Marcelo Chamecki. 2017. "Convective Storms and Non-Classical Low-Level Jets during High Ozone Level Episodes in the Amazon Region: An ARM/GOAMAZON Case Study." *Atmospheric Environment* 155: 199–209. doi:10.1016/j.atmosenv.2017.02.006.

Dias-Júnior, Cléo Quaresma, Edson P. Marques Filho, and Leonardo D A Sá. 2015. "A Large Eddy Simulation Model Applied to Analyze the Turbulent Flow above Amazon Forest." *Journal of Wind Engineering and Industrial Aerodynamics* 147. Elsevier: 143–53. doi:10.1016/j.jweia.2015.10.003.

Dias-Júnior, Cléo Quaresma, L. D A Sá, V. B. Pachêco, and C. M. de Souza. 2013. "Coherent Structures Detected in the Unstable Atmospheric Surface Layer above the Amazon Forest." *Journal of Wind Engineering and Industrial Aerodynamics* 115: 1–8. doi:10.1016/j.jweia.2012.12.019.

Dias-Júnior, Cléo Quaresma, Leonardo D A Sá, Edson P Marques, Raoni A Santana, Matthias Mauder, and Antônio O Manzi. 2017. "Turbulence Regimes in the Stable Boundary Layer above and within the Amazon Forest." *Agricultural and Forest Meteorology* 233. Elsevier B.V.: 122–32. doi:10.1016/j.agrformet.2016.11.001.

Dias-Júnior, Cléo Quaresma, Leonardo Deane de Abreu Sá, Edson P. Marques Filho, Raoni Aquino Silva de Santana, Matthias Mauder, and Antônio Ocimar Manzi. 2016.

"Turbulence Regimes in the Stable Boundary Layer above and within the Amazon Forest." *Agricultural and Forest Meteorology*.

Dupont, S., and E. G. Patton. 2012. "Momentum and Scalar Transport within a Vegetation Canopy Following Atmospheric Stability and Seasonal Canopy Changes: The CHATS Experiment." *Atmospheric Chemistry and Physics* 12 (13): 5913–35. doi:10.5194/acp-12-5913-2012.

Dupont, Sylvain, and Edward G. Patton. 2012. "Influence of Stability and Seasonal Canopy Changes on Micrometeorology within and above an Orchard Canopy: The CHATS Experiment." *Agricultural and Forest Meteorology* 157. Elsevier B.V.: 11–29. doi:10.1016/j.agrformet.2012.01.011.

Edson, J. B., and C. W. Fairall. 1998. "Similarity Relationships in the Marine Atmospheric Surface Layer for Terms in the TKE and Scalar Variance Budgets*." *Journal of the Atmospheric Sciences* 55 (13): 2311–28. doi:10.1175/1520-0469(1998)055<2311:SRITMA>2.0.CO;2.

Fairall, C. W., E. F. Bradley, D. P. Rogers, J. B. Edson, and G. S. Young. 1996. "Bulk Parameterization of Air-Sea Fluxes for Tropical Ocean-Global Atmosphere Coupled-Ocean Atmosphere Response Experiment." *Journal of Geophysical Research: Oceans* 101 (C2): 3747–64. doi:10.1029/95JC03205.

Fearnside, Philip M. 2005. "Do Hydroelectric Dams Mitigate Global Warming? The Case of Brazil's Curuá-Una Dam." *Mitigation and Adaptation Strategies for Global Change* 10 (4): 675–91. doi:10.1007/s11027-005-7303-7.

Finnigan, John. 2000. "Turbulence in Plant Canopies." *Annu. Rev. Fluid Mech.* 32: 519–71.

Fitzjarrald, David R., and Kathleen E. Moore. 1990. "Mechanisms of Nocturnal Exchange between the Rain Forest and the Atmosphere." *Journal of Geophysical Research: Atmospheres* 95 (D10): 16839–16850. doi:10.1029/JD095iD10p16839.

Fitzjarrald, David R., Kathleen E. Moore, Osvaldo M. R. Cabral, José Scolar, Antônio O. Manzi, and Leonardo D. de Abreu Sá. 1990. "Daytime Turbulent Exchange between the Amazon Forest and the Atmosphere." *Journal of Geophysical Research: Atmospheres* 95 (D10): 16825–16838. doi:10.1029/JD095iD10p16825.

Fitzjarrald, David R, Brian L Stormwind, Gilberto Fisch, and Osvaldo M R Cabral. 1988. "Turbulent Transport Observed Just above the Amazon Forest." *Journal of Geophysical Research* 93 (D2): 1551. doi:10.1029/jd093id02p01551.

Freire, L. S., T. Gerken, J. Ruiz-Plancarte, D. Wei, J. D. Fuentes, G. G. Katul, N. L. Dias, O. C. Acevedo, and M. Chamecki. 2017. "Turbulent Mixing and Removal of Ozone within an Amazon Rainforest Canopy." *Journal of Geophysical Research: Atmospheres* 122 (5): 2791–2811. doi:10.1002/2016JD026009.

Fuentes, JD, M Chamecki, RM Nascimento dos Santos, C Von Randow, PC Stoy, G Katul, D Fitzjarrald, et al. 2016. "Linking Meteorology, Turbulence, and Air Chemistry in the Amazon Rainforest during the GoAmazon Project." *Bulletin of the American Meteorological Society*, in review. doi:10.1175/BAMS-D-15-00152.1.

Garratt, J. R. 1972. "Studies of Turbulence in the Surface Layer over Water (Lough Neagh). Part II. Production and Dissipation of Velocity and Temperature Fluctuations." *Q. J. R.*

Meteorol. Soc. 98: 642–657.

Gash, J. H C, and C. A. Nobre. 1997. “Climatic Effects of Amazonian Deforestation: Some Results from ABRACOS.” *Bulletin of the American Meteorological Society* 78 (5): 823–30. doi:10.1175/1520-0477(1997)078<0823:CEOADS>2.0.CO;2.

Gerken, Tobias, Dandan Wei, Randy J. Chase, Jose D. Fuentes, Courtney Schumacher, Luiz A T Machado, Rita V. Andreoli, Marcelo Chamecki, Rodrigo A. Ferreira de Souza, et al. 2016. “Downward Transport of Ozone Rich Air and Implications for Atmospheric Chemistry in the Amazon Rainforest.” *Atmospheric Environment* 124 (1352–2310): 64–76. doi:10.1016/j.atmosenv.2015.11.014.

Gerken, Tobias, Dandan Wei, Randy J. Chase, Jose D. Fuentes, Courtney Schumacher, Luiz A T Machado, Rita V. Andreoli, Marcelo Chamecki, Rodrigo A. Ferreira de Souza, et al. 2016. “Downward Transport of Ozone Rich Air and Implications for Atmospheric Chemistry in the Amazon Rainforest.” *Atmospheric Environment* 124 (January 2016): 64–76. doi:10.1016/j.atmosenv.2015.11.014.

Gloor, M, L Gatti, R Brienen, T R Feldpausch, O L Phillips, J Miller, J P Ometto, H Rocha, and T Baker. 2012. “The Carbon Balance of South America : A Review of the Status , Decadal Trends and Main Determinants.” *Biogeosciences* 9: 5407–30. doi:10.5194/bg-9-5407-2012.

Kaimal, J. C., and J. J. Finnigan. 1994. *Atmospheric Boundary LayerFlows - Their Structureand Measurement*. *Oxford University Press. New York.* New York.: Oxford University Press. doi:10.1017/CBO9781107415324.004.

Kaimal, J. C., J. C. Wyngaard, Y. Izumi, and O. R. Coté. 1972. “Spectral Characteristics of Surface-Layer Turbulence.” *Quarterly Journal of the Royal Meteorological Society* 98 (417): 563–89. doi:10.1002/qj.49709841707.

Kaimal, J C, and J C Wyngaard. 1990. “The Kansas and Minessota Experiments.” *Boudary-Layer Meteorlogy* 50 (1952): 31–47.

Katul, Gabriel, Greg Kuhn, John Schieldge, and Cheng-I. Hsieh. 1997. “The Ejection-Sweep Character of Scalar Fluxes in the Unstable Surface Layer.” *Boundary-Layer Meteorology* 83 (1): 1–26. doi:10.1023/A:1000293516830.

Kruijt, B., Y. Malhi, J. Lloyd, A. D. Nobre, A. C. Miranda, M. G P Pereira, A. Culf, and J. Grace. 2000. “Turbulence Statistics above and within Two Amazon Rain Forest Canopies.” *Boundary-Layer Meteorology* 94 (2): 297–331. doi:10.1023/A:1002401829007.

Kundu, P K, and I M Cohen. 2002. *Fluid Mechanics*. *Comparative Biochemistry and Physiology Toxicology Pharmacology CBP*. Vol. 80. ACADEMIC PRESS. http://wobl.engineeringvillage.com/wobl/9780121782511/9780121782511.pdf?expires=1327426759207&ticket=f900c3de4a50f7f517e7dcc12fac5e70&custid=1001720&EISESSION=1_969c291350044e6b453bbses4.

Launiainen, Samuli, Timo Vesala, Meelis Mölder, Ivan Mammarella, Sampo Smolander, Üllar Rannik, Pasi Kolari, Pertti Hari, Anders Lindroth, and Gabriel G. Katul. 2007. “Vertical Variability and Effect of Stability on Turbulence Characteristics down to the Floor of a Pine Forest.” *Tellus* 59 (5): 919–36. doi:10.1111/j.1600-0889.2007.00313.x.

Lee, Xuhui. 1996. “Turbulence Spectra and Eddy Diffusivity over Forests.” *Journal of Applied Meteorology*.

Lima, Newton. 2014. “Sobre as Características de Formação de Estrutura Coerente E Turbulência Em Uma Floresta Densa de Terra Firme Com Medidas Em Até 80m de Altura: Projeto ATTO-CLAIRE / IOP - 1 - 2012.” Instituto Nacional de Pesquisas da Amazônia.

Lu, Cheng-Hsuan, and David Roy Fitzjarrald. 1994. “Seasonal and Diurnal Variations of Coherent Structures over a Deciduous Forest.” *Boundary-Layer Meteorology* 69: 43–69.

Lumiley, J. L., and H. A. Panosky. 1964. *The Structure Of Atmospheric Turbulence*. *Interscience*. New York: Interscience Publishers. doi:10.1038/178241b0.

Mahrt, L., Xuhui Lee, Andrew Black, Harold Neumann, and R. M. Staebler. 2000. “Nocturnal Mixing in a Forest Subcanopy.” *Agricultural and Forest Meteorology* 101 (1): 67–78. doi:10.1016/S0168-1923(99)00161-6.

Malhi, Y., E. Pegoraro, A. D. Nobre, M. G P Pereira, J. Grace, A. D. Culf, and R. Clement. 2002. “Energy and Water Dynamics of a Central Amazonian Rain Forest.” *Journal of Geophysical Research Atmospheres* 107 (20): 1–17. doi:10.1029/2001JD000623.

Marques Filho, Arí O., Ricardo G. Dallarosa, and Vanusa Bezerra Pachêco. 2005. “Radiação Solar E Distribuição Vertical de Área Foliar Em Floresta Reserva Biológica Do Cuieiras ZF2, Manaus.” *Acta Amazônica* 35 (4): 427–36. doi:10.1590/S0044-59672005000400007.

Marques Filho, E. P., L. D A Sá, H. A. Karam, R. C S Alvalá, A. Souza, and M. M R Pereira. 2008. “Atmospheric Surface Layer Characteristics of Turbulence above the Pantanal Wetland Regarding the Similarity Theory.” *Agricultural and Forest Meteorology* 148 (6–7): 883–92. doi:10.1016/j.agrformet.2007.12.004.

McGillis, W. R., J. E. Hare, and C. W. Fairall. 2001. “Direct Covariance Air-Sea CO2 Fluxes.” *Journal of Geophysical Research* 106 (C8): 729–45.

Molion, L. C. B. 1987. “On the Dynamic Climatology of the Amazon Basin and Associated Rain-Producing Mechanisms.” In *In Geophysiology of Amazonia*, edited by R. E. Dickinson, John Wiley, 391–407.

Moraes, Osvaldo L L, David R. Fitzjarrald, Otávio C. Acevedo, Ricardo K. Sakai, Matthew J. Czikowsky, and Gervásio A. Degrazia. 2008. “Comparing Spectra and Cospectra of Turbulence over Different Surface Boundary Conditions.” *Physica A: Statistical Mechanics and Its Applications* 387 (19–20): 4927–39. doi:10.1016/j.physa.2008.04.007.

Moura, Rildo Gonçalves de. 2001. “Estudos Das Radiações Solar E Terrestre Acima E Dentro De Uma Floresta Tropical Úmida.”

Nobre, Carlos A., J. H. C. Gash, J. M. Roberts, and R. L. Victoria. 1996. “Conclusions From ABRACOS.” In *Amazonian Deforestation and Climate*, 577–95.

Ohtaki, E, Y Iwatani, and Y Mitsuta. 1989. “Measurements of the Carbon Dioxide Flux over the Ocean.” *Meteolorogical Society of Japan* 67 (4): 541–54.

Oliveira, Pablo E S, Otávio C. Acevedo, Osvaldo L L Moraes, Hans R. Zimermann, and

Claudio Teichrieb. 2013. “Nocturnal Intermittent Coupling Between the Interior of a Pine Forest and the Air Above It.” *Boundary-Layer Meteorology* 146 (1): 45–64. doi:10.1007/s10546-012-9756-z.

Poggi, D., A. Porporato, L. Ridolfi, J. D. Albertson, and G. G. Katul. 2004. “The Effect of Vegetation Density on Canopy Sub-Layer Turbulence.” *Boundary-Layer Meteorology* 111 (3): 565–87. doi:10.1023/B:BOUN.0000016576.05621.73.

Raupach, M. R., J. J. Finnigan, and Y. Brunei. 1996. “Coherent Eddies and Turbulence in Vegetation Canopies: The Mixing-Layer Analogy.” *Boundary-Layer Meteorology* 78 (3–4): 351–82. doi:10.1007/BF00120941.

Raupach, M R, and A St Thom. 1981. “Turbulence in and above Plant Canopies.” *Annual Review of Fluid Mechanics* 13 (1): 97–129. doi:10.1146/annurev.fl.13.010181.000525.

Richey, Jeffrey E., John M. Melack, Anthony K. Aufdenkampe, Victoria M. Ballester, and Laura L. Hess. 2002. “Outgassing from Amazonian Rivers and Wetlands as a Large Tropical Source of Atmospheric CO2.” *Nature* 416 (6881): 617–20. doi:10.1038/416617a.

Sá, Leonardo Deane Abreu, and Vanusa Bezerra Pachêco. 2001. “Relações de Similaridade Para Os Perfis de Velocidade Média Do Vento Dentro Da Copa Da Floresta Amazônica Em Rondônia.” *Revista Brasileira de Meteorologia* 16 (1): 81–89.

Sá, Leonardo Deane de Abreu, and Vanusa Bezerra Pachêco. 2006. “Wind Velocity above and inside Amazonian Rain Forest in Rondônia.” *Revista Brasileira de Meteorologia* 21 (3a): 50–58.

Sahlée, Erik, Anna Rutgersson, Eva Podgrajsek, and Hans Bergström. 2014. “Influence from Surrounding Land on the Turbulence Measurements Above a Lake.” *Boundary-Layer Meteorology* 150 (2): 235–58. doi:10.1007/s10546-013-9868-0.

Sahlée, Erik, Ann-Sofi Smedman, Anna Rutgersson, and Ulf Högström. 2008. “Spectra of CO2 and Water Vapour in the Marine Atmospheric Surface Layer.” *Boundary-Layer Meteorology* 126 (2): 279–95. doi:10.1007/s10546-007-9230-5.

Sakai, Ricardo K., David R. Fitzjarrald, and Kathleen E. Moore. 2001. “Importance of Low-Frequency Contributions to Eddy Fluxes Observed over Rough Surfaces.” *Journal of Applied Meteorology* 40 (12): 2178–92. doi:10.1175/1520-0450(2001)040<2178:IOLFCT>2.0.CO;2.

Santana, Raoni Aquino Silva de, Cléo Quaresma Dias-Júnior, Roseilson Souza do Vale, Júlio Tóta, and David Roy Fitzjarrald. 2017. “Observing and Modeling the Vertical Wind Profile at Multiple Sites in and above the Amazon Rain Forest Canopy.” *Advances inMeteorology* 2017: 8.

Santana, Raoni Aquino Silva de, Julio Tóta, Rosa Maria Nascimento Santos, and Roseilson Souza Vale. 2015. “Estabilidade E Estrutura Da Turbulência Sob a Influência de Jatos de Baixos Níveis Noturnos No Sudoeste Da Amazônia.” *Revista Brasileira de Meteorologia* 30 (4): 405–14.

Santos, A. B, J. Tóta, M. A. L. Moura, D. R. Fitzjarrald, R. A. S. Santana, A. M. D. Andrade, and R. G. Carneiro. 2013. “Dinâmica Do Escoamento de Ar Acima E Dentro de Uma Floresta Tropical Densa Sobre Terreno Complexo Na Amazônia.” *Revista Brasileira de*

Geografia Física 6 (2): 308–19.

Santos, Daniel M., Otávio C. Acevedo, Marcelo Chamecki, José D. Fuentes, Tobias Gerken, and Paul C. Stoy. 2016. "Temporal Scales of the Nocturnal Flow Within and Above a Forest Canopy in Amazonia." *Boundary-Layer Meteorology*. Springer Netherlands, 1–26. doi:10.1007/s10546-016-0158-5.

Shaw, R. H., Y. Brunet, J. J. Finnigan, and M. R. Raupach. 1995. "A Wind Tunnel Study of Air Flow in Waving Wheat: Two-Point Velocity Statistics." *Boundary-Layer Meteorology* 76 (4): 349–76. doi:10.1007/BF00709238.

Sheppard, P. A., D. T. Tribble, and J. R. Garratt. 1972. "Studies of Turbulence in the Surface Layer over Water (Lough Neagh). Part I. Instrumentation, Programme, Profiles." *Quarterly Journal of the Royal Meteorological Society* 98 (417): 627–41. doi:10.1002/qj.49709841711.

Shuttleworth, W. J., J. H. C. Gash, V. P. Silva-Filho, L. C. B. Molion, L. D A Sá, C. A. Nobre, Osvaldo M. R. Cabral, S. R. Patel, and J. C. Moraes. 1984a. "Eddy Correlation Measurements of Energy Partition for Amazonian Forest." *Quarterly Journal of the Royal Meteorological Society* 110: 1143–62.

———. 1984b. "Observations of Radiation Exchange above and below Amazonian Forest." *Quarterly Journal of the Royal Meteorological Society* 110: 1163–69. doi:10.1002/qj.49711046623.

Silva Dias, M. A F, S. Rutledge, P. Kabat, P. L. Silva Dias, C. Nobre, G. Fisch, A. J. Dolman, et al. 2002. "Cloud and Rain Processes in a Biosphere-Atmosphere Interaction Context in the Amazon Region." *Journal of Geophysical Research D: Atmospheres* 107 (20). doi:10.1029/2001JD000335.

Souza, Cledenilson Mendonça, Cléo Quaresma Dias-Júnior, Júlio Tóta, and Leonardo Deane de Abreu Sá. 2016. "An Empirical-Analytical Model of the Vertical Wind Speed Profile above and within an Amazon Forest Site." *Meteorological Applications* 23 (1): 158–164. doi:10.1002/met.1543.

Stull, Roland B. 1988. *An Introduction to Boundary Layer Meteorology*. Dordrecht: Kluwer Academic Publishers.

Sun, Jielun, Larry Mahrt, Robert M. Banta, and Yelena L. Pichugina. 2012. "Turbulence Regimes and Turbulence Intermittency in the Stable Boundary Layer during CASES-99." *Journal of the Atmospheric Sciences* 69 (1): 338–51. doi:10.1175/JAS-D-11-082.1.

Tennekes, H. 1970. "Free Convection in the Turbulent Ekman Layer of the Atmosphere." *Journal of the Atmospheric Sciences* 27 (7): 1027–34.

Thomas, Christoph, and Thomas Foken. 2007. "Flux Contribution of Coherent Structures and Its Implications for the Exchange of Energy and Matter in a Tall Spruce Canopy." *Boundary-Layer Meteorology* 123 (2): 317–37. doi:10.1007/s10546-006-9144-7.

Tóta, Julio, David R. Fitzjarrald, Ralf M. Staebler, Ricardo K. Sakai, Osvaldo M M Moraes, Otávio C. Acevedo, Steven C. Wofsy, and Antonio O. Manzi. 2008. "Amazon Rain Forest Subcanopy Flow and the Carbon Budget: Santarém LBA-ECO Site." *Journal of Geophysical Research: Biogeosciences* 114 (1): 1–15. doi:10.1029/2007JG000597.

Tóta, Julio, David Roy Fitzjarrald, and Maria A. F. da Silva Dias. 2012. “Amazon Rainforest Exchange of Carbon and Subcanopy Air Flow: Manaus LBA Site—A Complex Terrain Condition.” *The Scientific World Journal* 2012: 1–19. doi:10.1100/2012/165067.

Vale, Roseilson Souza do. 2016. “Medições de Gases de Efeito Estufa E Variáveis Ambientais Em Reservatórios Hidrelétricos Na Amazônia Central.” Instituto Nacional de Pesquisas da Amazônia - Universidade do Estado do Amazonas.

Vesala, Timo, Werner Eugster, and Anne Ojala. 2012. “Eddy Covariance Measurements over Lake Fluxes.” In *Eddy Covariance - A Practical Guide to Measurement and Data Analysis*, edited by Marc Aubinet, Timo Vesala, and Dario Papale. Vol. 2. Springer Atmospheric Sciences.

Vickers, D., and L. Mahrt. 1997. “Quality Control and Flux Sampling Problems for Tower and Aircraft Data.” *Journal of Atmospheric and Oceanic Technology* 14: 512–26.

von Randow, C., A. O. Manzi, B. Kruijt, P. J. de Oliveira, F. B. Zanchi, R. L. Silva, M. G. Hodnett, et al. 2004. “Comparative Measurements and Seasonal Variations in Energy and Carbon Exchange over Forest and Pasture in South West Amazonia.” *Theoretical and Applied Climatology* 78 (1–3): 5–26. doi:10.1007/s00704-004-0041-z.

Von Randow, Celso, Bart Kruijt, Albert A M Holtslag, and Maria Betânia L de Oliveira. 2008. “Exploring Eddy-Covariance and Large-Aperture Scintillometer Measurements in an Amazonian Rain Forest.” *Agricultural and Forest Meteorology* 148 (4): 680–90. doi:10.1016/j.agrformet.2007.11.011.

Walter, Ryan K., Nicholas J. Nidzieko, and Stephen G. Monismith. 2011. “Similarity Scaling of Turbulence Spectra and Cospectra in a Shallow Tidal Flow.” *Journal of Geophysical Research: Oceans* 116 (10): 1–14. doi:10.1029/2011JC007144.

Wang, Jian, Paulo Artaxo, and Joel Brito. 2016. “Amazon Boundary Layer Aerosol Concentration Sustained by Vertical Transport during Rainfall.” *Nature* 539 (7629). Nature Publishing Group: 416–19. doi:10.1038/nature19819.

Wyngaard, J. C., O. R. Coté, and Y. Izumi. 1971. “Local Free Convection, Similarity, and the Budgets of Shear Stress and Heat Flux.” *Journal of the Atmospheric Sciences* 28 (7): 1171–82.

Xu, Xiyan, Chuixiang Yi, Leonardo Montagnani, and Eric Kutter. 2017. “Numerical Study of the Interplay between Thermo-Topographic Slope Flow and Synoptic Flow on Canopy Transport Processes.” *Agricultural and Forest Meteorology*. Elsevier B.V. doi:10.1016/j.agrformet.2017.03.004.

Yi, Chuixiang. 2008. “Momentum Transfer within Canopies.” *Journal of Applied Meteorology and Climatology* 47 (1): 262–75. doi:10.1175/2007JAMC1667.1.

Yi, Chuixiang, Russell K. Monson, Zhiqiang Zhai, Dean E. Anderson, Brian Lamb, Gene Allwine, Andrea A. Turnipseed, and Sean P. Burns. 2005. “Modeling and Measuring the Nocturnal Drainage Flow in a High-Elevation, Subalpine Forest with Complex Terrain.” *Journal of Geophysical Research Atmospheres* 110 (22): 1–13. doi:10.1029/2005JD006282.

Zahn, Einara, Nelson L. Dias, Alessandro Araújo, Leonardo Sá, Matthias Söergel, Ivonne Trebs, Stefan Wolff, and Manzi Antônio. 2016. “Scalar Turbulent Behavior in the

Roughness Sublayer of an Amazonian Forest." *Atmospheric Chemistry and Physics* 16 (17): 11349–66. doi:10.5194/acp-16-11349-2016.

Zeri, Marcelo, Leonardo Deane A Sá, and Carlos A. Nobre. 2015. "Contribution of Coherent Structures to the Buoyancy Heat Flux under Different Conditions of Stationarity over Amazonian Forest Sites." *Atmospheric Science Letters* 16 (3): 228–33. doi:10.1002/asl2.544.